



U.S. Department
of Transportation

**National Highway
Traffic Safety
Administration**



DOT HS 813 162

July 2021

Vehicle Technology Assessment, Model Development, and Validation of a 2019 Infiniti QX50

DISCLAIMER

This publication is distributed by the U.S. Department of Transportation, National Highway Traffic Safety Administration, in the interest of information exchange. The opinions, findings and conclusions expressed in this publication are those of the authors and not necessarily those of the Department of Transportation or the National Highway Traffic Safety Administration. The United States Government assumes no liability for its contents or use thereof. If trade or manufacturers' names are mentioned, it is only because they are considered essential to the object of the publication and should not be construed as an endorsement. The United States Government does not endorse products or manufacturers.

Suggested APA Format Citation:

Jehlik, F., Kim, N., Islam, E., Lohse-Busch, H., Rousseau, A., Stutenberg, K., & Vijayagopal, R. (2021, July). *Vehicle technology assessment, model development, and validation of a 2019 Infiniti QX50* (Report No. DOT HS 813 162). National Highway Traffic Safety Administration.

1. Report No. DOT HS 813 162		2. Government Accession No.		3. Recipient's Catalog No.	
4. Title and Subtitle Vehicle Technology Assessment, Model Development, and Validation of a 2019 Infiniti QX50				5. Report Date July 2021	
				6. Performing Organization Code	
7. Authors Jehlik, F., Kim, N., Islam, E., Lohse-Busch, H., Rousseau, A., Stutenberg, K., Vijayagopal, R.				8. Performing Organization Report No.	
9. Performing Organization Name and Address Argonne National Laboratory Energy Systems Division 9700 South Cass Avenue, Bldg. 362 Argonne, IL 60439-4854				10. Work Unit No. (TRAIS)	
				11. Contract or Grant No.	
12. Sponsoring Agency Name and Address National Highway Traffic Safety Administration 1200 New Jersey Avenue SE Washington, DC 20590				13. Type of Report and Period Covered Final Report	
				14. Sponsoring Agency Code	
15. Supplementary Notes					
16. Abstract NHTSA sets Corporate Average Fuel Economy (CAFE) standards for passenger cars, light trucks, and medium-duty vehicles, and contracted Argonne National Laboratory to conduct full vehicle simulations using Argonne's Autonomie software to provide input into the CAFE model to determine the contribution of vehicle technologies on fuel economy. The vehicle benchmarked in this report is a 2019 Infiniti QX50 equipped with the 2.0-liter, inline, 4-cylinder variable-compression-ratio (VCR) turbo engine coupled to a continuously variable transmission (CVT). This particular powertrain configuration is purported to provide favorable fuel economy results while delivering vehicle performance relative to previous V6-powered QX50 configurations. The evaluation focused on understanding the use of critical powertrain components and their impact on vehicle efficiency.					
17. Key Words CAFE, Argonne, Autonomie, 2019 Infiniti QX50, VCR, CVT				18. Distribution Statement Document is available to the public from the National Technical Information Service, www.ntis.gov .	
19. Security Classif. (of this report) Unclassified		20. Security Classif. (of this page) Unclassified		21. No. of Pages 106	22. Price

Form DOT F 1700.7 (8-72)

Reproduction of completed page authorized

Table of Contents

1. Executive Summary	1
2. Test Vehicle Description	3
2.1. Vehicle Specifications.....	3
2.2. Key Technology Features.....	4
2.3. Overview of Comparison Vehicles and Preliminary Analysis.....	5
3. Testing Overview	9
3.1. General Testing	9
3.2. Extended Testing.....	9
3.2.1. Vehicle Dynamometer Setup	9
3.2.2. Instrumentation	10
3.2.3. Test Plan Execution	14
3.2.4. Specialized Testing Overview	15
3.2.5. Test Fuel Specifications.....	17
3.2.6. Vehicle Setup	17
4. Vehicle Testing Analysis	19
4.1. Vehicle Operation Overview.....	19
4.2. Transient Cycle Results.....	20
4.2.1. Fuel Economy	20
4.2.2. Vehicle Efficiency Based on Tier 2 Fuel Testing.....	22
4.3. Analysis of Impact of Different Ambient Temperatures	23
4.4. Steady-State Speed Fuel Economy and Efficiency	26
4.5. Passing Maneuver Results and General Operation	28
4.6. Operation Over Maximum Acceleration.....	29
4.7. Results of Idle Fuel Flow Rate Test.....	30
4.8. Details of VCR Engine Operation.....	32
5. Component and Control Analysis	39
5.1. Signal Calculations for Control Analysis.....	39
5.2. Transmission Operation	42
5.2.1. Gear Ratio Control.....	42
5.2.2. Torque Converter Lockup Control.....	42
5.2.3. Lockup Variability	44
5.3. Deceleration Fuel Cutoff.....	45
5.4. PFI versus DI Operation.....	46
5.5. Engine Operation.....	47
5.5.1. Fuel Rate Map.....	47
5.5.2. Torque Pedal Map.....	47
5.6. Thermal Management Impact on Vehicle Controls	48
5.6.1. Engine Operation Under Cold Conditions	48
5.6.2. Engine Performance.....	51

5.6.3.	Fuel Consumption Analysis.....	51
5.7.	Accessory Load.....	52
5.8.	Energy Balance Diagram	54
6.	Autonomie Model Validation	57
7.	Conclusions	63
8.	References	64
9.	Acknowledgements.....	65
Appendix A:	Vehicle Build Sheet.....	A-1
Appendix B:	2019 Infiniti QX50 Test Signals.....	B-1
Appendix C:	2019 Infiniti QX50 Test Signals.....	C-1
Appendix D:	Test Summary	D-1
Appendix E:	Certification Fuel Specifications	E-1
Appendix F:	Test ID to Figure Matrix.....	F-1
Appendix G:	Comments From External Reviewers.....	G-1

List of Figures

Figure 1. Distribution of horsepower and equivalent test weight among comparable vehicles in the sample group	6
Figure 2. Distribution of unadjusted FTP fuel economy for comparison vehicles	7
Figure 3. Distribution of unadjusted HWFET fuel economy for comparison vehicles	7
Figure 4. Vehicle mounted for full testing inside the AMTL 4WD chassis dynamometer	9
Figure 5. Instrumentation of port and direct fuel Injection systems	11
Figure 6. Direct fuel flow measurements via fuel scale and Coriolis flow meters, system overview, and actual measurement system	12
Figure 7. Wiring of Hioki power analyzer on the 2019 Infiniti QX50 test vehicle	13
Figure 8. CAN breakout on the 2019 Infiniti QX50	13
Figure 9. Overview of steady-state ramp drive cycle	16
Figure 10. Vehicle acceleration with varying constant pedal inputs	16
Figure 11. 2019 Infiniti QX50 test vehicle mounted to the chassis dynamometer inside the test cell	18
Figure 12. Infiniti QX50 powertrain operation on cold start UDDS cycle	19
Figure 13. Daily drive cycle test sequence executed in the morning	20
Figure 14. Raw fuel scale fuel economy results: UDDS and HWFET certification cycles from Argonne	21
Figure 15. Raw fuel scale fuel economy results for certification cycles at different temperature conditions. Climate control is set to 22 °C in automatic mode for the -7 °C and 35 °C cold and hot ambient test. For the 22 °C ambient temperature test, climate control is off	23
Figure 16. Engine operation in the UDDS cycle at different temperatures	24
Figure 17. Powertrain and cabin temperature profiles at different temperatures	25
Figure 18. Steady-state stair-step speed profile at 0, 3, and 6% grades	26
Figure 19. Steady-state speed operation at 22 °C and 0% grade	26
Figure 20. Steady-state speed operation at 22 °C and 3% grade	27
Figure 21. Steady-state speed operation at 22 °C and 6% grade	27
Figure 22. Powertrain operation during the 55- to 80-mph passing maneuver	29
Figure 23. Powertrain operation during maximum acceleration	30
Figure 24. PFI to DI transition and initial 240 sec of the idle fuel flow test. Fuel power is the fuel flow rate multiplied by the fuel lower heating value	31
Figure 25. Infiniti VCR compression ratio and rate of change for 25°C hot start, US06, and 0–80 mph maximum effort cycles	33
Figure 26. Infiniti VCR operational overview for 25 °C hot start UDDS, HWFET, and US06 cycles	34
Figure 27. Infiniti VCR operational overview of positive tractive force for 25 °C hot start UDDS, HWFET, and US06 cycles	35
Figure 28. Infiniti VCR and boost operational map for 25 °C hot start UDDS, HWFET, and US06 cycles	36
Figure 29. Infiniti VCR histogram overview of positive tractive force for 25°C hot start UDDS, HWFET, and US06 cycles	36
Figure 30. Engine MAP histogram overview of positive tractive force for 25 °C hot start UDDS, HWFET, and US06 cycles	37
Figure 31. Comparison of ignition timing spark advance for UDDS, HWFET, and US06 cycles	38

Figure 32. Comparison of percentage DI operation for UDDS, HWFET, and US06 cycles. Additional figure generalizes regions of DI operation.	38
Figure 33. Schematic of the vehicle configuration	39
Figure 34. Calculation of missing signals for components.....	40
Figure 35. Time spent in each gear ratio segment for the UDDS, HWFET, and US06 cycles ...	42
Figure 36. Torque converter lockup operation: wheel torque versus vehicle speed.....	43
Figure 37. Torque converter lockup operation: vehicle speed versus CVT gear ratio	43
Figure 38. Torque converter operation points for clutch engaging versus disengaging.....	44
Figure 39. DFCO operation: Vehicle speed versus wheel torque.....	45
Figure 40. DFCO operation: Engine coolant temperature versus wheel torque.....	45
Figure 41. Operating behavior of the fuel injection mode according to engine coolant temperature	46
Figure 42. Operating behavior of the fuel injection mode according to engine speed	46
Figure 43. Engine fuel rate map according to engine speed and torque.....	47
Figure 44. Torque pedal map.....	48
Figure 45. Engine operation at the launch of the vehicle differs according to engine coolant temperature	49
Figure 46. Engine idle speed is controlled according to coolant temperature	50
Figure 47. Behaviors of engine coolant temperatures on UDDS in different test conditions	50
Figure 48. Fuel rate according to engine power for different coolant temperatures.....	51
Figure 49. Accumulated fuel consumption trajectories on the UDDS cycle under different test conditions.....	52
Figure 50. Engine output power when vehicle is fully stopped.....	53
Figure 51. Electrical consumption when vehicle is fully stopped	53
Figure 52. Fan duty when vehicle is fully stopped	54
Figure 53. Example of energy calculation for one component on Autonomie.....	54
Figure 54. Energy balance diagram for the UDDS cycle in Autonomie	55
Figure 55. Energy balance diagram for the HWFET cycle in Autonomie	56
Figure 56. Validation process for 2019 Infiniti QX50 on Autonomie.....	57
Figure 57. Simulation and test results for the UDDS cycle.....	58
Figure 58. Simulation and test results for the HWFET cycle.....	59
Figure 59. Vehicle speed at which torque converter locked up.....	61
Figure 60. Vehicle speed at which engine fuel cutoff occurred	61

List of Tables

Table 1. Technical specifications of the 2019 Infiniti QX50 test vehicle	3
Table 2. Standard data streams collected for all vehicles tested at the Argonne AMTL.....	10
Table 3. Summary of the executed general test plan	14
Table 4. Main specifications of the EPA Tier 2 EEE fuel	17
Table 5. Chassis dynamometer target parameters for the 2019 Infiniti QX50 test vehicle	18
Table 6. Raw fuel scale fuel economy results for the UDDS and HWFET certification cycles from EPA and Argonne	21
Table 7. Results of raw Tier 2 fuel scale fuel economy drive cycles, ambient temperate 22 °C..	22
Table 8. Powertrain efficiencies based on J2951 positive cycle energy [5]	22
Table 9. Powertrain efficiencies at different ambient test conditions based on Tier 2 fuel.....	24
Table 10. Time duration for acceleration events (seconds)	28
Table 11. Aggregate engine thermal efficiency for UDDS, HWFET, and US06 cycles relative to VCRs.....	35
Table 12. Parameter values used for calculating additional signals	41
Table 13. Percentage of time torque converter lockup in each cycle	44
Table 14. NCCP value for the UDDS and HWFET cycles	60
Table 15. Percentage of time for torque converter lockup and engine fuel cutoff	62
Table 16. Fuel consumption in testing and simulation of UDDS and HWFET cycles	62
Table 17. Facility and Vehicle Signal list.....	C-2
Table 18. CAN Signal list.....	C-3
Table 19. Certificate of Analysis for Tier 2 test fuel used for all the testing.....	E-2

Definitions and Abbreviations

Acronym	Description
2WD	two-wheel drive
4WD	four-wheel drive
AMTL	Advanced Mobility Technology Laboratory (Argonne)
Autonomie	Argonne full vehicle simulation software, https://www.autonomie.net/
AWD	all-wheel drive
CAN	controller area network
CAFE	Corporate Average Fuel Economy
ccps	cubic centimeters per second
CEd	positive driven cycle energy
CVT	continuously variable transmission
DAQ	data acquisition system
DFCO	deceleration fuel cut-off
DFI	direct fuel injected
DI	direct Injection
DOHC	double overhead cam
EGR	exhaust gas recirculation system
ETW	equivalent test weight
FTP	Federal test procedure (EPA defined)
FWD	Front-wheel drive
GDI	gasoline direct injection
gps	grams per second
HWFET	EPA certification testing: Highway Fuel Economy Test
JC08	Japanese JC08 Cycle
LA92	California unified driving schedule
lb-ft	foot-pound(s)
lbm	pound-mass
MPI	multipoint injection
MSRP	manufacturer's suggested retail price
Nm	Newton-meters (torque)
NCCP	normalized cross correlation power
Nm	Newton-meters (torque)
PFI	port fuel injected
SC03	EPA certification test (Air conditioning test)
UDDS	EPA certification test: urban dynamometer driving schedule
US06	EPA certification test: US06 dynamometer driving schedule
Volpe	Volpe National Transportation Systems Center
VCR	variable compression ratio
WLTP	World harmonized light-duty vehicles test procedure
WOT	Wide open throttle

Symbols	Description
$F_{chassis}$	force obtained from the dynamometer
J_{TC}	Inertia of torque converter
$P_{acc_{mech}}$	power of accessory load
r_t	radius of tire
$R_{xy}(\tau)$	cross-correlation over the range of lags between two signals (x, y)
$T_{acc_{mech}}$	torque of accessory load
T_{eng}	torque of engine
$T_{fd,in}$	torque in of final drive
$T_{fd,out}$	torque out of final drive
$T_{gb,in}$	torque in of gearbox
$T_{gb,out}$	torque out of the gearbox
T_{ratio}	torque ratio of torque converter
$T_{TC,in}$	torque in of torque converter
$T_{TC,out}$	torque out of torque converter
$T_{trq_{cpl},out}$	torque out of torque-coupling
$T_{wheel,brake}$	brake torque of wheel
$T_{wheel,loss}$	torque loss of wheel
$T_{wheel,out}$	torque out of wheel
$v_{chassis}$	linear speed of vehicle
γ_{fd}	ratio of the final drive
η_{fd}	transfer coefficient of final drive
τ	displacement, also known as lag
ω_{eng}	rotational speed of engine
$\omega_{gb,out}$	rotational speed out of gearbox
ω_{ratio}	speed ratio of turbine speed to impeller speed for torque converter
ω_{TC}	rotational speed of impeller for torque converter
ω_{wheel}	rotational speed of wheel

1. Executive Summary

The National Highway Traffic Safety Administration (NHTSA) is an agency within the U.S. Department of Transportation (DOT) that sets Corporate Average Fuel Economy (CAFE) standards for passenger cars, light trucks, and fuel efficiency standards for medium-duty and heavy-duty engines and vehicles. NHTSA contracted with Argonne National Laboratory (Argonne) to conduct a full vehicle simulation using Autonomie (www.autonomie.net/) to provide input into the CAFE model to determine optimum average fuel economy based on numerous technological and economic factors. Autonomie relies on vehicle and component data for model development and validation. The Argonne Advanced Mobility Technology Laboratory (AMTL) provides the laboratory test data in Autonomie. NHTSA funded a project at Argonne to perform a benchmark study of a 2019 Infiniti QX50 SUV, resulting in an extensive dataset and analysis, model development, and validation with Argonne's Autonomie to assess the fuel-saving technologies of this advanced powertrain.

The vehicle benchmarked in this report is a 2019 Infiniti QX50 equipped with the 2.0-liter, inline, 4-cylinder variable-compression-ratio (VCR) turbo engine coupled to a continuously variable transmission (CVT). This particular powertrain configuration is purported to provide favorable fuel economy results while delivering vehicle performance relative to previous V6-powered QX50 configurations [1]). The evaluation focused on understanding the use of critical powertrain components and their impact on vehicle efficiency. The vehicle was instrumented to provide data to support model development and validation in conjunction with providing the data for the analysis in the report. Tests were performed on a chassis dynamometer in a controlled laboratory environment across a range of certification drive cycles and other testing conditions relevant for model development and validation. Furthermore, focused testing was performed to characterize the performance of different powertrain components.

Testing results showed that the VCR system is continually dynamic in usage rather than using a static set point of operation. The system is capable of varying compression ratio from 8.0:1 to 14.0:1 in one second. The VCR system is used extensively at high-compression ratios for the Environmental Protection Agency's city, highway, and the more aggressive US06 certification cycles. For the city cycle, highway, and US06 cycle, the engine used a compression ratio of 14.0:1 for 89%, 71%, and 53% of the drive cycle time, respectively. Turbo boost levels remained relatively low (sub-atmospheric pressure). Higher levels of boost are used for very high and full-load efforts in which the VCR system reduces the compression ratio to 8.0:1 and maximized boost. All cold starts use the direct injection (DI) system before transitioning to any blended levels of the port fuel injection (PFI) system. PFI usage is low, with most of the speed load utilization map showing high DI usage.

A comparison of the adjusted fuel economy on the federal test procedure (FTP) cycle against a sample group of 28 other comparative vehicles with similar vehicle weight and powertrain power shows the QX50 demonstrates relatively high fuel economy on the FTP cycle, only less than the hybrid powertrains of the Lexus NX300h and Volvo XC60 T8, and the conventional powertrains of the Jaguar F-Pace and Cadillac XT4. On the HWFET cycle, the Infiniti QX50 demonstrates the second-highest fuel economy of the sample group of 44.4 mpg. Only the Jaguar F-Pace displayed a higher highway fuel economy of 47.3 mpg.

The detailed analysis in this report is presented in several sections. Initial discussions describe vehicle instrumentation and setup throughout the testing program. Discussions then focus on

vehicle level operation, fuel economy, and efficiency results in certification drive cycles; this includes the impact of ambient temperature and details on VCR operation. Finally, model development, analysis, and validation are presented.

2. Test Vehicle Description

2.1. Vehicle Specifications

In 2019 Infiniti began offering a new powertrain lineup, with engine technology marketed as “VC-Turbo Engine”[1]. This powertrain technology was portrayed as providing many improvements over previous generations. This new engine contains a broad range of technologies: Port and direct injection fueling systems (PFI, DI), turbo-charging, variable compression ratio (VC/VCR), variable intake and exhaust valve timing allowing for Atkinson and regular combustion cycles, and active manifold tuning. Additional friction reduction technologies, particularly in the engine bore finish, are cited. The engine variable compression ratio varies and optimizes compression ratio depending upon load, which is cited to decrease fuel consumption by 35% in the front-wheel-drive configuration for the city/highway combined 2-cycle tests while maintaining performance relative to the previous 6-cylinder engine it replaced. In addition, the vehicle features a CVT. An overview of the vehicle’s technical specifications is presented in Table 1.

Table 1. Technical specifications of the 2019 Infiniti QX50 test vehicle

Test vehicle	2019 Infiniti QX50 /2.0L I-4 VC-Turbo Engine with automatic CVT
VIN	3PCAJ5M39KFI25022
Engine	2.0 L turbocharged, I-4, DOHC 16 V, Atkinson cycle capable, 200 kW (268 hp) @ 5,600 rpm 380 Nm (280 ft*lb-ft) @ 1,600–4,800 rpm compression ratio 8.0:1–14.0:1 port and direct fuel-Injection
Transmission	Xtronic automatic CVT [2] low gear ratio 2.371, high gear ratio 0.439, total gear reduction ratio of 5.41:1 235/55 R19 tires
Test vehicle weight	1,928 kg (4250 lbs.)
Climate control	Dual-zone automatic climate control belt-driven air-conditioning compressor
EPA label fuel economy (mpg) ^a	24 city, 30 highway, 26 combined, premium gasoline

^a Data from fueleconomy.gov.

Appendix A: Vehicle Build Sheet provides the full details of the actual test vehicle.

2.2. Key Technology Features

The 2019 Infiniti QX50 was produced with a new generation of Infiniti internal combustion engines labeled “VC-Turbo Engine.” The engine is a new design featuring a VCR, direct and port fuel injection, Atkinson cycle-enabled combustion, and a unique turbo exhaust manifold, resulting in claimed efficiency improvements throughout the powertrain. The Infiniti’s manufacturer, Nissan Motor Corporation, states, “Equipped with the VC-Turbo engine, the QX50 is competitively efficient, delivering gasoline fuel economy of 27 mpg (U.S. combined, front-wheel drive; 26 mpg all-wheel drive). In front-wheel-drive specification, this offers a 35 percent improvement in fuel efficiency over the V6 gasoline engine in the previous QX50, while the new all-wheel drive model's 26 mpg represents a 30 percent improvement” [2]. The engine is a turbocharged, in-line 4-cylinder (I-4), 2.0-liter, 16-valve, dual overhead cam (DOHC) engine. The engine operates under VCRs ranging from 8:1 under high load to 14:1 under low load, in addition to high-expansion-ratio Atkinson cycles under certain load regimes, to provide improved engine performance, noise-vibration-harshness (NVH), and fuel economy.

The following new technologies are used in this engine (Nissan Motor Corporation 2017 [2]).

- Multilink enabled VCR system (8:1–14:1) including a harmonic drive to improve engine noise, vibration, harshness:
 - Under the Atkinson cycle, air and fuel intakes overlap, allowing combustion gases in the combustion chamber to expand to larger volumes for greater efficiency (late exhaust valve opening).
 - The engine operates the Atkinson cycle under higher compression ratios, with longer piston strokes allowing the intake valves to open for a short time as the compression stroke starts.
 - As the compression ratio drops, the engine reverts to a regular combustion cycle assisted by turbocharging—intake, compression, combustion, exhaust—to enable greater performance.
- Variable intake port tumble ratio for combustion stability and optimization.
- Lightweight aluminum for block and heads.
- Multipoint injection (MPI) and gasoline direct injection (GDI) to balance efficiency and power in all conditions:
 - GDI improves combustion efficiency and performance and enables the engine to avoid knocking at higher compression ratios.
 - MPI mixes fuel and air earlier, enabling complete combustion in the chamber for greater efficiency at low engine loads.
 - The engine switches between both MPI and GDI at regular engine speeds, with both sets of injectors able to work in conjunction under higher loads.
- Engine low-friction mirror bore coating contributes to a cited 44% reduction in cylinder friction.

2.3. Overview of Comparison Vehicles and Preliminary Analysis

To provide insights into the possible impact of this unique powertrain combination on the market, the 2019 Infiniti QX50 test vehicle was compared with 11 other vehicles in the same market segment of the same model year. The 2019 Infiniti QX50 resides in the compact luxury crossover SUV vehicle class. The vehicle was offered in multiple trim levels, Pure, Luxury, and Essential trim levels, all equipped with the 2.0-L I-4 VCR engine coupled to a CVT.

For this comparison, all vehicle models and trim levels in the compact luxury crossover SUV segment with a starting manufacturer's suggested retail price (MSRP) of \$33,000 to \$45,000 and peak power of less than 268 kW were considered. The price range was selected based on the price of the varying trim levels of the QX50 platform, while power limit was chosen to remove non-comparable performance-oriented vehicles. The resulting list of comparable vehicles from the 2019 model year is summarized as follows

- *Infiniti QX50 (test vehicle)*
- Cadillac XT4
- Lexus NX300
- Acura RDX
- Lincoln MKC
- Mercedes Benz GLC-Class¹
- Jaguar F-Pace
- Alfa Romeo Stelvio
- Audi Q5
- BMW X3
- Volvo XC60
- Land Rover Range Rover Evoque

Following vehicle selection based on these broad criteria, data on all trim levels of each model were captured from the EPA vehicle test car list database [3]. The full subset of selected vehicles used for this comparison is listed in Appendix E.

Although all the vehicles compared are in the compact luxury crossover class, vehicle weight and power varies widely because this class has a variety of optional powertrains and trim levels available. A distribution of the weight and power of the comparison vehicles is displayed in Figure 1.

¹ Vehicle starting MSRP is \$40,000 to \$45,000.

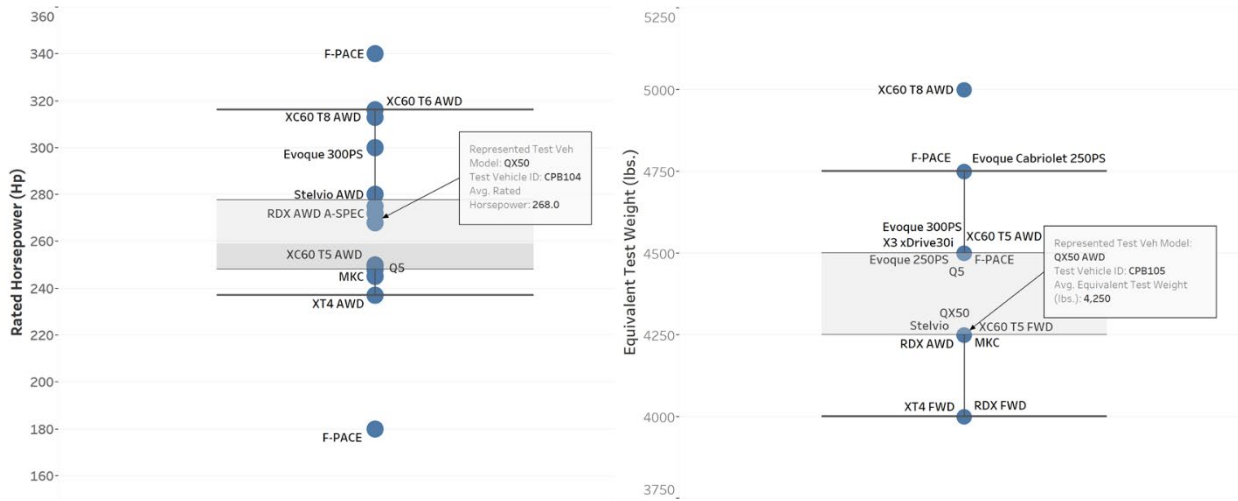


Figure 1. Distribution of horsepower and equivalent test weight among comparable vehicles in the sample group

At 200 kW, the 2.0-L turbocharged VCR engine is the median point of the sample group, in which the available power ranged from 134 to 253 kW. The equivalent test weight (ETW) ranged from a minimum of 1,814 kg (4,000 lb) to a maximum of 2,268 kg (5,000 lb), with a median ETW of 1,928 kg. Both versions of the QX50 available in the dataset, one front wheel drive (FWD) and one AWD, fell into the test weight class of 1,928 kg.

Similar to vehicle weight and powertrain power, fuel economy in this category varies considerably based not only on model but also on specific powertrain and trim selection. A comparison the unadjusted fuel economy on the federal test procedure (FTP) cycle for the sample set is shown in Figure 2.

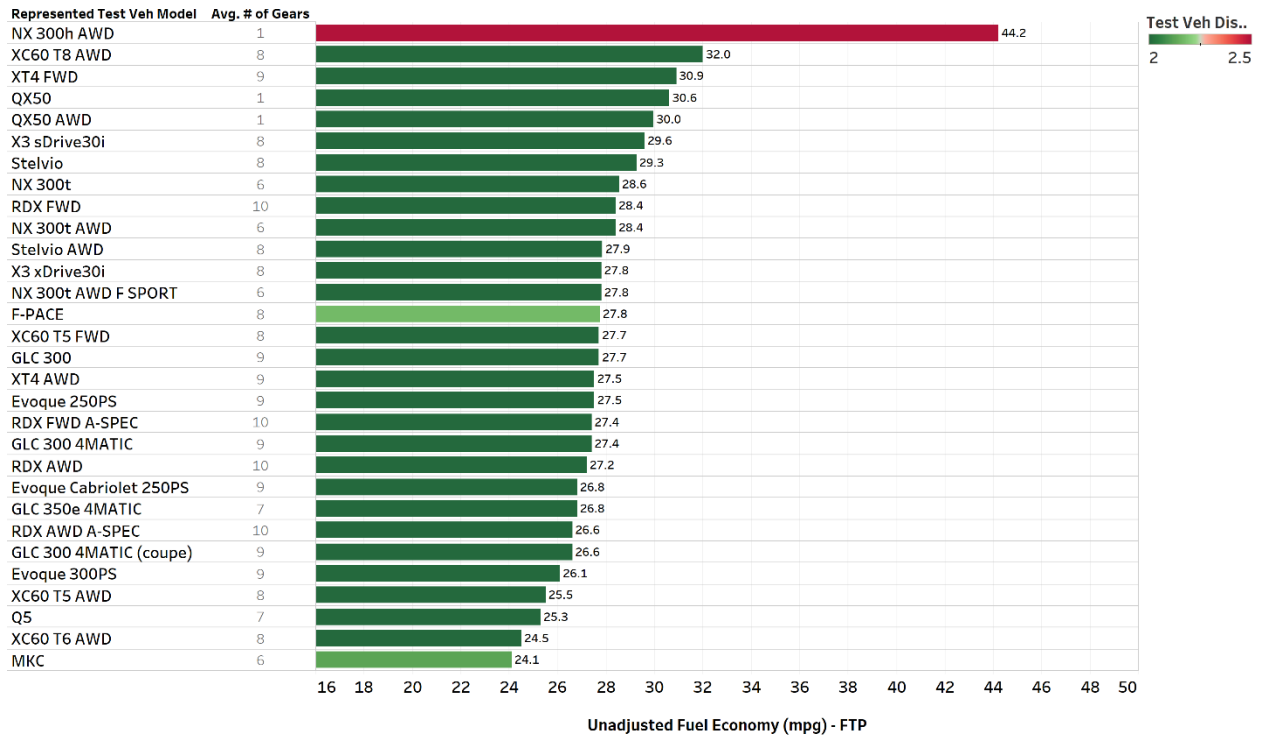


Figure 2. Distribution of unadjusted FTP fuel economy for comparison vehicles

The unadjusted fuel economy on the Highway Fuel Economy Test (HWFET) cycle of the 2019 Infiniti QX50 is shown in Figure 3.

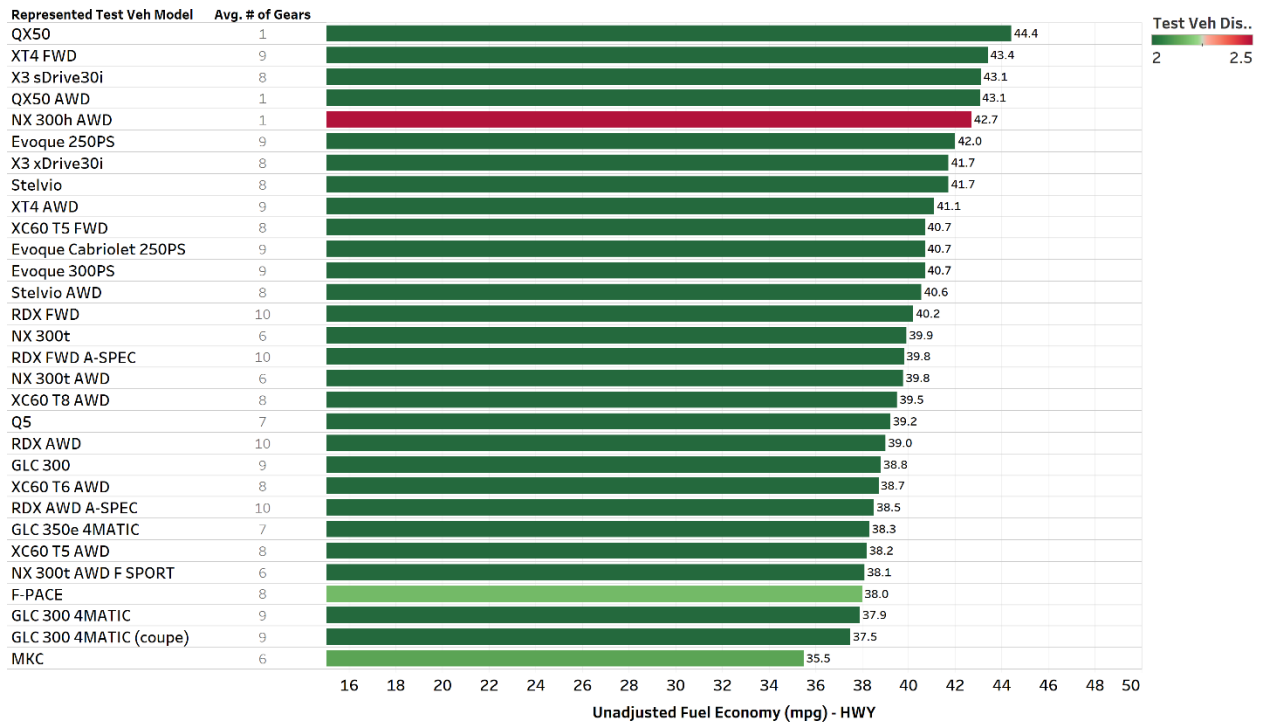


Figure 3. Distribution of unadjusted HWFET fuel economy for comparison vehicles

In the sample group the QX50 demonstrated relatively high fuel economy on the FTP cycle, only less than the hybrid powertrains of the Lexus NX300h and Volvo XC60 T8, and the conventional powertrains of the Cadillac XT4. On this cycle, which simulates operation within a city, regenerative braking and flexibility in powertrain operation enabled by the hybrid powertrain demonstrated large improvements in vehicle efficiency over that of the NX300h. On the HWFET cycle, the Infiniti QX50 demonstrated the highest fuel economy of the sample group of 44.4 mpg.

Following a joint review of possible powertrain configurations by the project team and a review of available vehicles that met the time goals of this project, a 2019 Infiniti QX50 of the Essential trim level was selected for this research because of its unique powertrain combination incorporating a VCR engine enabling improved vehicle efficiency.

3. Testing Overview

3.1. General Testing

Vehicle trim level selection followed a review of available vehicle options that could have an impact on vehicle energy use and fuel economy. One system determined to have a high impact on consistent vehicle operation was automatic climate control. Because testing was performed above and below an ambient temperature of 22 °C, automatic climate control offers insights in the climate control system operations that may have an impact on vehicle energy consumption. Above ambient (hot) temperatures, the air-conditioning system is an extra load on the powertrain, which can be affected by controlled cabin temperature, controlled airflow, and air-conditioning compressor operation. At low temperatures, the climate control system has an impact on the rate at which fluid temperatures rise, as coolant flow is routed to the passenger cabin, reducing waste heat available for the powertrain. In addition, all-wheel drive (AWD) systems may reduce efficiency because of additional powertrain friction losses.

A review of the 2019 Infiniti QX50 trim levels found that the Essential trim level provided all desired features and thus was chosen for the test vehicle. The test vehicle was purchased new from an Infiniti dealership, providing a known (zero mile) starting point of vehicle maintenance and operation history.

A new vehicle must be broken in for stability and consistent vehicle losses in tires and in moving and rotating components, and to ensure catalyst “de-greening.” The industry standard is 4,000 miles (6,437 km) for proper vehicle break-in [4]. On the test vehicle, this 4,000-mile (6437 km) break-in was accomplished through on-road driving. Computer area network (CAN)-based vehicle instrumentation was completed prior to break-in, providing data for preliminary results and instrumentation validation and refinement.

3.2. Extended Testing

3.2.1. Vehicle Dynamometer Setup

The following sections provide details of the vehicle setup and an overview of the test methodology specific to this test vehicle. The AMTL Test Methodology report provides further information on the methods of vehicle testing [4]. The vehicle was tested on the four-wheel drive (4WD) chassis dynamometer in the AMTL, as shown in Figure 4.



Figure 4. Vehicle mounted for full testing inside the AMTL 4WD chassis dynamometer.

3.2.2. Instrumentation

Vehicle instrumentation was developed to be sufficiently comprehensive to provide overall insight into vehicle operation, and to supply enough detail to develop models, calibrate control strategies, and validate simulation results. This section describes the vehicle specific instrumentation installed, in addition to the generic facility instrumentation listed in Table 2.

Table 2. Standard data streams collected for all vehicles tested at the Argonne AMTL

Facility Data	Drive Cycle Input	Emissions Data	Generic Vehicle Data
Dyno_Spd [mph]	Drive_Schedule_Time [s]	Dilute_CH4 [mg/s]	Engine_Oil_Dipstick_Temp [°C]
Dyno TractiveForce [N]	Drive_Trace_Schedule [mph]	Dilute_NOx [mg/s]	Cabin_Temp [°C]
Dyno_LoadCell [N]	Exhaust_Bag []	Dilute_COlow [mg/s]	Tire_Rear_Temp [°C]
DilAir_RH [%]		Dilute_COmid [mg/s]	Tire_Front_Temp [°C]
Tailpipe_Press [inH2O]		Dilute_CO2 [mg/s]	
Cell_Temp [°C]		Dilute_HFID [mg/s]	
Cell_RH [%]		Dilute_NMHC [mg/s]	
Cell_Press [inHg]		Dilute_Fuel [g/s]	

The following is a categorized list of the signals decoded on the vehicle communication bus, both diagnostic and broadcast messaging.

- Driver input and vehicle signals
 - Drive_trace_grade_per
 - Drive_trace_speed_mph
 - Pedal_accel_CAN2_per
- Engine
 - Eng_spd_CAN2_rpm
 - Eng_torque_TCM_Nm
 - Eng_turbo_boost_pressure_PCM_psi
 - Eng_wategate_act_position_PCM_cm
 - Eng_ignition_timing_PCM_deg
 - VCR_angle_actual_CAN5_deg
- Cooling system
 - Engine_coolant_bypass_valve_pos_PCM_deg
 - Eng_coolant_temp_CAN2_C
 - Eng_fan_duty_PCM_per
 - Eng_radiator_coolant_temp_PCM_C
- Transmission
 - Eng_torque_CVT_input_shaft_TCM_Nm
 - Input_CVT_Shaft_Rev_TCM_rpm
 - Trans_CVT_fluid_temp_CAN2_C
 - Trans_CVT_fluid_temp_TCM_C

This list is only a subset of signals collected. The complete list for the test vehicle is presented in Appendix C: 2019 Infiniti QX50 Test Signals.

3.2.2.1. Fuel Flow Measurements

The 2.0-L I-4 VC-Turbo engine has two fuel injection systems: a direct injection (DI) system and a port fuel injection (PFI) system. Figure 6 illustrates the direct fuel flow meter locations used for the fuel flow instrumentation on the test vehicle. The total fuel flow was measured by metering the fuel line between the tank and the engine bay using a Coriolis fuel flow meter and a positive displacement flow meter whose signals are Eng_FuelFlow_Direct2 [g/s] and Eng_FuelFlow_Direct [cm³/s], respectively. To determine the fuel usage between the PFI and DI systems, a positive displacement meter was placed on the fuel line to the PFI fuel injection rail, whose signal is Eng_FuelFlow_Direct3 [cm³/s]. By having the total fuel flow from the tank and the fuel flow to the PFI rail, the DI flow could be ascertained by subtracting the two.

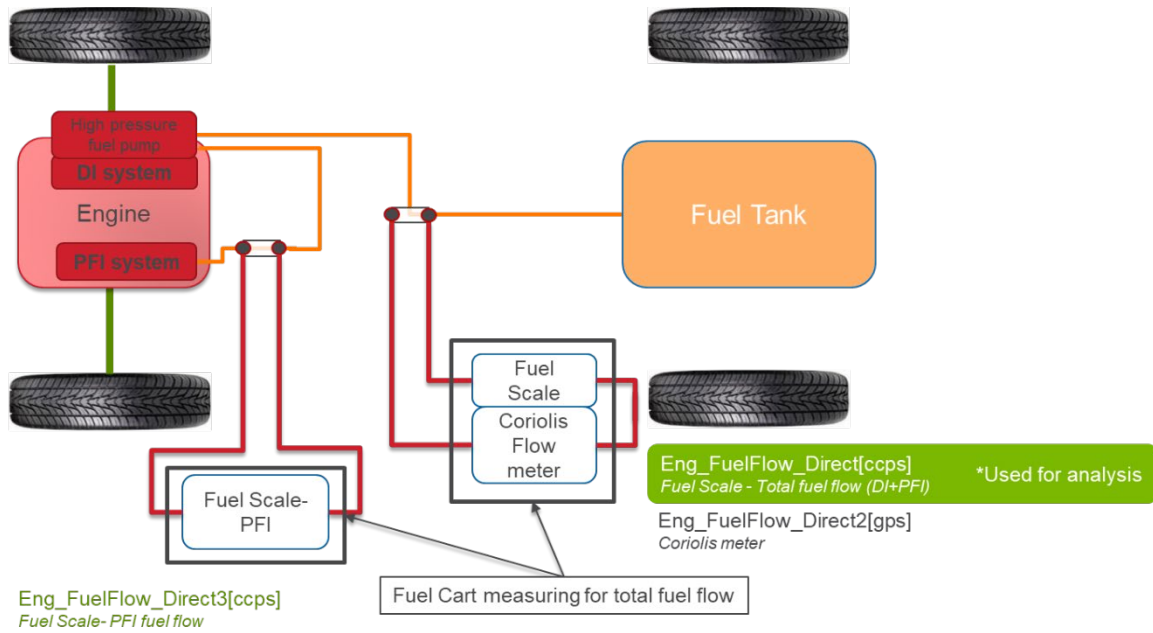


Figure 5. Instrumentation of port and direct fuel Injection systems

Note that the addition of hosing to connect the meters to the fuel system results in a transport signal delay because of fuel storage in the hoses. Detailed analysis is required to align the flow signals with another signal (i.e., engine torque, vehicle tractive force, engine revolutions per minute [rpm]) to time-align the entire dataset. This alignment was done for the analyses requiring time-synced flow rates in this report. Figure 6 shows the physical implementation of the fuel flow meters and the connecting hoses.

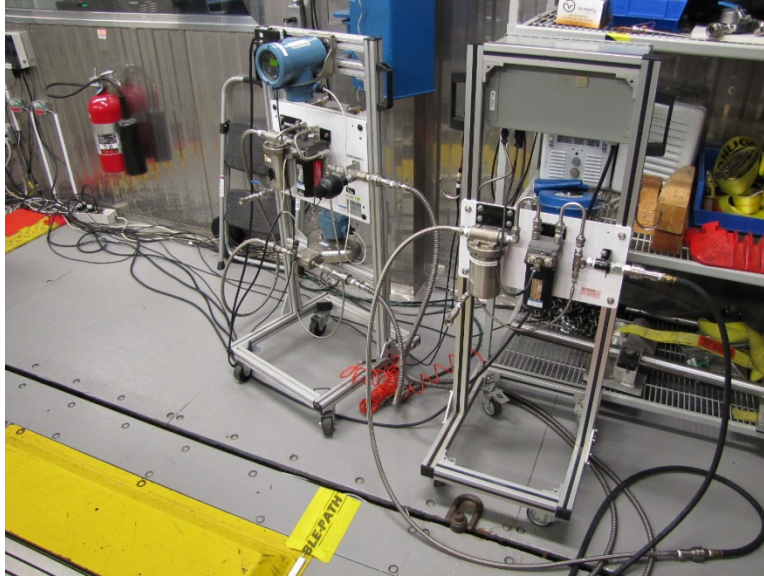


Figure 6. Direct fuel flow measurements via fuel scale and Coriolis flow meters, system overview, and actual measurement system

In addition, fuel flow was measured using the emissions bench, which included a bag fuel economy measurement for entire drive cycles in addition to modal fuel rate measurements. During the testing of the Infiniti QX50, the emissions bench did not accurately capture the fuel cutoff events. Typically, fuel cutoff events during deceleration in conventional powertrains are accurately captured with a slow decay of the fuel flow signal to zero, whereas direct measurements capture the step-type function. Considering the challenges of the modal fuel flow measurements for this vehicle, the team decided to use the direct fuel flow measurements for the analysis. The direct fuel measurements were used for the drive cycle level fuel economy analysis instead of the bench measurements for consistency in analysis.

3.2.2.2. Hioki Setup

The vehicle's 12-V electrical power flows were measured with a 4-channel Hioki 3390-10 power analyzer. Three channels were instrumented, each with a direct measurement of current with Hioki CT6843 200A current probes. Voltage for each channel was measured across the 12-V battery, which was then bridged to act as the source for all three channels. From the measured current and voltage channels, power and energy use were calculated in the analyzer. An overview of vehicle wiring is shown in Figure 7.

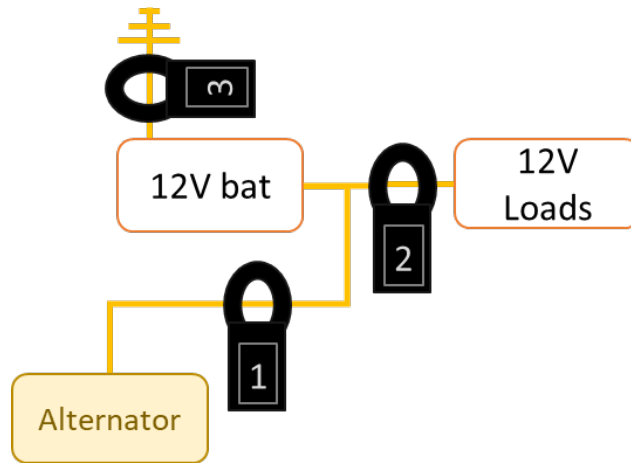


Figure 7. Wiring of Hioki power analyzer on the 2019 Infiniti QX50 test vehicle

3.2.2.3. Computer Area Network Signals

A core capability of the AMTL staff is the ability to decode the vehicle and powertrain internal communication messages. Over the last few years, AMTL staff has developed powerful tools that enable the decoding of both broadcast and diagnostic CAN messages. These tools rely on the understanding of CAN messaging structure, the correlation of changes in CAN messages with known instrumentation signals, and the ability to use the chassis dynamometer environment to safely control planned scenarios to enable the decoding of certain signals. The corresponding logging and communication of CAN messages was completed through a combination of custom scripting in Intrepid Control Systems Vehicle Spy software, and with National Instruments LabVIEW software located on the AMTL custom-built data acquisition system (DAQ).

This instrumentation included the determination and probing of eight separate CAN networks across the vehicle, which joined to a single measurement location for data collection, as shown in Figure 8. The complete list of CAN messages for the test vehicle is presented in Appendix C: 2019 Infiniti QX50 Test Signals.



Figure 8. CAN breakout on the 2019 Infiniti QX50

3.2.3. Test Plan Execution

3.2.3.1. Overview of Testing Matrix

Table 3 provides a summary of the tests that were executed as part of the general test plan. The test sequence was repeated three times at 22 °C, while testing at -7 °C and 35 °C did not include any repeat testing. Additional testing with varied octane fuel was not conducted because of the manufacturer’s recommendation of high-octane fuel only (93).

Table 3. Summary of the executed general test plan

Test Cycle/Test Conditions	22 °C	35 °C + solar loading = 850 W/m ²	-7 °C
UDDSx3, including cold start (Three UDDS cycles back to back)	Repeat 3 times ^a	UDDSx2, 1 test	X
HWFETx2 (Two HWY cycles back-to-back)	Repeat 3 times ^a	1 test	x
US06x2 (4bag) (Two US06 cycles back-to-back)	Repeat 3 times ^a	1 test	X
SC03x2 (Two SC03 cycles back-to-back, per EPA protocol)	N/A	1 test	N/A
Steady-state speed testing 0%, 3%, 6% grade	1 test	1 test	X
Passing 0%, 3%, 6% grade	1 test		
Wide open throttle (WOT) x3	1 test		

^a Two cycles completed with speed match fan, one without. Cycle without speed match fan is EPA Certification style with hood open, fan fixed at 6 mph.

Additional testing was included in order to provide further insight into vehicle energy consumption and operation. The additional testing included the following:

- 22 °C cold start idle, that is, mapping out the idle fuel flow consumption as a function of powertrain temperature;
- 22 °C cold start, California unified driving schedule (LA92);
- 22 °C cold start, US06 dynamometer driving schedule, transmission mapping through
 - Constant accelerator tip-ins tests, and
 - Accelerator tip-ins with vehicle locked at constant speed; and
- High-load engine and transmission mapping.

Appendix D: Test Summary summarizes all the final tests performed in this effort.

3.2.3.2. Driver Selection (Human versus Robotic)

Argonne has experienced dynamometer drivers who have driven test cycles on chassis rolls for decades. Vehicle operation on all drive cycles was completed with trained human drivers. In order to supplement their efforts and provide greater control for specific tests such as mapping or steady-state speeds, Argonne uses a robot driver. These focused tests perform best when step change inputs can be executed and subsequently held constant on braking or accelerator inputs, an operation that is more easily performed by an actuator. The driver used for each specific test is provided in the test plan in Appendix D: Test Summary.

3.2.3.3. Vehicle and Test Cell Setup

Aside from the EPA certification 5-cycle testing protocol, Argonne staff changed specific aspects of the drive cycle test procedures to prioritize vehicle operation in real world conditions. As a result, Argonne standard testing deviates from standard certification testing to fulfill Argonne's goal of research fidelity. One example would be to use a vehicle speed matching fan to emulate forced convection across the powertrain as would be realized in real world driving. Further detail on standard vehicle and test setup is discussed in the AMTL Testing Methodology Report [4]. Specific details on how a test was performed are given in Appendix D: Test Summary.

All testing on the 4WD chassis dynamometer was conducted with the Forward Collision Warning and Pre-collision braking systems disabled through the driver control interface. Although these systems were disabled, the vehicle was found to enter a fault mode when operated on the chassis dynamometer. To resolve this issue, a dynamometer mode was found and initiated each day prior to testing. This manufacturer-enabled mode disabled several systems so that relative control parameters (i.e., deceleration fuel cutoff) would remain consistent. Prior to testing, several runs were completed and compared with on-road testing data to ensure consistent vehicle operation across both scenarios.

3.2.4. Specialized Testing Overview

Determination of component and controls operation and limitations is best realized by specialized testing in which vehicle operation can be controlled. This section provides an overview of the methods and testing developed specifically for this assessment.

3.2.4.1. Steady-State Speeds

Steady-state speed tests evaluate vehicle operation while the vehicle is operated at a constant speed and load point. Steady-state cycles are conducted by following a ramp type driving schedule and are completed with a minimum 30 seconds at each speed until stability is determined. Vehicle speed is increased in 10-mph increments up to 80 mph, held for the set period of time, and then decreased to a stop in 10-mph increments. This is shown in Figure 9. Holding each speed following both increasing and decreasing speed captures variability in powertrain operation. Steady-state cycles may be repeated at varying grades to capture variations in vehicle loading at a steady state.

Prior to each steady-state speed cycle, the vehicle is warmed to an engine oil temperature of over 80 °C, or similar to that seen on a transient drive cycle. On the 2019 Infiniti QX50, steady-state speed cycles were performed at the test temperatures of 22 °C (0% grade), 35 °C (0%, 3%, and 6% grade), and -7 °C, as shown in Appendix D: Test Summary.

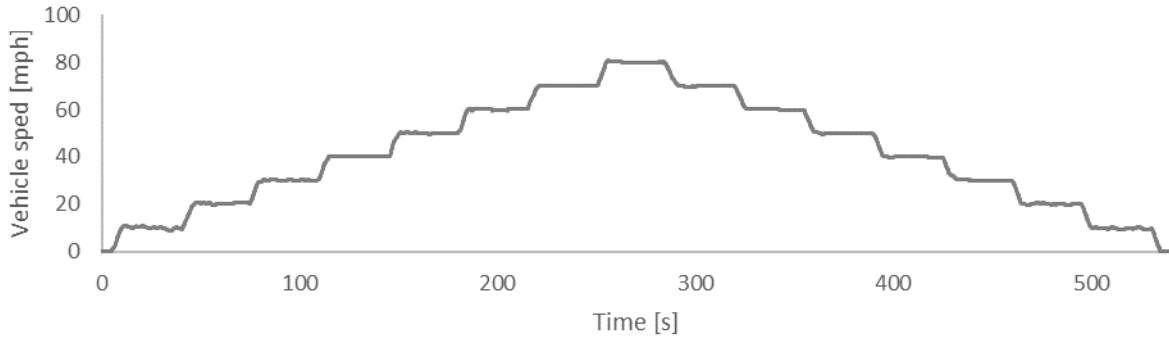


Figure 9. Overview of steady-state ramp drive cycle

3.2.4.2. Powertrain Mapping Cycles

Operation of the vehicle powertrain at its limits is not commonly seen during standard regulatory transient drive cycles. To fully map powertrain operation, supplemental custom cycles are used to test these extreme vehicle operations and effectively map component operation. To map powertrain operation on the 2019 Infiniti QX50, a combination of custom drive cycles, a robotic driver, and feedback from focused instrumentation were used. Mapping was performed using the U. S. Environmental Protection Agency (EPA) drive cycle data in addition to a vehicle mapping data. For the mapping data, the dynamometer was placed in road load simulation mode, and the vehicle accelerated with fixed accelerator pedal inputs. A representation of this is shown in Figure 10.

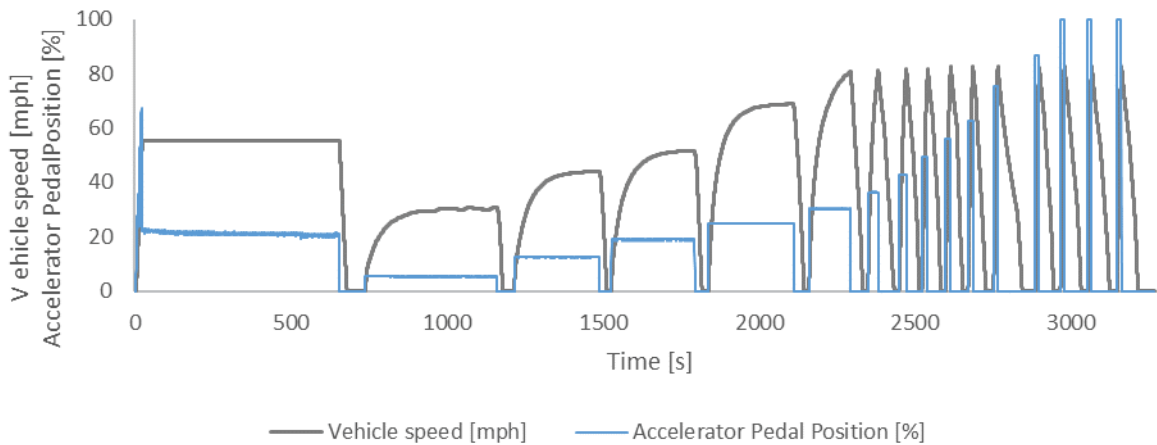


Figure 10. Vehicle acceleration with varying constant pedal inputs

This test provides a map of load demand and CVT shifting strategies for the full range of powertrain operations. Accelerator pedal inputs were held in 2.5% increments to a position of 20%, 5% increments to 50%, and then 10% increments to full throttle.

3.2.5. Test Fuel Specifications

One important factor in fuel economy during chassis dynamometer testing is the test fuel. Test fuels vary in many ways including energy content, octane, heating value, and so on. The 2019 Infiniti QX50 recommends a premium fuel. EPA certification testing was performed on Tier 2 EEE, high-octane certification fuel. The certification fuel was procured through Haltermann Solutions under the product code of HF0437. Table 5 provides the major specifications for the Tier 2 certification fuel used. The full chemical analysis of the certification fuel is presented in Appendix E: Certification Fuel Specifications.

Table 4. Main specifications of the EPA Tier 2 EEE fuel

Specification	Value
Ethanol content	0%
Carbon weight fraction	0.8663
Density	0.743 [g/ml]
Net heating value	43,317 [kJ/kg]
Research octane number	96.8
Motor octane number	89.1
R+M/2	93.0
Sensitivity	7.7

3.2.6. Vehicle Setup

Argonne used the test weight and road load coefficients published by the EPA of the manufacturer certification documentation[3]. The vehicle was tested in 4WD mode as it was an AWD vehicle. The vehicle was restrained on the chassis dynamometer from lateral motion using chains attached to straps affixed to the front sub-frame of the vehicle. The chains were connected to towers at the front corners of the vehicle. Longitudinal movement of the vehicle was restrained with specialized wheel chocks applied to the rear wheels. The team performed the vehicle coast down and vehicle loss determination evaluations before formal testing began. Table 5 provides the chassis dynamometer setup parameters for the Infiniti QX50 which includes the EPA target coefficients and the dynamometer set coefficients. Figure 11 shows a picture of the test vehicle mounted to the chassis dynamometer.

Table 5. Chassis dynamometer target parameters for the 2019 Infiniti QX50 test vehicle

Test weight	4,250 lbs. (1,928 kg)	
Chassis dyno setup	4WD on rolls with dyno mode	
	Target (EPA)	Set (Dynamometer)
Road load A term	45.470 lbf [202 N]	-19.30 lbf [-86N]
Road load B term	-0.1558 lbf/mph [-0.1059 N/(m/s)]	0.3231 lbf/mph [-3.2149 N/(m/s)]
Road load C term	0.02382 lbf/mph ² [0.52019 N/(m/s) ²]	0.02150 lbf/mph ² [0.47855 N/(m/s) ²]



Figure 11. 2019 Infiniti QX50 test vehicle mounted to the chassis dynamometer inside the test cell

Further details on vehicle dynamometer coefficients used for specific tests are given in Appendix D: Test Summary.

4. Vehicle Testing Analysis

4.1. Vehicle Operation Overview

Figure 12 provides a general overview of vehicle operation on a section of the EPA certification test urban dynamometer driving schedule (UDDS) cycle. The Infiniti QX50 does not have an engine idle stop feature, so the vehicle enters into this acceleration with the engine at idle. When the vehicle accelerates, the CVT transitions smoothly through the gear ratios to allow the engine speed to accelerate to 2,400 rpm and then transitions steadily to a low speed of approximately 1,300 rpm. At the relative low vehicle speed of 35 mph, the transmission has adjusted to its lowest CVT ratio. During the relatively light acceleration period, the engine only slightly reduces the engine compression ratio below 14:1. Manifold pressure remains low (low boost), and the engine uses high percentages of direct injection. During deceleration, the fuel to the engine is cut off while the engine is spun through the transmission and locked torque converter using the kinetic energy of the vehicle. The engine resumes fueling again before the vehicle comes to a full stop.

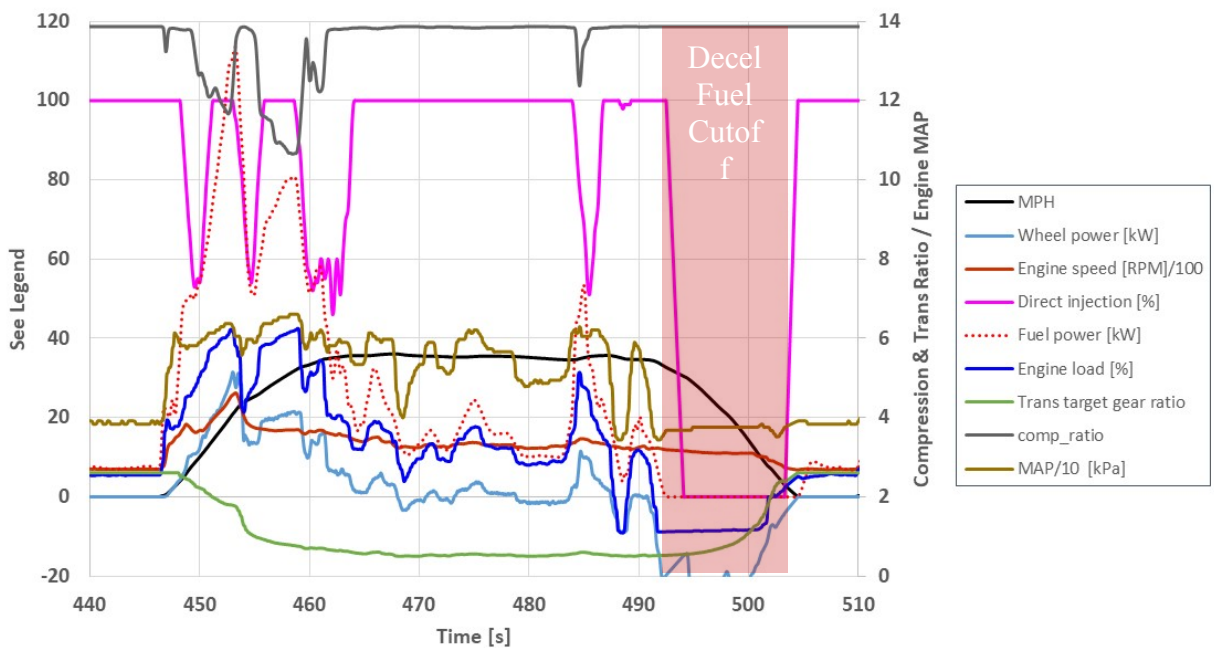


Figure 12. Infiniti QX50 powertrain operation on cold start UDDS cycle

4.2. Transient Cycle Results

4.2.1. Fuel Economy

4.2.1.1. Standard Fuel Economy Test Sequence Overview

The fuel economy testing focus is on the UDDS, HWFET, and US06 drive cycles at an ambient temperature of 22 °C. The test sequence includes a cold start UDDS, a hot start UDDS, a third UDDS, an HWFET pair, and a US06 pair. Preparation for the cold start test consists of completing a UDDS cycle at 22 °C and leaving the vehicle to thermally soak at 22 °C for more than 12 hours. The overnight soak is done on the chassis dynamometer in the test cell since the vehicle stayed mounted on the rolls for the duration of the testing. The graph in Figure 13 shows the sequence of drive cycles executed, which was repeated three times to determine test-to-test variability. Note that a 10-minute soak period is held between the UDDS cycles (not shown in the Figure due to size constraints). The third UDDS, while not used in the EPA 5-cycle calculation, is used to examine further thermal warm up effects. The fuel economy numbers in this report are based on the test phases highlighted by the pink boxes (discounting UDDS#3). The phases for the US06 drive cycle are the split city and highway phases needed to calculate the EPA 5-cycle fuel economy label. These are highlighted in the red outlined boxes.

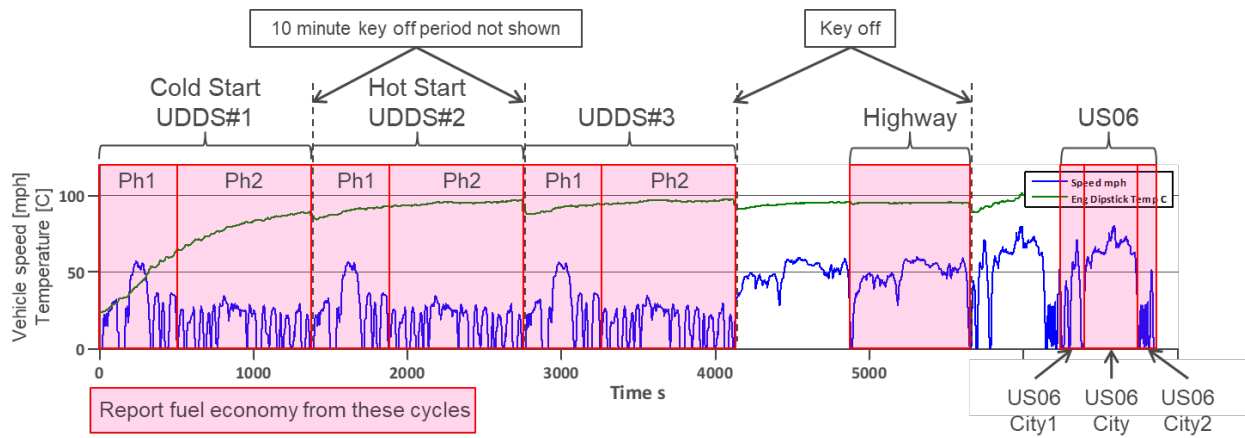


Figure 13. Daily drive cycle test sequence executed in the morning

4.2.1.2. CAFE Certification Cycle Fuel Economy Results

Figure 14 and Table 6 compare the three test sequences completed at the AMTL. The fuel economy results from the testing at Argonne compare closely to the fuel economy results published by EPA under the data on cars used for Testing Fuel Economy. The EPA published unadjusted fuel economy results from the manufacturer for phases 1, 2, and 3 of the UDDS as well as the HWFET cycle. The vehicle setup at Argonne is different from the certification testing in that Argonne tests the vehicle with the hood closed and the test cell fan in vehicle speed match mode. The test results summarized in Table 6 show high test-to-test repeatability, with the highest deviation of any phase to the average fuel economy of all the tests less than 1.2% (HWFET cycle).

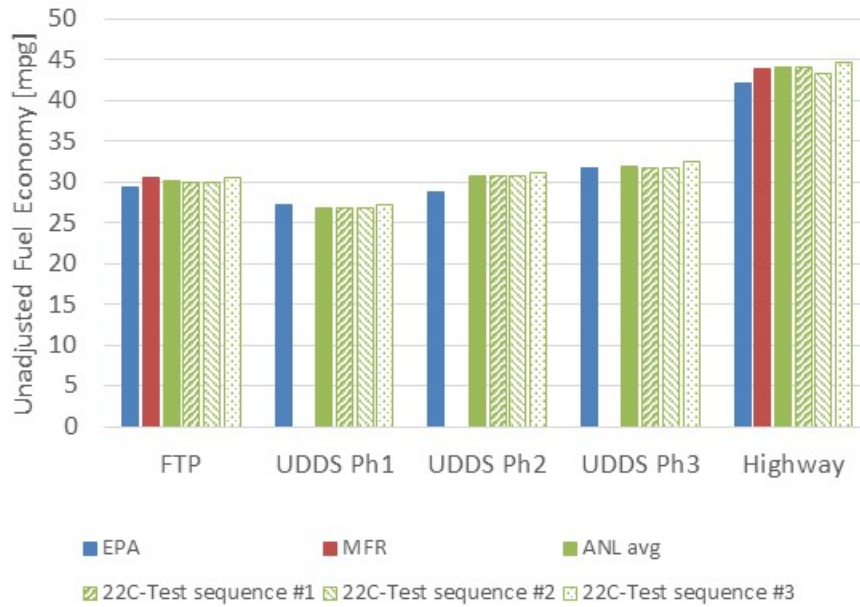


Figure 14. Raw fuel scale fuel economy results: UDDS and HWFET certification cycles from Argonne

Table 6. Raw fuel scale fuel economy results for the UDDS and HWFET certification cycles from EPA and Argonne

Drive Cycle	EPA by MFR (Tier 2)	ANL Avg. (Tier 2)	Test Sequence 1	Test Sequence 2	Test Sequence 3	Deviation from Avg.
UDDS phase 1	27.3	26.9	26.8	26.8	27.2	0.66%
UDDS phase 2	28.8	30.8	30.7	30.7	31.1	0.56%
UDDS phase 3	31.8	31.9	31.7	31.7	32.4	1.13%
HWFET	42.2	44.0	44.1	43.3	44.6	1.23%

4.2.1.3. Tier 2 Fuel Economy Results for Standard Drive Cycles

The fuel economy results for standard drive cycles are presented in Table 7. The drive cycles include the cold start UDDS (phases 1 and 2), the hot start UDDS (phase 3), a third UDDS cycle, the HWFET cycle, and the US06 cycle. The third UDDS cycle is not part of the certification testing; however, it is performed to understand the fuel economy changes at higher powertrain temperatures. Both the Highway and US06 drive cycles included 2 phases of testing. Note the test results shown here were conducted with the vehicle speed fan set to match vehicle speed with the vehicle hood closed.

Table 7. Results of raw Tier 2 fuel scale fuel economy drive cycles, ambient temperature 22 °C

Drive Cycle	Test Sequence 1	Test Sequence 2	Test Sequence 3	Average
UDDS #1 cold start	28.7	28.7	29.0	28.8
UDDS #1 phase 1	26.8	26.8	27.1	
UDDS #1 phase 2	30.7	30.7	31.1	
UDDS #2 hot start	31.4	31.4	32.0	31.6
UDDS #2 phase 1	31.7	31.7	32.4	
UDDS #2 phase 2	31.1	31.1	31.7	
UDDS #3	31.6	31.5	32.2	31.8
UDDS #3 phase 1	31.4	30.9	31.7	
UDDS #3 phase 2	31.8	32.2	32.6	
WFET	44.0	44.1	43.3	43.8
US06	24.7	24.8	25.0	24.8

4.2.2. Vehicle Efficiency Based on Tier 2 Fuel Testing

The vehicle efficiency is calculated by dividing the cumulative measured dynamometer positive cycle tractive force energy by the integrated fuel energy used over the drive cycle. Table 8 provides the calculated vehicle efficiencies for the drive cycles in each test sequence.

Table 8. Powertrain efficiencies based on J2951 positive cycle energy [5]

Drive Cycle	Test Sequence 1	Test Sequence 2	Test Sequence 3	Average
UDDS #1 cold start	21.5%	21.5%	21.8%	21.6%
UDDS #2 hot start	23.6%	23.7%	24.0%	23.8%
UDDS #3	23.7%	23.8%	24.0%	23.8%
HWFET	31.7%	31.0%	32.0%	31.6%
US06	28.4%	28.6%	28.9%	28.6%

The lowest average vehicle efficiency occurs on the UDDS cycle, which is typical for conventional vehicles. The UDDS cycle is a stop-and-go drive cycle with very mild power requirements. On the UDDS cycle the engine operates at low load with a relatively low throttle opening, which increases the pumping losses. The powertrain efficiency increases by 2.2% from the cold start cycle to the third cycle when the powertrain has reached its operating temperature. This efficiency increase is due to reduced friction and transition to closed-loop operation, which is a typical result of higher temperatures in all components within the powertrain.

The average powertrain efficiency is the highest on the HWFET drive cycle. On this cycle, the powertrain can take full advantage of the higher gear ratios and a lack of transient operation. The

engine down-speeding coupled with the high compression ratio Atkinson cycle operation engine enables the vehicle to achieve more than 30% vehicle efficiency on the HWFET cycle.

The average powertrain efficiency on the US06 drive cycle is more than 28%. This drive cycle requires high engine loads. Although the loading is high, the engine is still able to operate under high compression ratios during most of the cycle (to be shown in detail in Section 6.5 Engine Operation).

4.3. Analysis of Impact of Different Ambient Temperatures

The UDDS cycles, the HWFET cycle, and the US06 cycle were also tested at -7 °C and at 35 °C with 850 W/m² of solar load, which are the two extreme temperature conditions for the EPA five-cycle fuel economy label. Figure 15 provides the test results for those conditions and drive cycles.

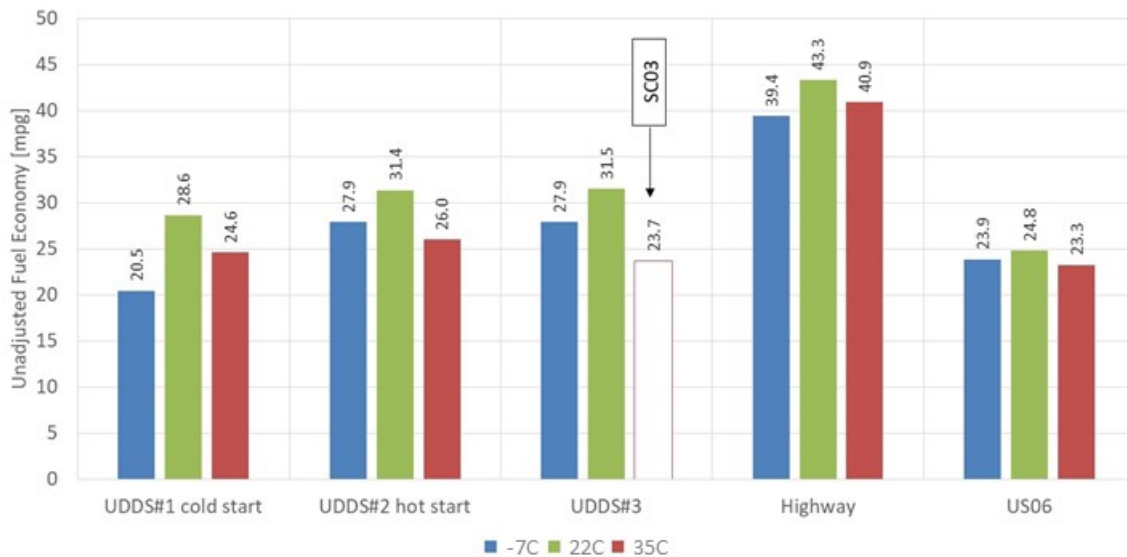


Figure 15. Raw fuel scale fuel economy results for certification cycles at different temperature conditions. Climate control is set to 22 °C in automatic mode for the -7 °C and 35 °C cold and hot ambient test. For the 22 °C ambient temperature test, climate control is off.

The fuel economy for the cold start UDDS cycle at -7 °C is decreased by 26% compared to that for the same test at 22 °C, yet the fuel economy for the second urban cycle at -7 °C is only 13% lower than that for the same test at 22 °C. The powertrain has to overcome significantly increased friction losses throughout the drive train on the cold start at -7 °C, however once the powertrain reaches a steady operating temperature, those friction losses become less significant. The fuel economy penalty at -7 °C compared to that at 22 °C becomes smaller as the powertrain temperature increases.

The fuel economy at the 35 °C test condition is also reduced compared to that for the 22 °C test condition. At 35 °C the fuel economy decreases by 8% and 10% for the cold start UDDS and the hot start UDDS, respectively, compared to that for the 22 °C test condition. The fuel economy reduction is driven by the additional power required to operate the air-conditioning system to cool down the cabin. Contrary to the cold temperature testing, this compressor load is a

permanent energy penalty needed to maintain the comfort of the occupants in the vehicle. The deceleration fuel cutoff is reduced (13.8% of the time for deceleration fuel cutoff (DFCO) UDDS cold start at 22 °C compared to 11.9% at 35 °C) because the engine restarts fueling sooner to provide power to the air-conditioning compressor when the kinetic energy of the vehicle is not enough. Note that for the 35 °C testing, the third UDDS cycle was replaced by SC03 drive cycles.

Table 9 provides the calculated vehicle efficiencies for the different ambient test conditions. The impact of the cold powertrain temperatures is apparent in the efficiency for the -7 °C cold start. As the powertrain temperatures rise throughout the tests in the test sequence, the vehicle efficiencies at -7 °C start to approach the vehicle efficiencies at 22 °C ambient temperature. The impact of the auxiliary load from the air-conditioning compressor at 35 °C is also apparent in this table. Note that the impact of the air-conditioning compressor on efficiency is lower on the high-power US06 drive cycle as the ratio between the air-conditioning power to the average wheel power is lower compared to the same ratio for the low-power UDDS cycle.

Table 9. Powertrain efficiencies at different ambient test conditions based on Tier 2 fuel

Drive Cycle	-7 °C	22 °C	35 °C
UDDS #1 cold start	15.4%	21.6%	18.8%
UDDS #2 hot start	21.0%	23.8%	19.8%
UDDS #3	N/A	23.8%	N/A
HWFET	28.2%	31.6%	29.4%
US06	27.4%	28.6%	26.8%

Figure 16 shows the engine operating areas for the cold start and hot start UDDS cycles at each of the three ambient temperature conditions. The 22 °C plot in the middle serves as the reference. At -7 °C the engine operation is slightly shifted to higher speeds and higher loads to overcome heat transfer and viscous losses. At 35 °C the average absolute engine load shifts upward slightly. The overall absolute engine load envelop is increased, which is also due to the additional power required for the air-conditioning compressor.

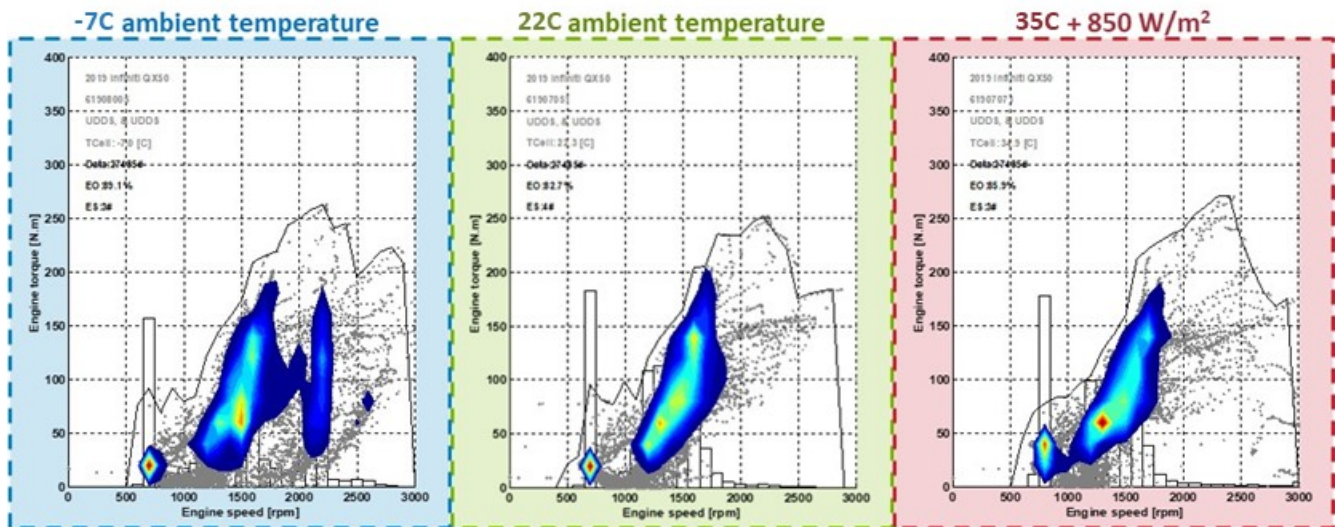


Figure 16. Engine operation in the UDDS cycle at different temperatures

Figure 17 shows some relevant powertrain and ambient temperature profiles over the completion of the test sequences. In order to obtain thermally stable results, three pairs of HWFET drive cycles were tested at -7°C . The SC03 at 35°C ambient temperature replaced the third UDDS cycle as this is the EPA certification cycle to test air conditioning impacts. These graphs also show the targeted 22°C cabin temperature that the climate control system tries to achieve in the -7°C and 35°C test conditions.

Per the -7°C test, the first UDDS consumption is much greater than the following cycle due to catalyst light off strategies, cold idle stability enrichment, and increased friction and heat transfer due to the engine being cold. Similar results are seen for the 22°C , however, the losses are relatively smaller. Consumption increases in the $+35^{\circ}\text{C}$ case are associated with the increased engine load of air-conditioning cabin pull-down.

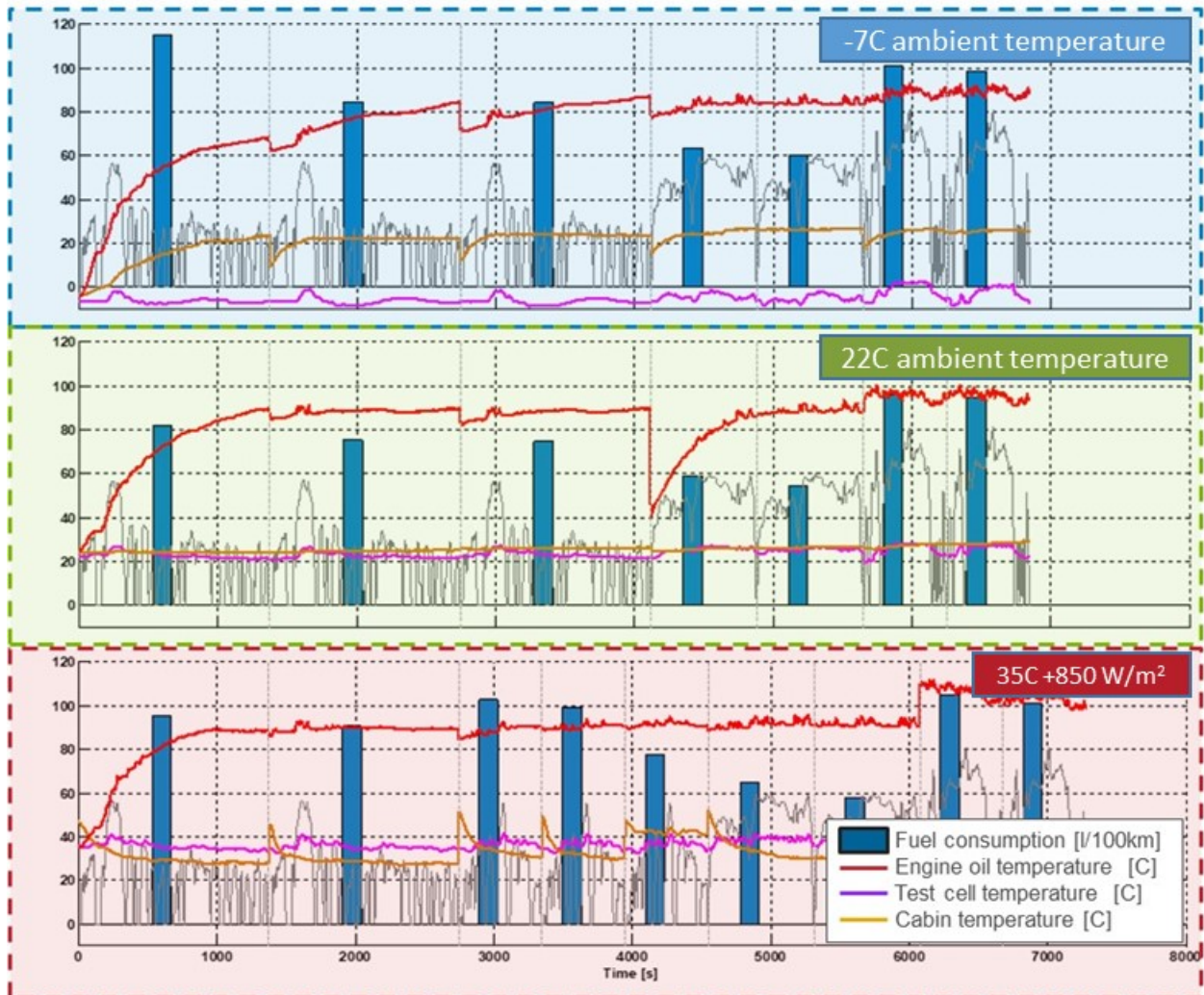


Figure 17. Powertrain and cabin temperature profiles at different temperatures

The engine oil temperature is representative of the powertrain temperature. For the $22^{\circ}\text{C}/35^{\circ}\text{C}$ ambient temperature conditions the final engine oil temperature for the US06 cycle was about 100°C , while for the -7°C test was $\sim 90^{\circ}\text{C}$. In past testing of light-duty vehicles, Argonne has observed that in a number of these vehicles the average powertrain temperatures in the -7°C test never rise to the average powertrain temperatures at 22°C . The QX50 engine has an

electronically controlled thermostat as well as an electric water pump, which enable high engine temperatures even at cold temperatures.

4.4. Steady-State Speed Fuel Economy and Efficiency

One characterization test was the steady-state speed drive cycle, which holds vehicle speed for one minute at speeds from 10 to 80 mph in increments of 10 mph. The vehicle is first accelerated to constant steady state speeds, held at that speed for 30 seconds, followed by decelerations through the speed set points down to idle. This is done three times, each time at a different grade: 0, 3%, and 6%. The speed profile is shown in Figure 18. From this test, fuel economy results as well as some vehicle efficiency characterization parameters are calculated.

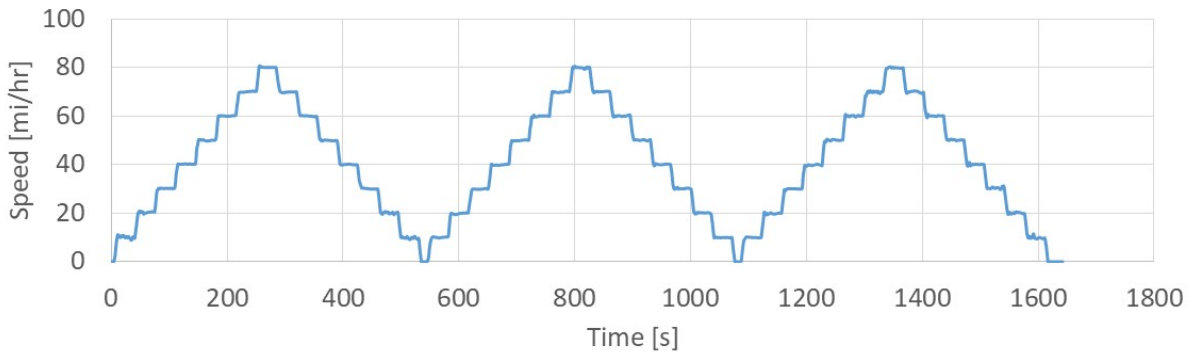


Figure 18. Steady-state stair-step speed profile at 0, 3, and 6% grades.

Results from the three grades are presented in Figure 19 through Figure 21. The hood remained closed during testing with the variable speed fan matching the driven vehicle speed. For each steady-state speed, the vehicle efficiency, the power required at the wheel, and the engine speed were calculated.

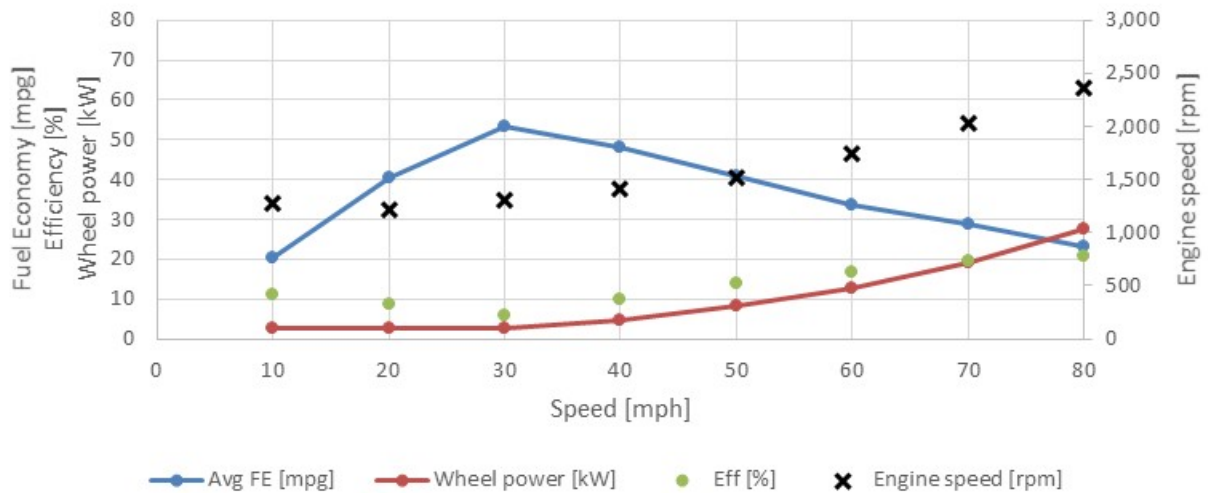


Figure 19. Steady-state speed operation at 22 °C and 0% grade

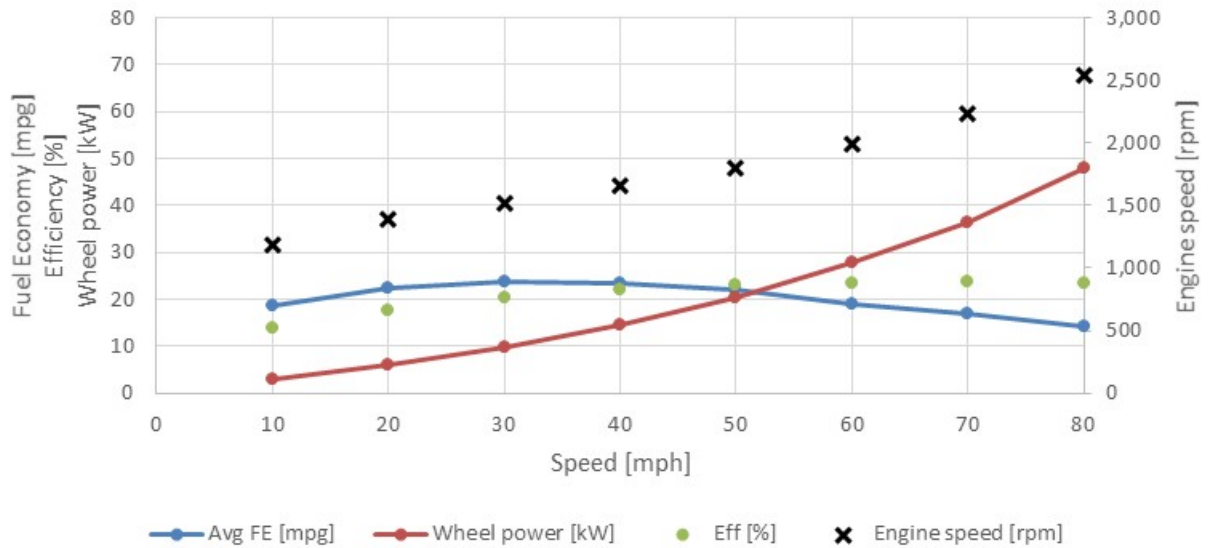


Figure 20. Steady-state speed operation at 22°C and 3% grade

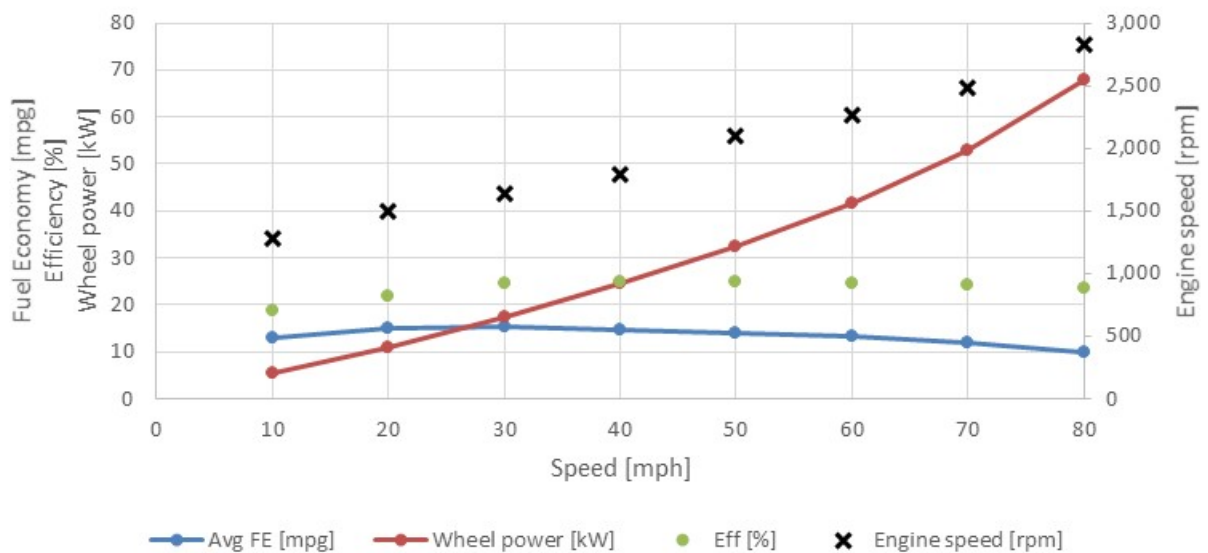


Figure 21. Steady-state speed operation at 22°C and 6% grade

The highest fuel economy at each of the grades was realized at a vehicle speed of 30 mph. Below 30 mph, low vehicle efficiency results in reduced fuel economy for all grades, whereas required wheel power remains low. This behavior may be explained due to low load conditions for throttled gasoline engines reducing efficiency due to throttling pumping losses. At higher loads, pumping losses decrease with increasing throttle openings. For the 3 and 6% grade tests, vehicle efficiency increased up to approximately 50 mph as vehicle speed increased; beyond that the efficiency flattened. The additional wheel power required offset any improvements to efficiency, reducing overall fuel economy. Engine speed increased as the vehicle speed increased from 1,250 to 2,500 rpm for the 3% test, and 1,300 to 2,750 RPM for the 6% grade test. Engine speed changes for the 0% grade test was slightly lower than the 3% grade test.

4.5. Passing Maneuver Results and General Operation

In order to develop an understanding of vehicle performance when a high transient response is requested, such as when overtaking on a highway, Argonne has developed a test to simulate these events on a chassis dynamometer. This passing maneuver drive cycle includes accelerations from 35 to 55 mph, 55 to 65 mph, 35 to 75 mph, and 55 to 80 mph. In addition, to determine vehicle operation at higher loads, such as on an incline, this test is repeated at dynamometer grade settings of 0%, 3%, and 6%. For each passing maneuver, the vehicle is held at an initial steady-state speed; then the driver applies 100% accelerator pedal until the vehicle passes the desired end speed. Table 10 summarizes the time it took the QX50 to complete each event using Tier 2 fuel.

Table 10. Time duration for acceleration events (seconds)

Acceleration	0% Grade	3% Grade	6% Grade
35-55 mph	4.0	4.2	3.9
55-65 mph	2.1	2.2	2.5
35-70 mph	6.6	6.7	7.3
55 80 mph	5.5	5.7	7.8

A plot of the powertrain details for the passing maneuver from 55 to 80 mph is shown in Figure 22. Immediately upon 100% pedal application, the engine transitions into the lowest compression ratio (8.0:1), while engine boost builds up to the maximum pressure of 19 PSI (1.3 bar). During the building of engine boost, the engine transitions solely to DI, followed by a transition to a blend of PFI/DI operation once peak boost is achieved. Engine speed steadily builds as the transmission remains at a fixed ratio between speeds of 55 and 70 mph. The transmission then smoothly transitions above this speed to meet the requirements of vehicle speed.

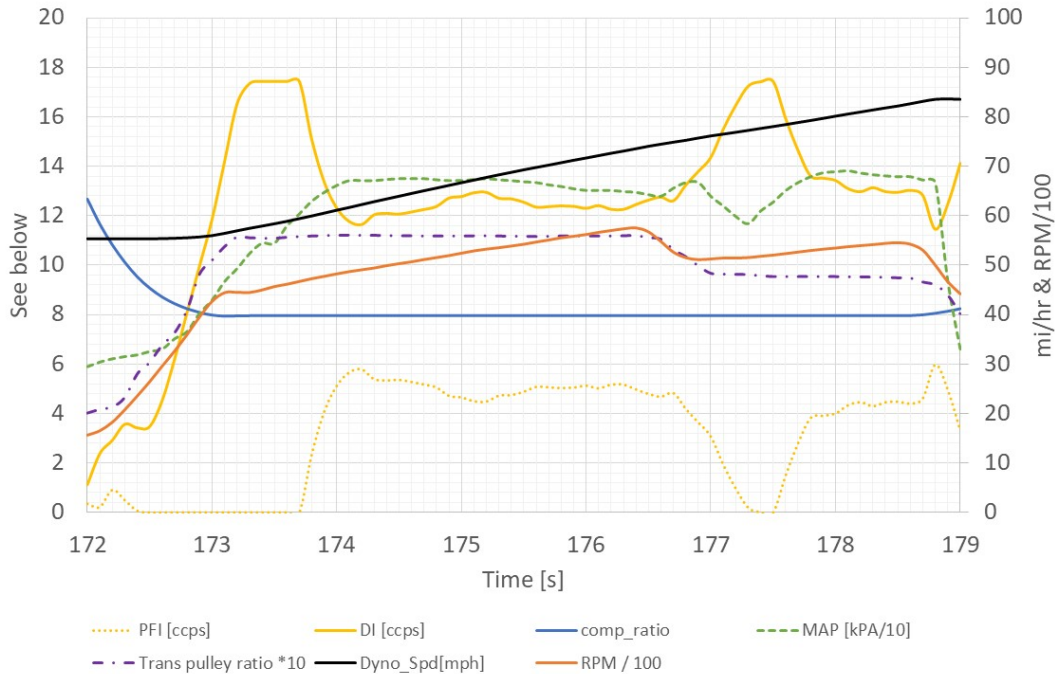


Figure 22. Powertrain operation during the 55- to 80-mph passing maneuver

4.6. Operation Over Maximum Acceleration

Maximum acceleration performance tests were performed on the chassis dynamometer. The test is performed from a rolling start to reduce slip between the tire and the steel roll. The throttle is rapidly depressed to 100% and the vehicle accelerates to 90 mi/hr at which point the throttle is set to zero and the vehicle coasts to a standstill. The two graphs in Figure 23 show the details of powertrain operation during the maximum acceleration test. The DI fuel system is largely used during the acceleration phase with PFI assistance occurring during transmission upshifts. No down-shift are observed during decelerations. The torque convertor signal exhibits the maximum noted slip value of 125 rpm during the onset of the acceleration, which then tapers out above speeds of 40 mph. During maximum acceleration events, the compression ratio reduces to 8.0:1, while engine boost maximizes pressure in a manner similar to that in the passing maneuver (Figure 22). The engine speed reaches a maximum of approximately 5,700 rpm between the simulated shifts.

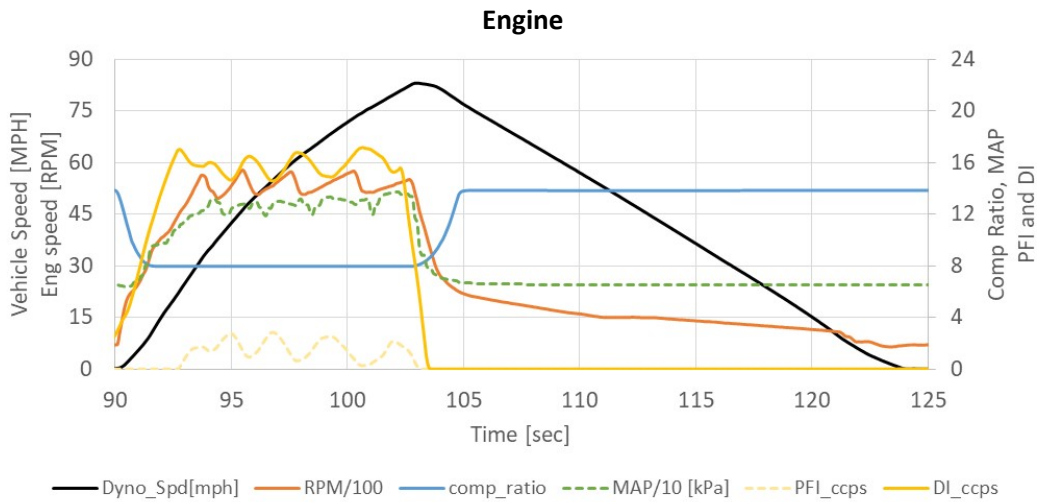
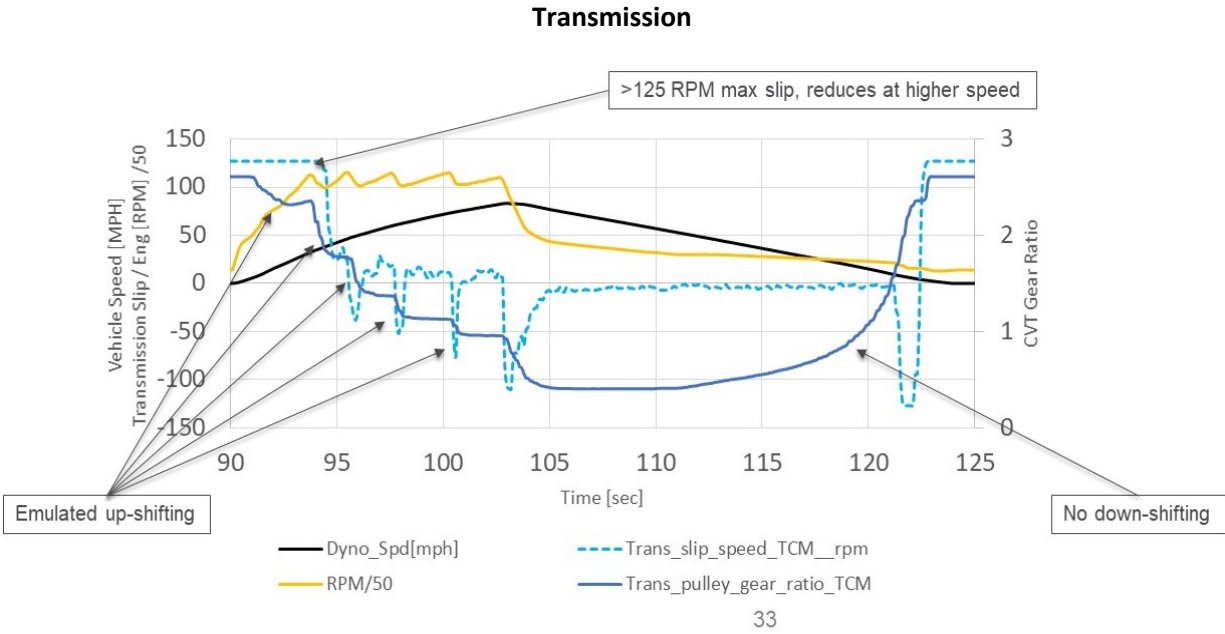


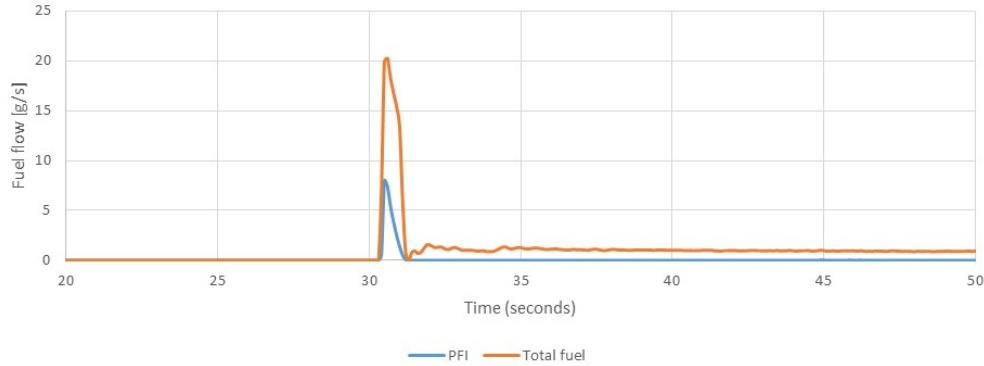
Figure 23. Powertrain operation during maximum acceleration

4.7. Results of Idle Fuel Flow Rate Test

A 30-minute engine idle test in cold start conditions was performed with the transmission in park, following an overnight soak at the test temperature of 22 °C. This test is designed to characterize engine behavior and fuel flow rate as the powertrain warms up at idle. The vehicle was soaked overnight for no less than 12 hours at ambient test cell temperature, started and left at idle for 30 minutes (at which point engine oil operational temperature of 90 °C has been reached). For this analysis, particular attention is paid to the VCR and injection strategies. Figure 24 shows the first 240 sec of the cold-start engine idle test. Following engine start, engine speed increased to more than 1,700 rpm before settling to approximately 1,450 rpm. The ignition was retarded to help with the warm-up of the exhaust-after-treatment system. The engine starts at a compression ratio of 9.0:1 and then transitions to 14.0:1 once the engine coolant reaches 60 °C. During engine start the engine uses a mix of PFI and DI, quickly transitioning to DI only. The fuel injection pressure remains high (15 MPa) until the coolant temperature reaches 40 °C. Once this

temperature is reached, injection pressure reduces to 6 MPa and the retarded ignition timing advances to normal operating timing. Beyond the 240 seconds shown, no additional changes were observed from 240 seconds until completion of the idle test at 30 minutes.

PFI to DI Transition



Engine Start Idle Details

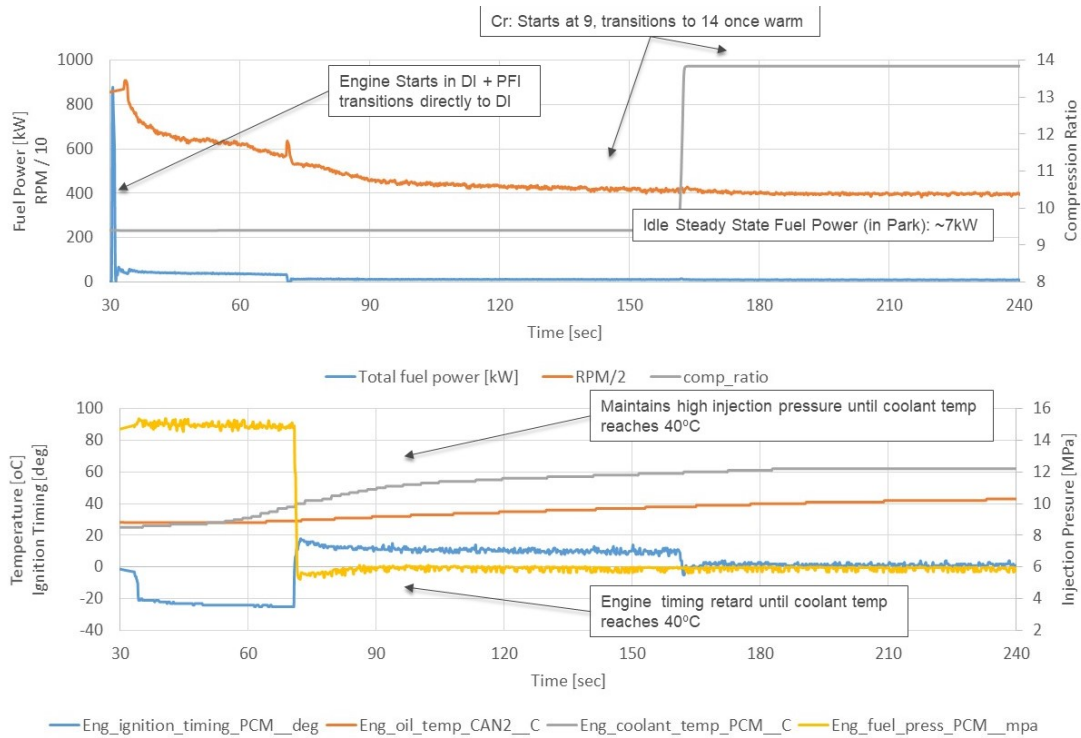


Figure 24. PFI to DI transition and initial 240 sec of the idle fuel flow test. Fuel power is the fuel flow rate multiplied by the fuel lower heating value

4.8. Details of VCR Engine Operation

Data from the test cycles was used to determine operation of the VCR mechanism to gain an understanding of the engine speeds/loads in which higher and lower compression ratios were used. To determine the real-time compression ratio, the VCR_angle_actual_CAN5_deg CAN signal was used to infer compression ratio changes. The VCR angle is the actuator that rotates the first link to the connecting rod/crankshaft junction, thereby changing the compression ratio. Detailed engine measurements were completed to determine the kinematic relationship between the electric motor CAN signal and the physical change in compression height of the piston. These kinematics were validated against literature data of the change in stroke and compression ratio of the engine.

All tests were performed with the dynamometer operating in 4WD mode, with a closed hood and a vehicle speed-match fan at an ambient test temperature of 22 °C to best simulate real world conditions. Analysis focused on the data in which the vehicle powertrain was at warm operational temperature to avoid transient thermal operation affecting results. Hot start UDDS, HWFET, US06, and maximum acceleration cycles were used for the analysis.

The maximum rate of compression ratio change during the US06 and 0–80 mph WOT cycles was analyzed. For positive tractive force, the maximum observed compression ratio change over the US06 cycles was 6 compression ratio units/sec. For negative tractive force (deceleration), the maximum compression ratio change was also 6 units/sec. For the WOT cycle test, the maximum rate of change was just over 6 units/sec., exhibiting results identical to those of the US06 analysis, the results of which are shown in Figure 25. In this figure both the absolute compression ratio and rate of change may be viewed. From these results it may be seen that the compression ratio may change from its lowest to highest compression ratio, and vice versa, in 1 sec.

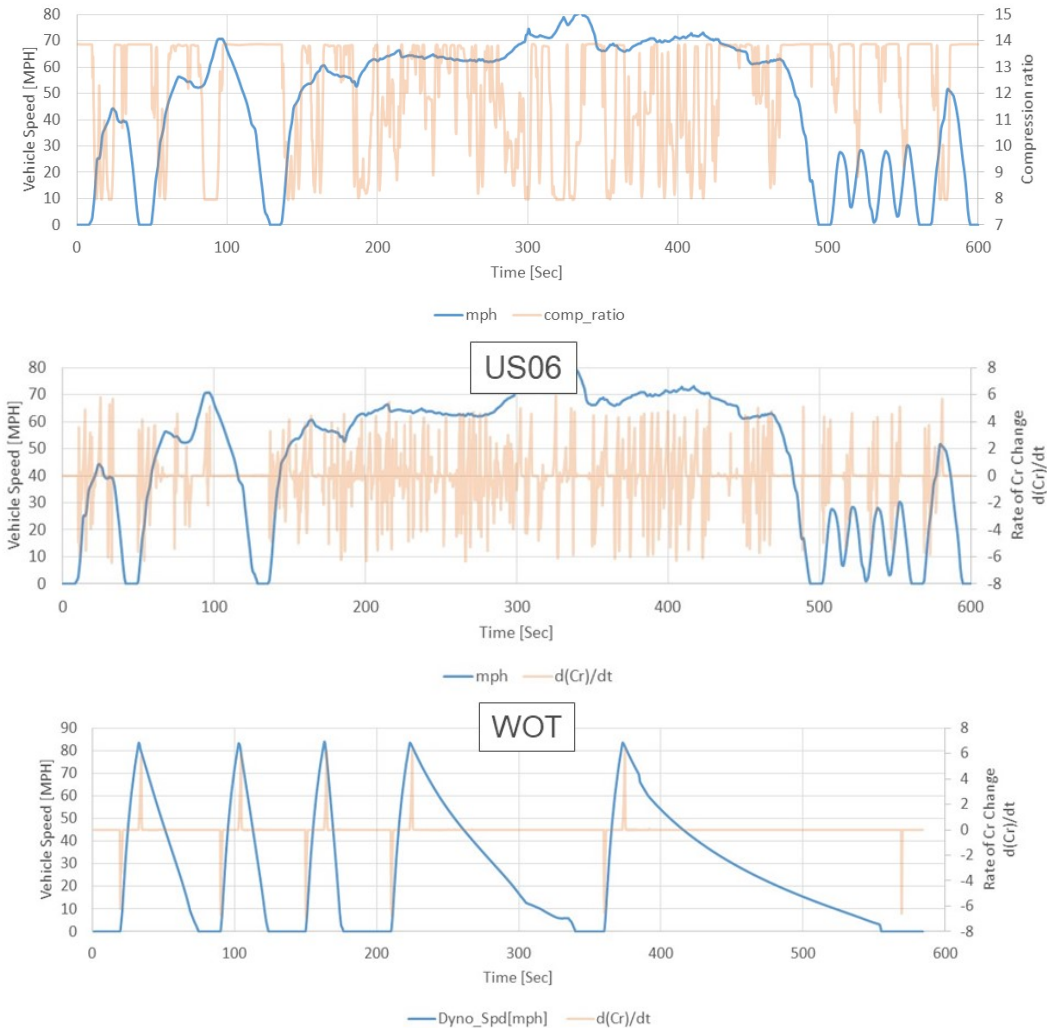
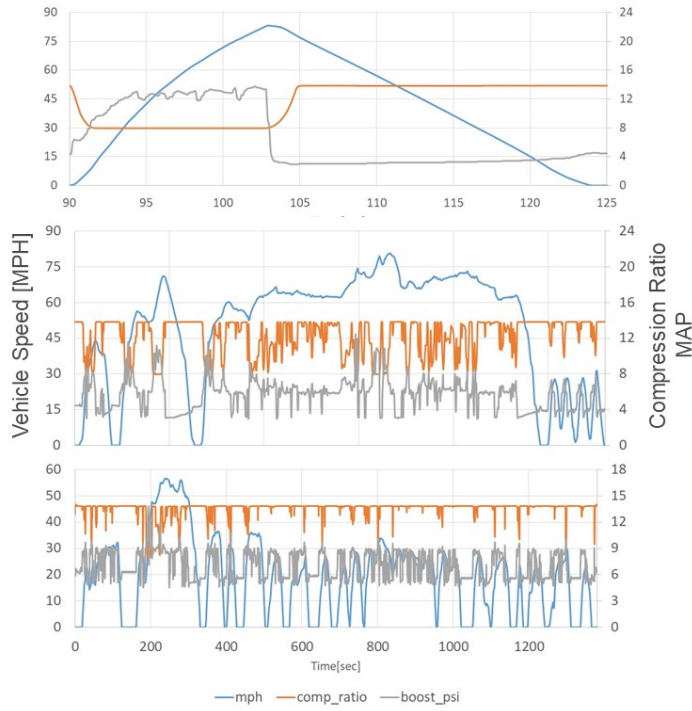


Figure 25. Infiniti VCR compression ratio and rate of change for 25°C hot start, US06, and 0–80 mph maximum effort cycles

Figure 26 summarizes the observed operation of the engine VCR system relative to maximum effort acceleration, the high-load US06, and the light-load UDDS drive cycles. During maximum effort, the compression ratio drops to the lowest level (8.0:1) and boost increases to the maximum level of 19 psi. This is done to maximize engine power while reducing knock. For the high-loaded US06 cycle, the compression ratio occasionally drops to 8.0:1. During the low-loaded cycles (i.e., UDDS), engine strategies center around maximizing high compression ratios and minimizing boost. During acceleration the compression ratio drops, yet the loading is low enough that it rarely drops below 12.0:1, thereby maintaining higher ratios and thermal efficiency.



Acceleration

- Transitions to lowest Cr
- Boost increases as Cr lowers
- Returns to highest Cr for engine decelerations

US06

- Highest loaded cycle uses lower average Cr
- Cr reduces for high acceleration rates

UDDS

- Highest overall use of high Cr
- Low loaded cycle enables higher Cr use

Figure 26. Infiniti VCR operational overview for 25°C hot start UDDS, HWFET, and US06 cycles

Figure 27 exhibits the engine thermal efficiency for the UDDS, HWFET, and US06 cycles. Included in these figures are the engine operational points. The engine operates largely in the 30+% engine efficient regions of the operating map for all cycles. Table 11 summarizes the engine thermal efficiency relative to the compression ratio using the combined data of the UDDS, HWFET, and US06 cycles shown in Figure 27. The results shown are calculated from the positive tractive force portions of the cycles only; the thermal efficiency ranges from 31% at 8.0:1 to 36% at 14.0:1.

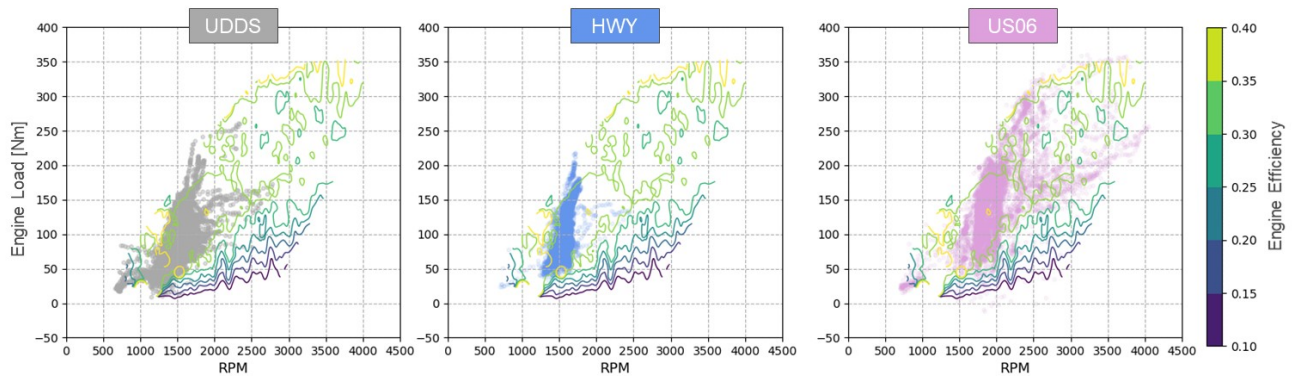


Figure 27. Infiniti VCR operational overview of positive tractive force for 25°C hot start UDDS, HWFET, and US06 cycles

Table 11. Aggregate engine thermal efficiency for UDDS, HWFET, and US06 cycles relative to VCRs

Range of VCR	Aggregate Engine Efficiency	Efficiency Gain over Baseline, Cr = 8
Between 8 and 9	32.5%	(baseline)
Between 9 and 10	34.3%	5.5%
Between 10 and 11	35.8%	10.2%
Between 11 and 12	36.6%	12.6%
Between 12 and 13	36.5%	12.3%
Between 13 and 14	35.8%	10.2%

Figure 28 summarizes the VCR and engine manifold pressure as a function of the speed/load operating range. Data for these figures were collected from hot start UDDS, HWFET, and US06 cycles only. These figures can be contrasted with those in Figure 27 to show the engine operational points for each type of cycle. Analysis shows that the engine operates at high compression ratios (>12.0:1) for engine torques below a range of 150–200 Nm, exhibiting an increase in allowable compression ratio relative to higher engine speeds (higher engine speeds reduce volumetric efficiency and knock propensity, thereby allowing the higher compression ratio). Boost levels remain relatively low (below atmospheric pressure) until the engine load is greater than 275 Nm. Similar to the compression ratio, there is a secondary effect of engine speed allowing higher boost at higher speeds. Figure 28 contrasts the engine compression ratio

usage, and Figure 30 summarizes the engine boost via histograms for the hot start UDDS, HWFET, and US06 cycles.

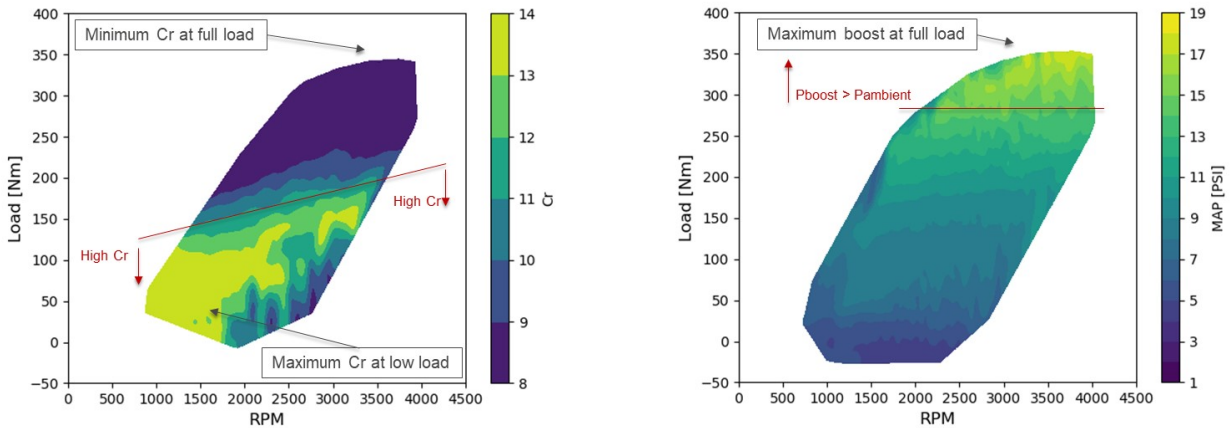


Figure 28. Infiniti VCR and boost operational map for 25°C hot start UDDS, HWFET, and US06 cycles

Figure 29 shows that the engine operates at very high percentages at a compression ratio of 14.0:1 for the UDDS and HWFET cycles. The system is able to take advantage of the relatively low loading of these cycles and maximize thermal efficiency, with the UDDS cycle exhibiting 89% and the HWFET cycle exhibiting 71% maximum compression ratio usage. Including all compression ratio usage, the UDDS cycle exhibits an average compression ratio of 13.6:1 and the HWFET, 13.2:1. Because of the higher loading of the US06 cycle, maximum compression ratio usage is 61% with an average compression ratio of the entire cycle of 12.2:1.

	UDDS	HWY	US06
Mean	13.6	13.2	12.2
Median	13.8	13.8	13.4
Range	6.0	6.0	5.9
Minimum	8.0	8.0	8.0
Maximum	14.0	14.0	13.9

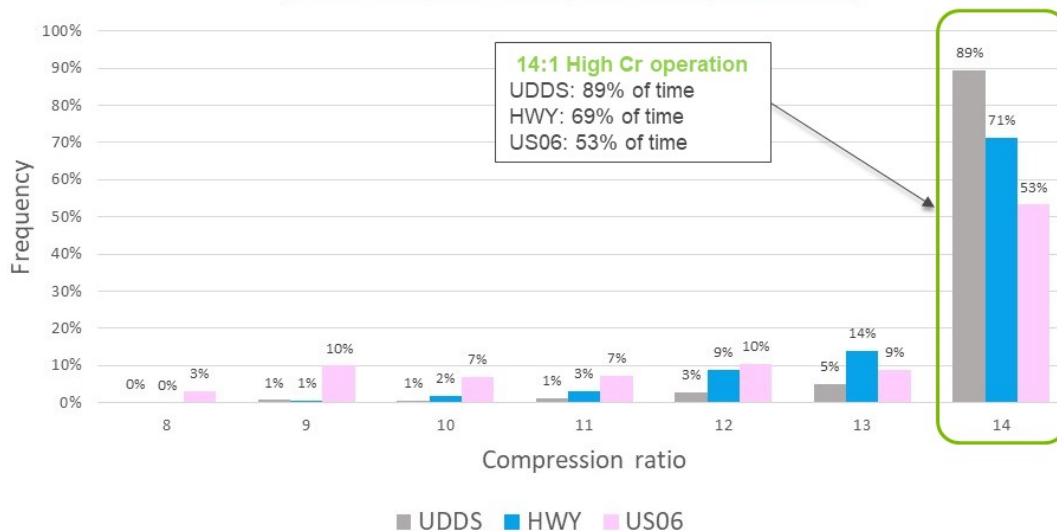


Figure 29. Infiniti VCR histogram overview of positive tractive force for 25°C hot start UDDS, HWFET, and US06 cycles

Figure 30 contrasts the engine manifold pressures for the hot start UDDS, HWFET, and US06 cycles. Because of the relatively low loading of the cycles, manifold pressure above atmospheric (101 kPa) are almost never realized, with the UDDS and US06 being the only cycles in which pressure boost levels were recorded (less than 5% of the cycle time for the US06 and less for the UDDS). The average manifold pressure for the cycles was in a relatively narrow band of 48-47 kPa (gauge). As shown in Figure 27, the engine load for the cycles was rarely more than 200 Nm; therefore, high boost levels remain low while compression ratio is maximized for efficiency.

	UDDS	HWY	US06
Mean	48.6	56.8	57.0
Median	47.1	59.7	59.7
Range	72.9	53.9	99.0
Minimum	29.6	30.4	28.9
Maximum	102.5	84.3	127.9

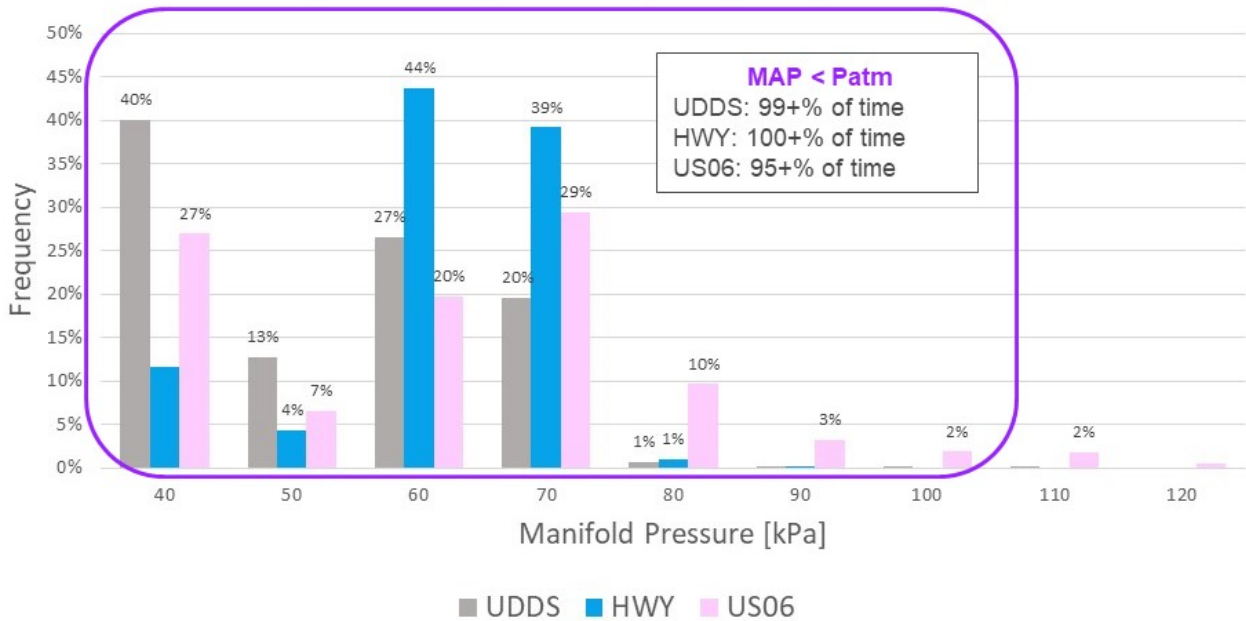


Figure 30. Engine MAP histogram overview of positive tractive force for 25°C hot start UDDS, HWFET, and US06 cycles

Figure 31 shows the engine spark advance for the hot start UDDS, HWFET, and US06 cycles. In general, engine spark advances with increasing engine speed approaching 40 degrees at lower loads and 20 degrees at higher loads.

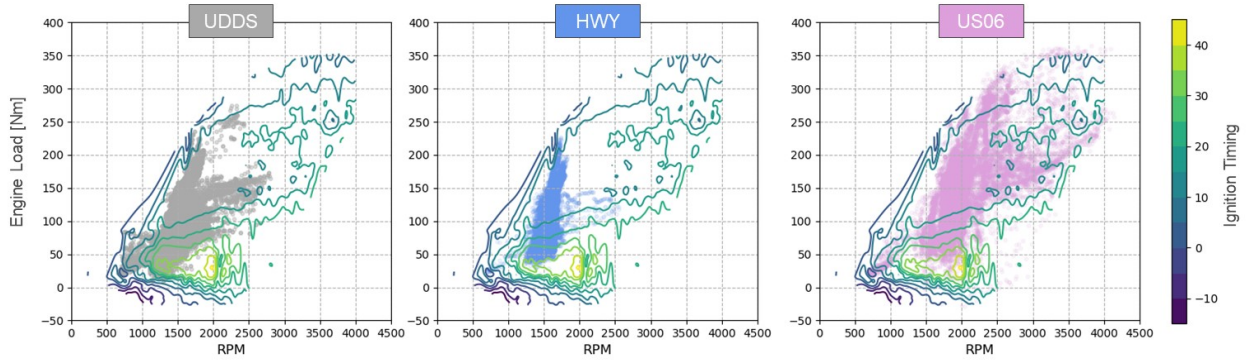


Figure 31. Comparison of ignition timing spark advance for UDDS, HWFET, and US06 cycles

Figure 32 presents the percentage usage of DI over the UDDS, HWFET, and US06 cycles. The VCR engine relies heavily on DI use with PFI blended use occurring mostly in moderate speeds and loads (1,500 rpm, 100 Nm of load). For high- and full-load operation, the engine operates almost exclusively on DI.

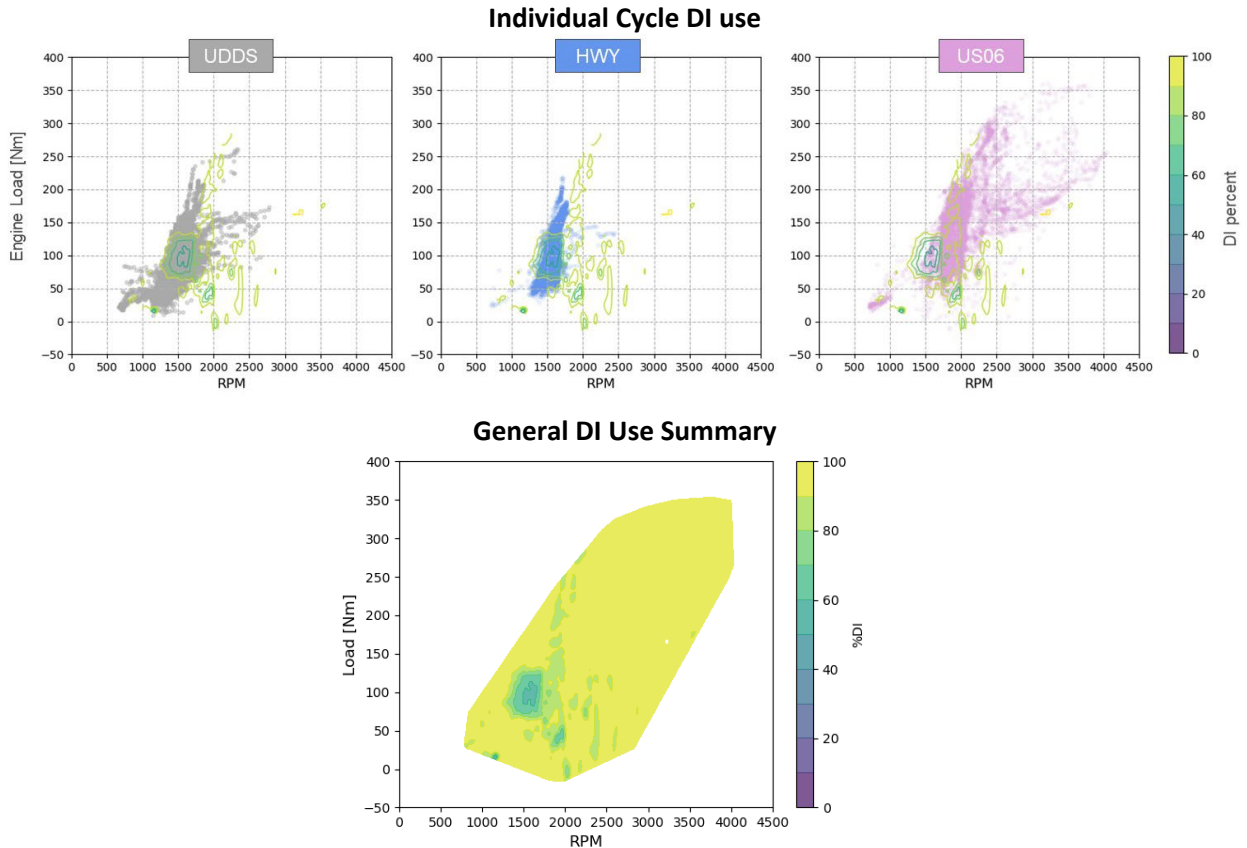


Figure 32. Comparison of percentage DI operation for UDDS, HWFET, and US06 cycles. Additional figure generalizes regions of DI operation.

5. Component and Control Analysis

This section describes the vehicle component controls, including transmission shifting, torque converter lockup, engine fuel cutoff, and detailed component control concepts. Models and control calibrations developed through this analysis have been implemented in Autonomie.

5.1. Signal Calculations for Control Analysis

The vehicle component control analysis is conducted using Autonomie “Import Test Data” process. This process automatically changes signal names and test data units to match Autonomie nomenclature based on pre-defined conversion methods. During the test data import process, additional parameters required to analyze the component operating conditions are calculated from the test data. In Figure 33 the signals labeled in black, blue, and green are obtained directly from the test. At the energy management strategy level, the signals used to calculate the engine and battery power are critical, and directly obtained from the test. While not all signals can be recorded during testing, some can be easily calculated from the measured ones. For example, the output torque and speed of the transmission were calculated by the dyno force and speed. Transmission input signals are calculated by engine torque and speed, using assumptions of the torque converter efficiency map used in FRM (final rulemaking) study [5]. Techniques used in the process will be described in the following section.

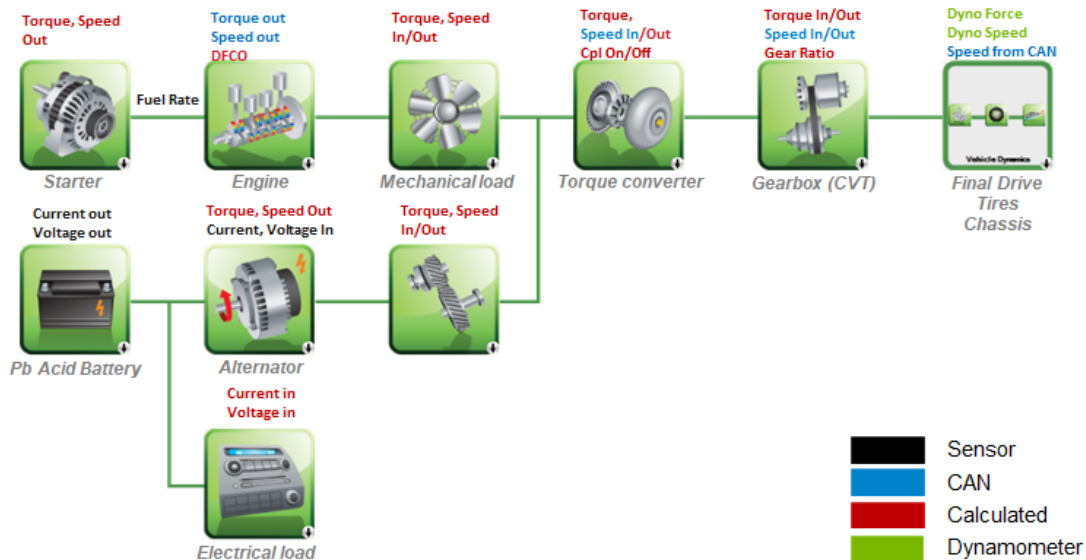


Figure 33. Schematic of the vehicle configuration

Since not all signals can be recorded, additional ones are calculated based on measured ones and additional information obtained by external source [1]. First, the time-based rotating speed and torque of each component is calculated as shown in Figure 34.

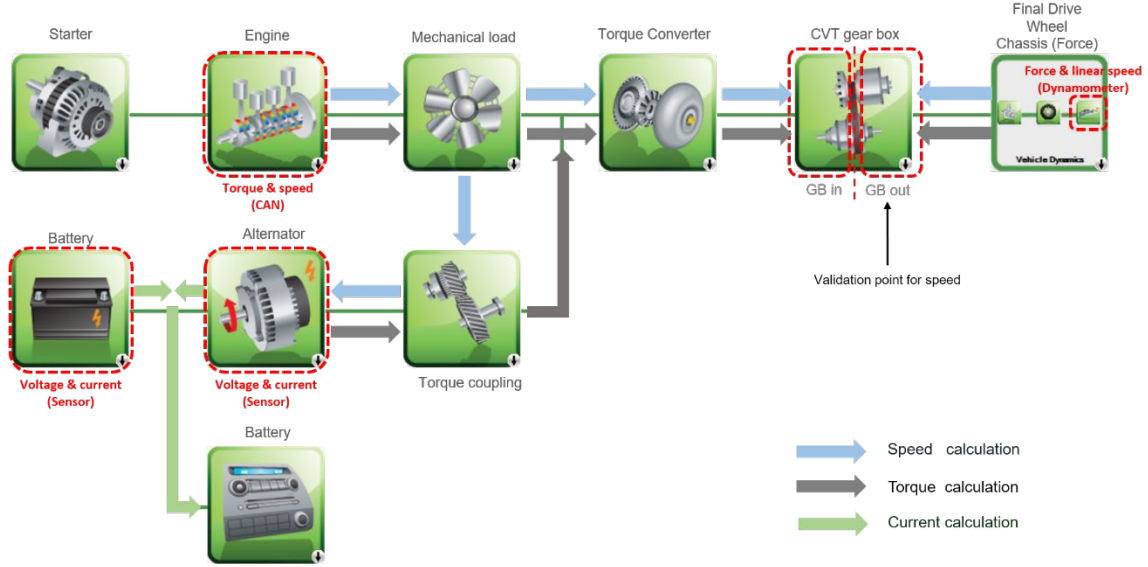


Figure 34. Calculation of missing signals for components

The wheel speed can be calculated from the speed signal, which is obtained from the dynamometer:

$$\omega_{gb,out} = \gamma_{fd} \frac{1}{r_t} v_{chassis}$$

Equation 1

where r_t is the tire radius and γ_{fd} is the final drive ratio. Because the exact tire radius in driving conditions is unknown, the speeds can be validated by comparing the two values of $\omega_{gb,out}$ and $v_{chassis}$ by adjusting the tire radius. While there may be no discrepancy in speed for the wheel and chassis, the torque calculations should be carefully handled because each component torque measurements include uncertainties.

Figure 34 shows the flow of the calculation for torque signals. Since an accurate transmission efficiency map is not available, the torque calculation process is divided into two parts—from the transmission output to the wheel and from the engine to the transmission input. The output torque of the final drive is calculated from the force obtained from the dynamometer:

$$T_{fd,out} = T_{wheel,out} + T_{wheel,loss} - T_{wheel,brake} = r_t \times F_{chassis} + T_{wheel,loss} - T_{wheel,brake}$$

Equation 2

The output torque of the gearbox is calculated from $T_{fd,out}$, which can be expressed as

$$T_{gb,out} = T_{fd,in} = \frac{1}{\eta_{fd}^k} \times \frac{1}{\gamma_{fd}} \times T_{fd,out}$$

Equation 3

where η_{fd} is the transfer coefficient of the final drive, and k is 1 if the power flows from the final drive to the wheel or -1 if the power flows in the other direction. These values are generic and are applied to following calculations in this report:

$$k = \begin{cases} 1 & \text{if power flows from power sources to the wheel} \\ -1 & \text{if power flows from wheel to power sources} \end{cases}$$

Equation 4

The torque converter input torque is calculated from the mechanical accessory load torque and the torque-coupling torque.

$$T_{acc_{mech}} = T_{eng} - P_{acc_{mech}} \div \omega_{eng}$$

Equation 5

$$T_{TC,in} = T_{acc_{mech}} + T_{trq_{cpl,out}}$$

Equation 6

where $P_{acc_{mech}}$ is the mechanical accessory power the system needs.

The transmission input torque is calculated from the torque converter torque input and the torque converter characteristics. The speed ratio can be calculated from CAN signals for transmission input and engine output speed:

$$T_{gb,in} = T_{TC,out} = (T_{TC,in} - \dot{\omega}_{TC} \times J_{TC}) \times T_{ratio} [= f(\omega_{ratio})]$$

Equation 7

where T_{ratio} is the torque ratio of the torque converter, and ω_{ratio} is the speed ratio of turbine speed to impeller speed for the torque converter.

All the equations for torque calculation are based on static equilibrium. The parameter values used in the calculations are listed in Table 12.

Table 12. Parameter values used for calculating additional signals

Parameter	Value
Tire radius, r_t	0.3376 m
Gear ratio range of CVT	0.383 ~ 2.413
Gear ratio of the final drive, γ_{fd}	5.846
Vehicle test weight	1,928 kg

In addition to the signals introduced in this section, other signals representing efforts and flows are calculated based on reasonable assumptions [7].

5.2. Transmission Operation

The 2019 Infiniti QX50 has a CVT. The control algorithm in Autonomie used to select the CVT gear ratio relies on multiple parameters that need to be calibrated for each individual vehicle. The transmission operation was analyzed to estimate the control parameters to be used in Autonomie. The details of this analysis are explained in the subsequent sections.

5.2.1. Gear Ratio Control

To understand the choice of reduction ratio in CVT, we divided the infinite gear range into 55 sub-ratio segments. Figure 35 shows the time spent in each gear ratio segment for each cycle.

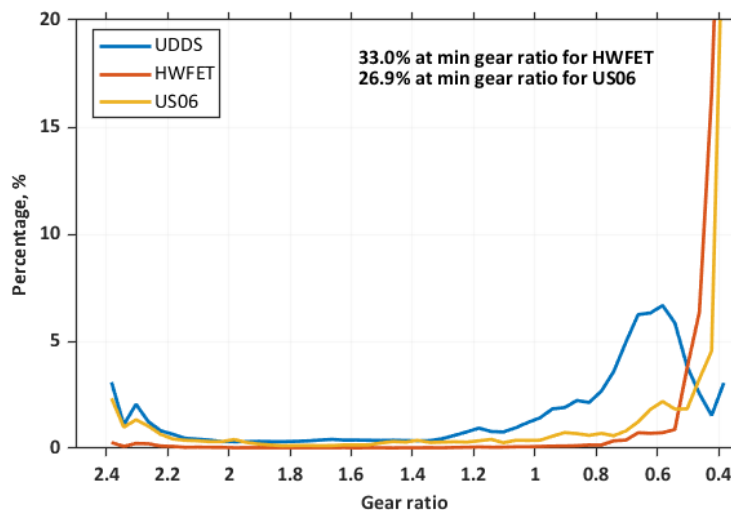


Figure 35. Time spent in each gear ratio segment for the UDDS, HWFET, and US06 cycles

The highest gear ratio (lowest gear range) is used more frequently in the UDDS cycle (about 3.5% of the time) than in the HWFET cycle (less than 1% of the time). In addition, the low gear ratios (highest gear range) are used more frequently (more than 50% of the time) in the high-speed drive cycle (HWFET & US06). However, the lowest gear ratio is not used much in the UDDS drive cycle, since it is running at a slightly higher ratio range than the lowest gear ratio.

Understanding the choice of ratio at various vehicle speeds and acceleration scenario is essential in developing an accurate CVT control.

5.2.2. Torque Converter Lockup Control

In order to determine the overall behavior of the torque converter lockup status, all operating points of the vehicle from all test data are shown in Figure 36 and Figure 37. The graphs show the clutch is locked up above a certain speed regardless of wheel torque. Figure 36 shows that the clutch is locked when the vehicle speed is about 8 mph or more. In particular, in the high-torque region of low vehicle speed, the torque converter is unlocked to use the torque-multiplying effect.

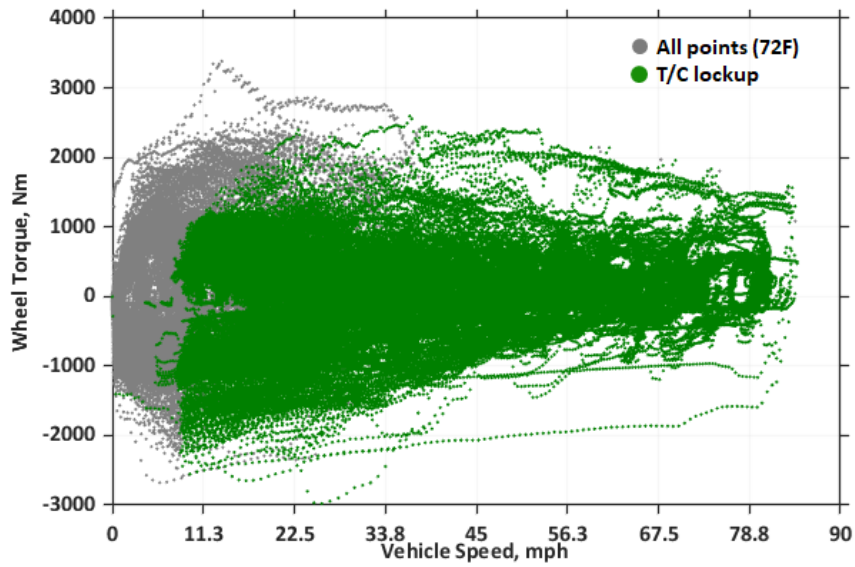


Figure 36. Torque converter lockup operation: wheel torque versus vehicle speed

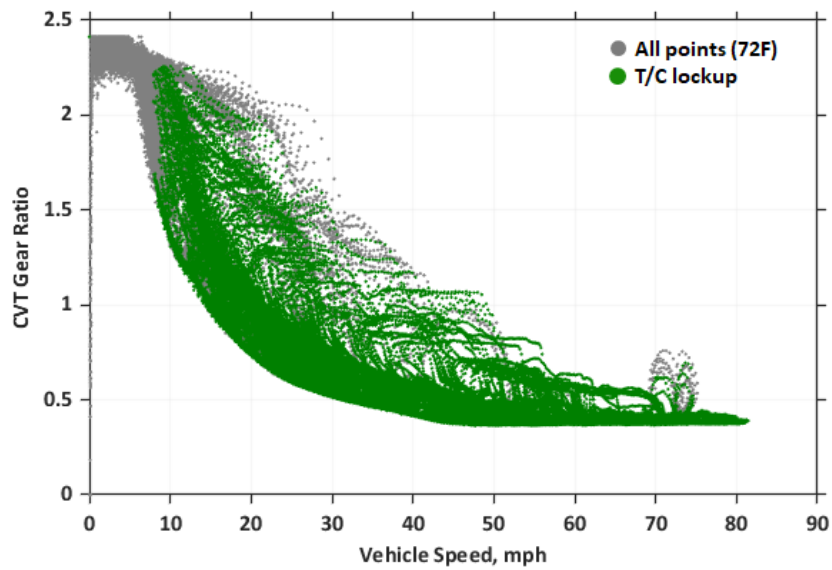


Figure 37. Torque converter lockup operation: vehicle speed versus CVT gear ratio

The percentage of torque converter lockup per cycle is summarized in Table 13. On the UDDS cycle, the torque converter is locked up at about 60%, but it can be locked up almost any time during high-speed driving.

Table 13. Percentage of time torque converter lockup in each cycle

Test Cycle	Time of Lockup
UDDS	68.04%
HWFET	98.40%
US06	81.57%
WLTP	69.10%
JC08	49.18%
California unified driving schedule (LA92)	63.84%

5.2.3. Lockup Variability

To analyze how torque converter lockup is controlled, the points at which the clutch is engaged and the points at which the clutch is released were analyzed.

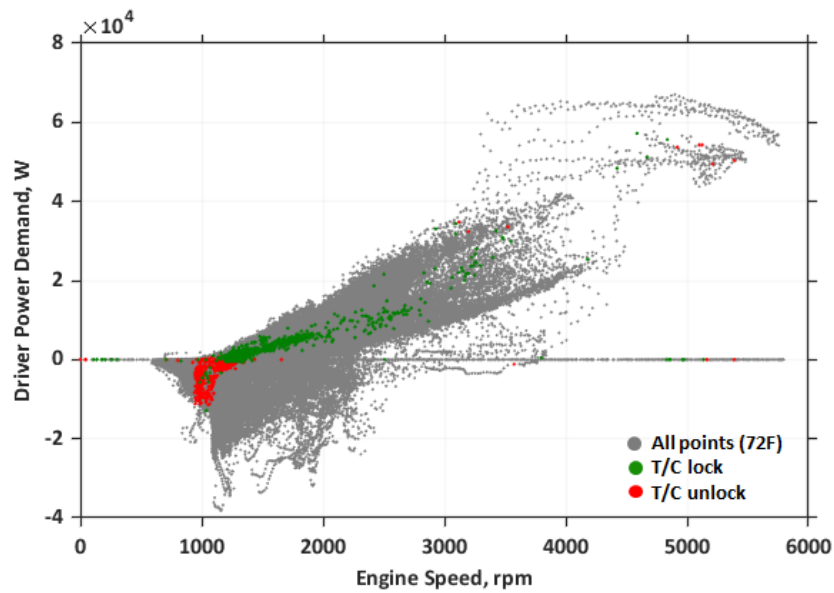


Figure 38. Torque converter operation points for clutch engaging versus disengaging

In Figure 38 the points at which the torque converter clutch is engaging are indicated in green, and the points at which the clutch is disengaging in red in the domain of engine speed and driver power demand. The points at which the clutch of the torque converter is engaged and disengaged are clearly visible in the form of lines. When the power demand increases, the clutch is engaged to minimize power loss from the torque converter.

5.3. Deceleration Fuel Cutoff

DFCO is a feature in many modern-day engine control units (ECUs) that detects whether the vehicle is coasting downhill and then cuts fuel to the engine and allows the wheels to keep the engine running. In this section, the DFCO enabling conditions will be determined in terms of vehicle speed, wheel torque requirement and engine coolant temperatures.

As shown in Figure 39, DFCO is active only when the wheel torque is negative.

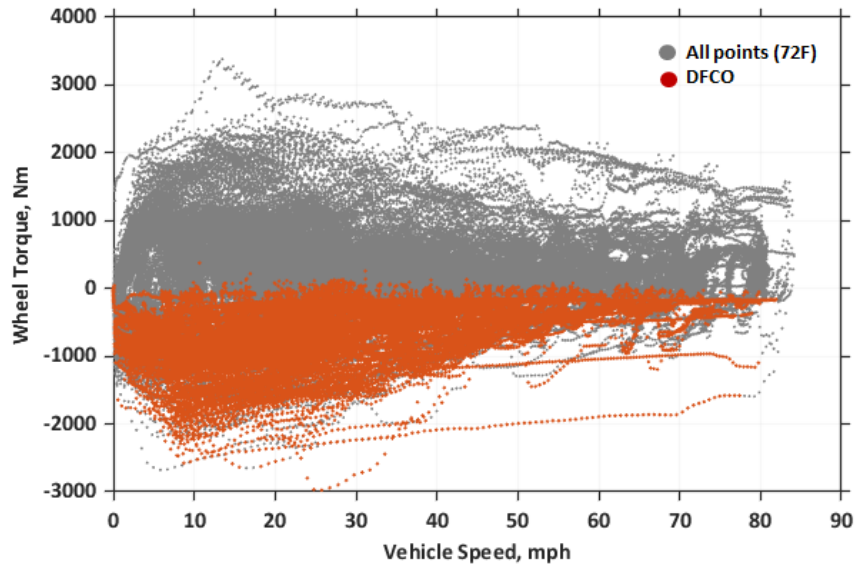


Figure 39. DFCO operation: Vehicle speed versus wheel torque

Figure 40 shows that DFCO does not activate below an engine coolant temperature of 60 °C.

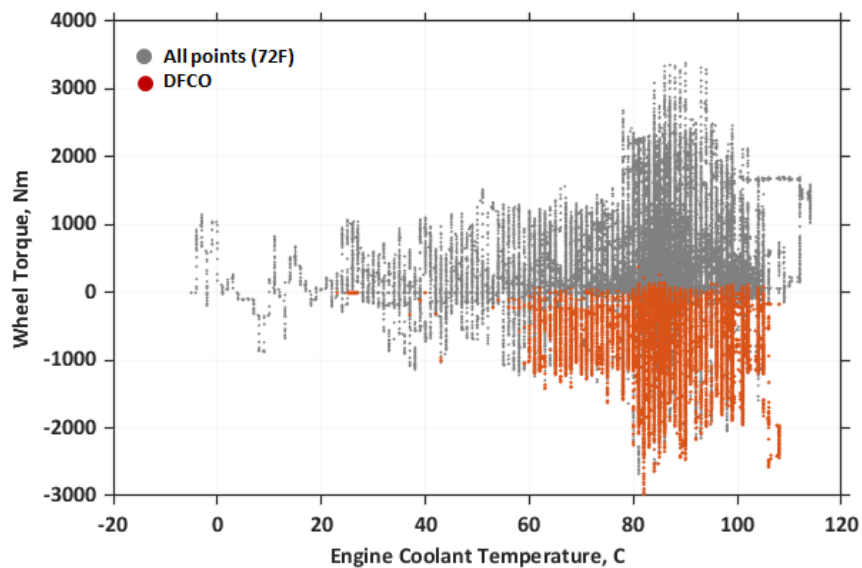


Figure 40. DFCO operation: Engine coolant temperature versus wheel torque

5.4. PFI versus DI Operation

The 2019 Infiniti QX50 is equipped with multi-injection mode (DI and PFI). In order to analyze how the injection mode of the engine is determined, we first checked the engine power points by engine coolant temperature. Figure 41 shows that fuel injection mode depends on the engine coolant temperature for all drive cycles at normal ambient temperature. When the initial engine is started cold, the fuel is injected only in DI mode until the coolant temperature becomes warm (about 60 °C). When the engine coolant temperature is above 60 °C, the fuel is injected in DI mode for the initial low power section and in PFI mode for the second lower power section, and only DI mode is performed in the higher power range. Figure 42 shows that the engine operates in PFI-only mode at above 1,300 rpm and low torque range, and the DI mode is used in the region of high speed and high torque of engine.

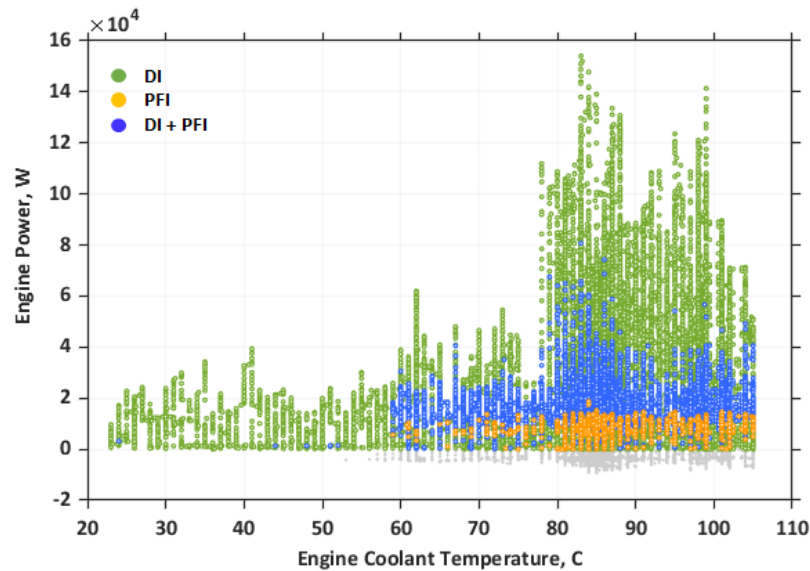


Figure 41. Operating behavior of the fuel injection mode according to engine coolant temperature

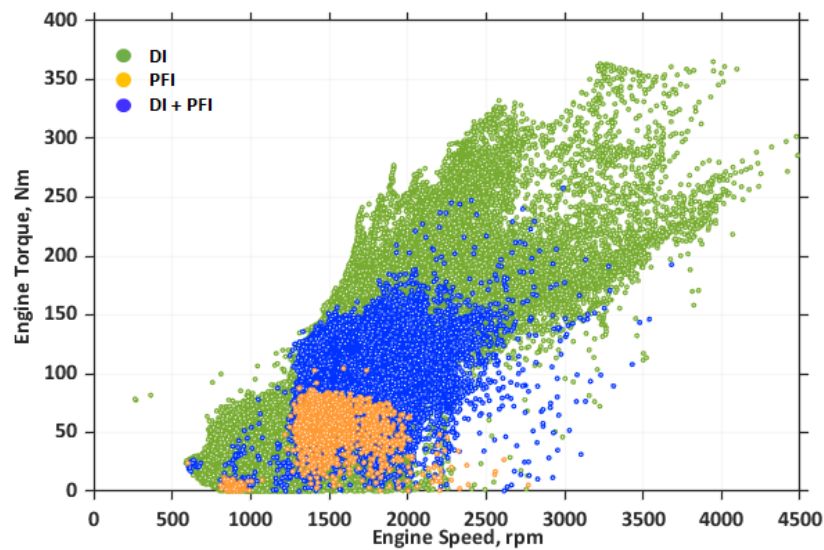


Figure 42. Operating behavior of the fuel injection mode according to engine speed

5.5. Engine Operation

5.5.1. Fuel Rate Map

The engine fuel rate map was generated based on the engine mapping test data, as shown in Figure 43. Since the components modeled in Autonomie were assumed to be in their warmed-up state, the fuel map is generated from test data where engine coolant temperature is above 60 °C. Figure 43 shows only the points at which the time derivative of the acceleration pedal is below 0.1/s and the engine coolant temperature is above 60 °C, by which it is assumed that the points are obtained under steady operating conditions.

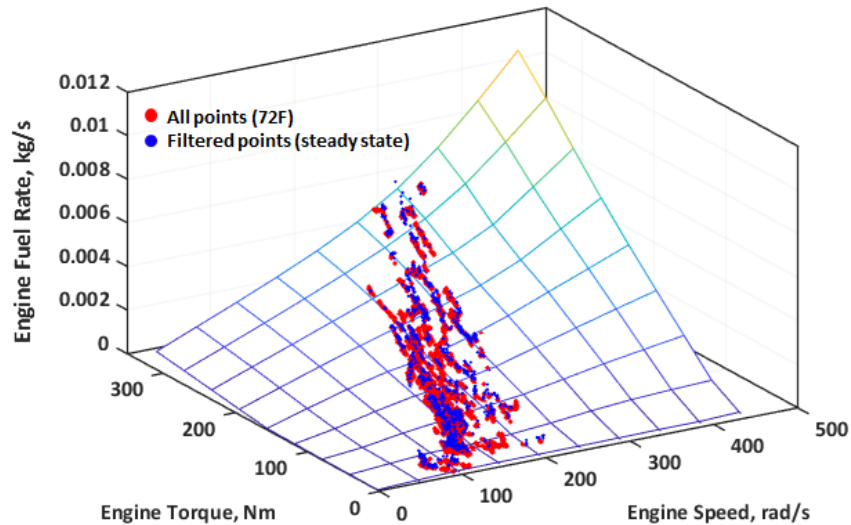


Figure 43. Engine fuel rate map according to engine speed and torque

5.5.2. Torque Pedal Map

The accelerator pedal is not a simple way of directly moving the throttles on the engine, because with an ECU, the traditional Bowden cable between the pedal and throttle is replaced with a pedal position sensor and a map. The torque pedal map does not depend on conditions like engine speed or transmission gear ratio. Instead, the engine throttle has a linear correlation in the middle of the accelerator pedal in positions 0.25 to 0.6. A given pedal position and a given engine speed generate an engine torque demand, which is fed to the ECU to deliver the required amount of torque. In the low accelerator pedal position, the engine throttle responds in a more gradual manner as shown in Figure 44.

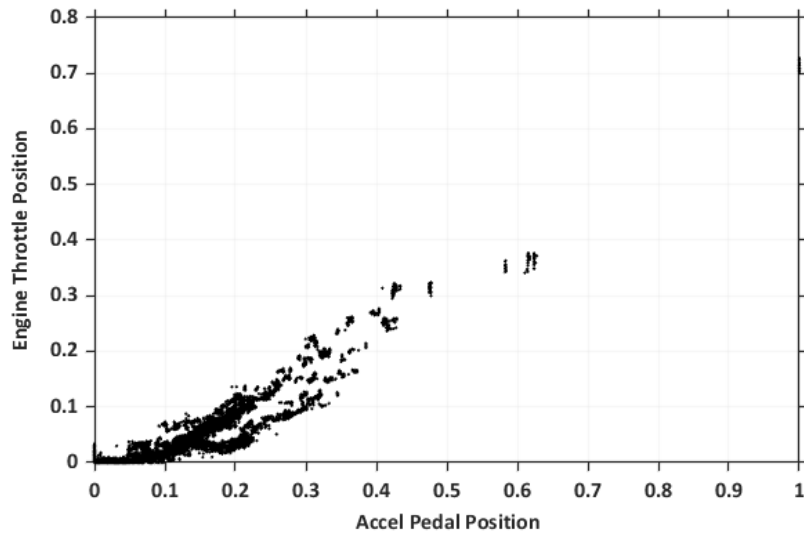


Figure 44. Torque pedal map

5.6. Thermal Management Impact on Vehicle Controls

In this section we will focus on additional vehicle controls and how they are affected by thermal conditions. The impact of thermal conditions on performance and on the vehicle control are important issues. The effect of thermal conditions on control behavior will be discussed first, followed by performance analysis in different thermal conditions.

5.6.1. Engine Operation Under Cold Conditions

Engine thermal management systems are designed to heat up the engine as soon as possible with advanced techniques. However, it is difficult to completely avoid operating the engine at a low temperature. While the engine has a cooling system when the engine temperature is too high, the coolant temperature can be increased — and the engine warmed up — only by the waste heat from combustion. In other words, the way to warm up the engine is to start the engine. Typically passenger cars do not use an electrical heater to warm up the engine itself.

Figure 45 shows three different control behaviors under different engine coolant temperatures.

- The engine operates normally and the coolant temperature is warm at start-up (hot start).
- When the coolant temperature is between 20 °C and 60 °C, the engine stays on higher speed than normal idle speed (of about 700 rpm) even if there is no power demand. This control behavior is specific to vehicle start-up, and the engine operates normally once the coolant temperature rises above approximately 60 °C.
- When the engine coolant is very low (below 0 °C) in cold ambient temperatures, the engine operates at an even higher speed until the engine coolant temperature warms up, as shown in Figure 45.

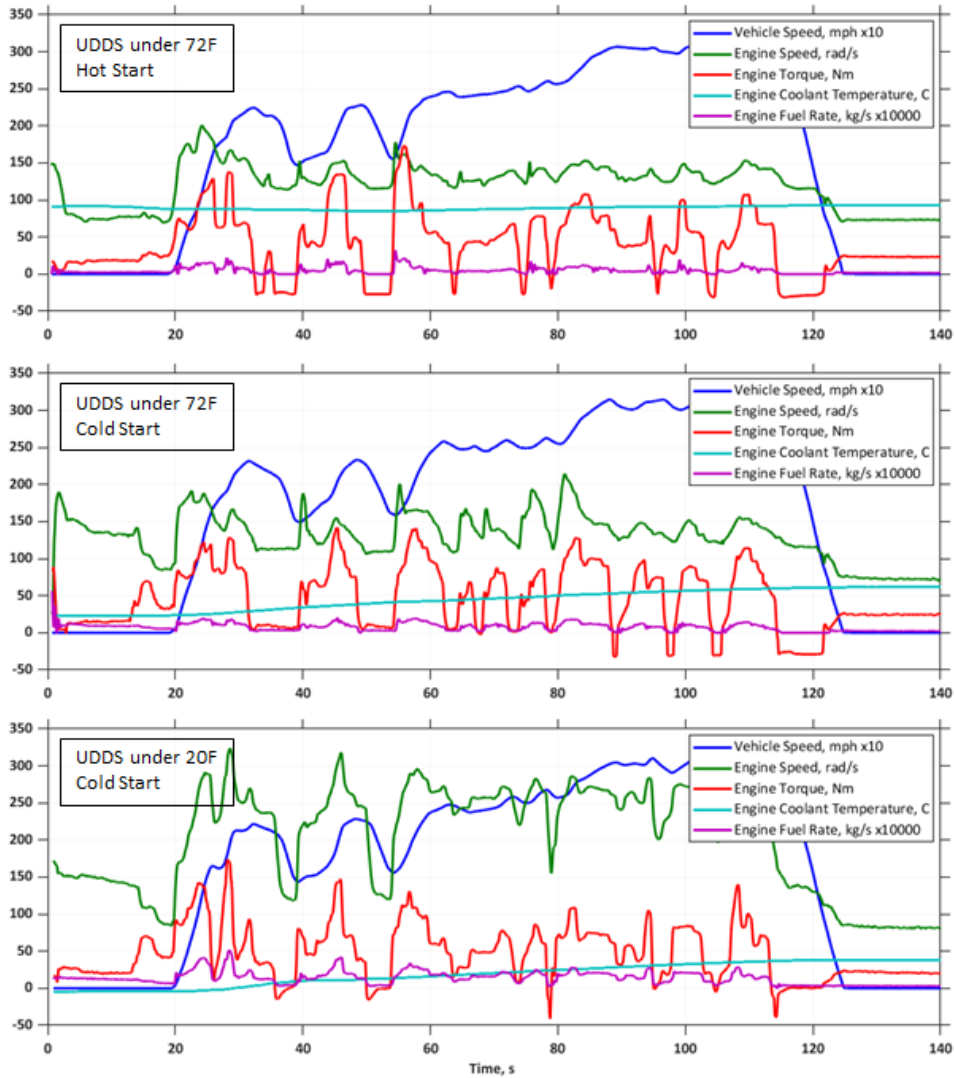


Figure 45. Engine operation at the launch of the vehicle differs according to engine coolant temperature

As shown in Figure 46, the engine speed is controlled based on the engine coolant temperature, which means that the idle speed has a strong correlation with the engine coolant temperature in cold conditions.

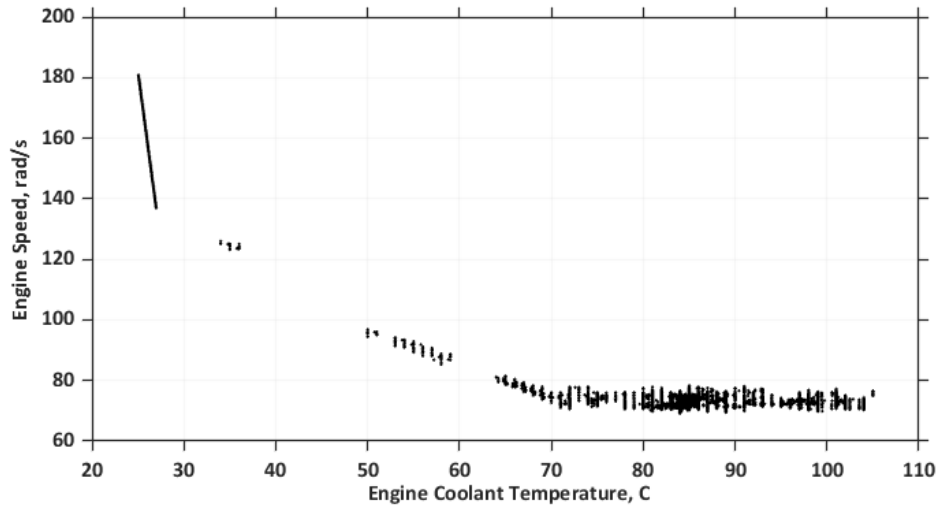


Figure 46. Engine idle speed is controlled according to coolant temperature

On the other hand, Figure 47 shows the effect of start-up coolant temperatures in driving conditions. The coolant cannot easily reach its optimal temperature when the vehicle is operated with the heater on in cold ambient temperatures.

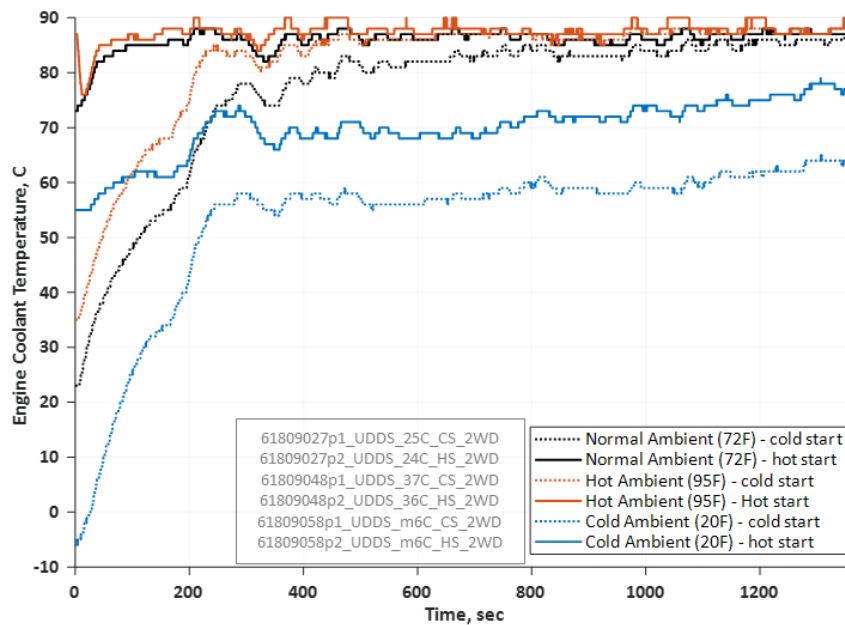


Figure 47. Behaviors of engine coolant temperatures on UDDS in different test conditions

5.6.2. Engine Performance

Thermal conditions not only affect the control of the components but also the performance as well. Engine performance noticeably deteriorates in very cold conditions. While we do not have complete component test data for different steady thermal conditions, the performance degradation caused by thermal conditions can be analyzed from the vehicle test data.

An engine generates a great deal of heat. Approximately one-third of the input power is converted to mechanical work, and another third is exhausted as emission gas, so the last third of the input power contributes to heating the engine block and cooling system. Therefore, the engine temperature increases very fast as long as the engine is turned on; however, the coolant temperature is not sustained if the ambient temperature is very cold. Figure 48 shows that the fuel consumption rate is significantly affected by the thermal condition.

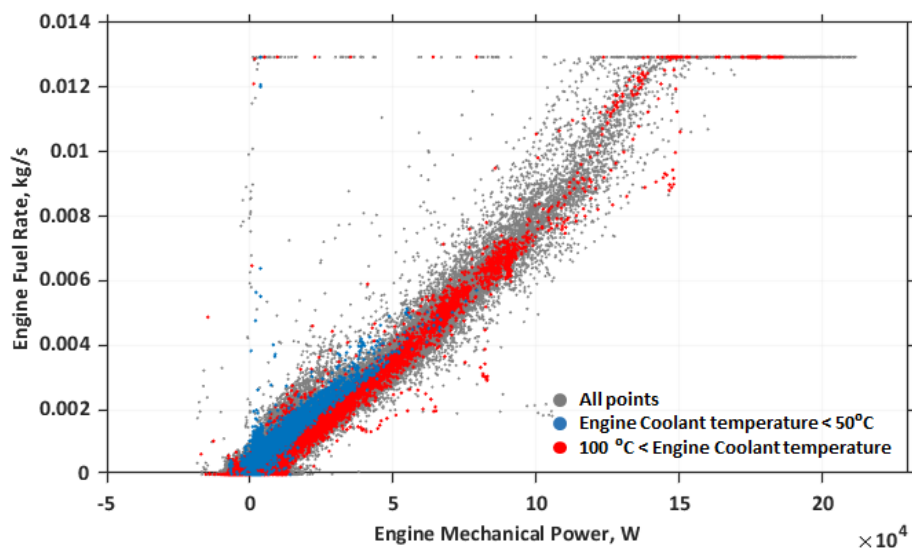


Figure 48. Fuel rate according to engine power for different coolant temperatures

The operating points in Figure 48 are grouped by the engine coolant temperature range and show meaningful trends in fuel consumption according to engine coolant temperature. Although cylinder temperature might have a stronger correlation with the engine efficiency than the coolant temperature, it is not measured in our tests, and the coolant temperature can be considered as the closest temperature to the heat source.

5.6.3. Fuel Consumption Analysis

Changes in component performance affect the fuel consumption of the vehicle, and the thermal impact on fuel consumption can be explained by the performance of the components. Figure 49 shows the fuel consumption in several tests performed on the UDDS cycle but under different test conditions.

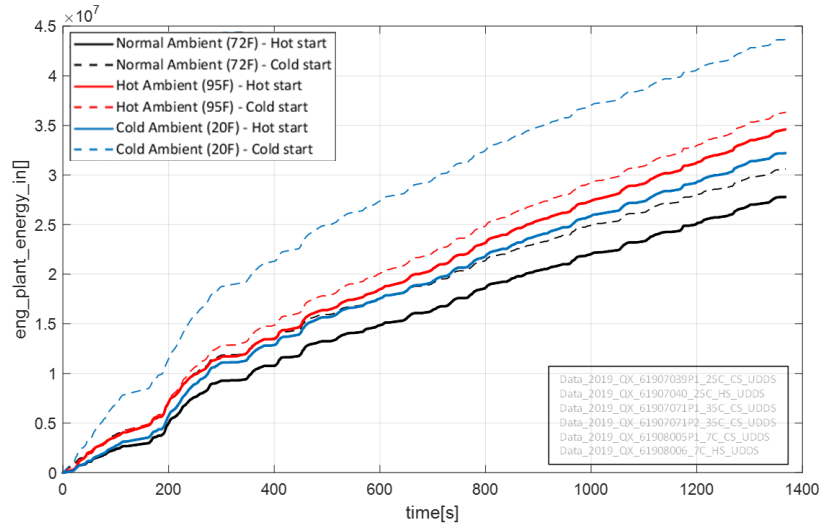


Figure 49. Accumulated fuel consumption trajectories on the UDDS cycle under different test conditions

In Figure 49 different colors are used to indicate the different ambient temperatures and the dotted lines mean that the engine starts at cold temperature (cold-start). The results show that the car operated in normal ambient temperatures with the heating and air-conditioning system off shows the best fuel economy. When the air-conditioning system is operating, the fuel economy decreases although there are variations according to the initial engine and transmission temperature. However, the vehicle operated at cold ambient condition, the vehicle consumes only about 10% more fuel if the engine starts at the “hot” condition. At certain hot ambient temperatures, fuel consumption is higher than that for the cold ambient condition since the air-conditioning system consumes more energy than the heating system. Fuel consumption is dramatically increased if the engine starts at cold temperature and the cabin heater is turned on, because the engine cannot use all the waste heat to increase the engine temperature. When the engine temperature is not well maintained, the engine consumes more fuel, which leads to lower fuel economy.

5.7. Accessory Load

There is no electrical heater for the cabin in the 2019 Infiniti QX50, so the most significant impact on the accessory load is the air-conditioning system under hot ambient conditions. There are two kinds of accessory load for heating and air-conditioning. The first is the electrical accessory load from the battery to operate the fan that ventilates air. The second is the mechanical accessory load from the engine to operate the water pump and compressor for the air-conditioning. While we have data for the electrical accessory load in our test data, we do not have the specific mechanical accessory load. However, we can deduce it from the information shown in Figure 50, which shows engine output power while the vehicle is fully stopped for the hot ambient condition and the cold condition. More energy is consumed in the hot ambient condition than in the cold ambient condition. It can be deduced that the compressor for the air-conditioning consumes about 900 W when the vehicle is fully stopped.

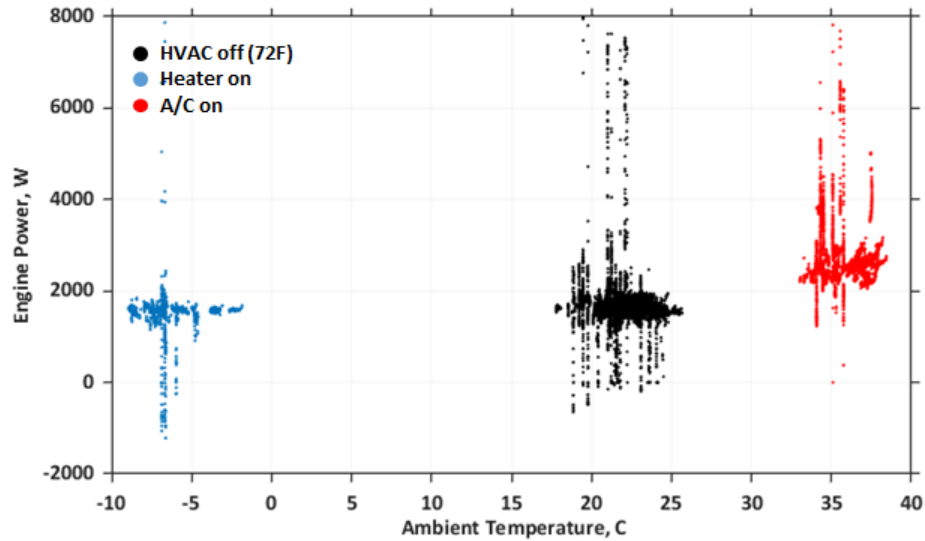


Figure 50. Engine output power when vehicle is fully stopped

Figure 51 shows the accessory power while the vehicle is fully stopped. The operating points are grouped according to operating conditions. The black points are the accessory power when the air-conditioning or heater is turned off. The required power without any demand for air-conditioning or heating is about 360 W regardless of thermal conditions. The battery power increases 140 W or more if the air-conditioning system in the passenger compartment is turned on under the hot condition (red points). In cold conditions (ambient temperature below 0 °C), when the heater is turned on and the battery power increases about 140 W (blue points). Because only the fan operates, blowing hot air from the engine into the cabin, the power required for heating is relatively small compared to that for the AC system.

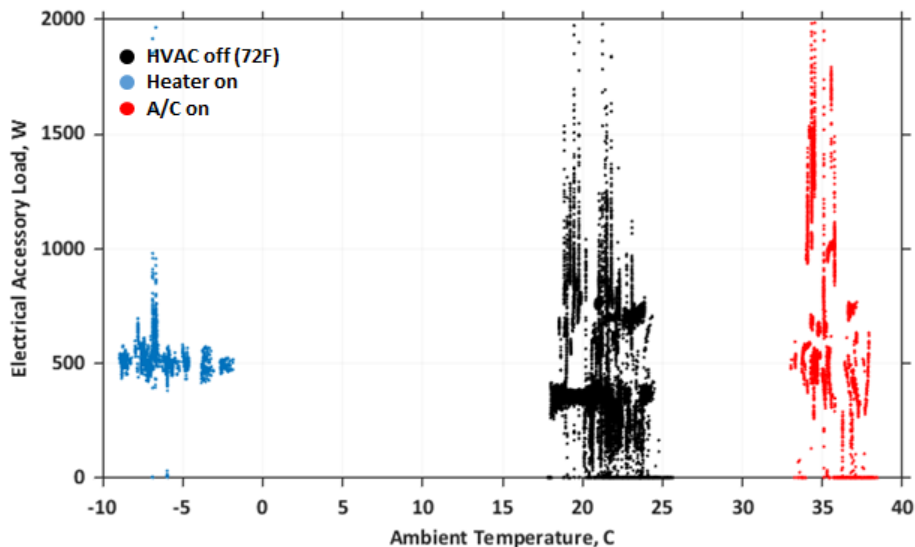


Figure 51. Electrical consumption when vehicle is fully stopped

Figure 52 shows why accessory load is higher in the hot condition. When the air-conditioning is on, the fan duty changes according to the difference between the cabin and the ambient temperature.

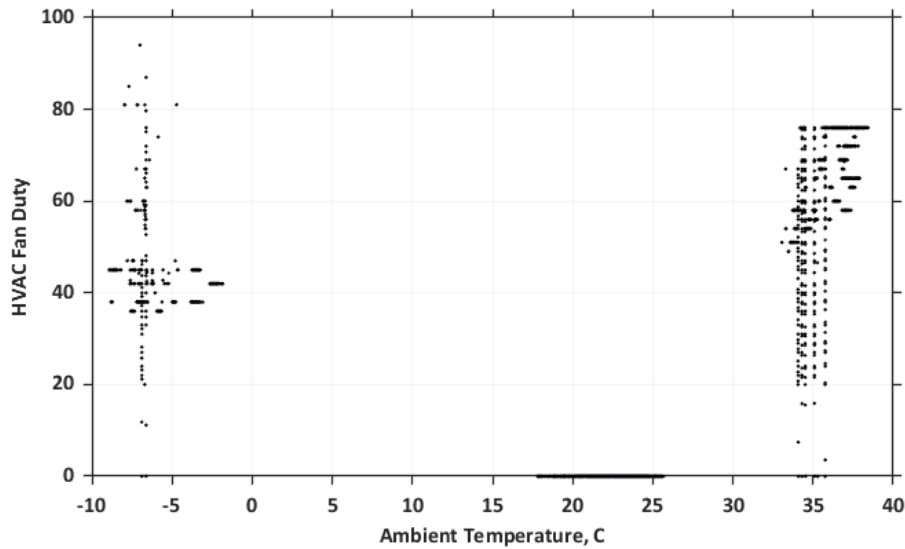


Figure 52. Fan duty when vehicle is fully stopped

5.8. Energy Balance Diagram

In section 5.1, the additional signals were calculated based on other signals or additional information from external sources [7]. Based on the additional signals for each component, the total amounts of energy in and out can be computed by the post-processing process in Autonomie. The terms input and *output* can be confusing because their roles can be exchanged. Therefore, in this discussion, each port means one power flow, and all components have two ports in Autonomie. For example, Figure 53 shows the energy in and out for two ports and the efficiency values for the final drive component.

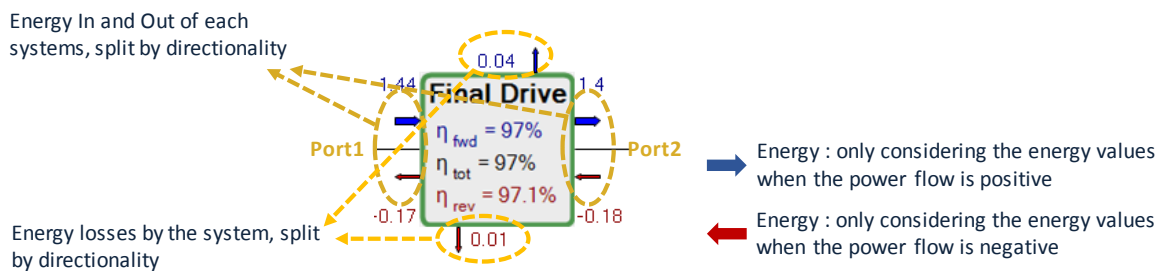


Figure 53. Example of energy calculation for one component on Autonomie

The total efficiency can be computed on each port in different ways. The following are the definitions of efficiency values.

- η_{fwd} = total efficiency when the power on port 1 and 2 is positive (positive positive);
- η_{tot} = total aggregate efficiency; and
- η_{rev} = total efficiency when the power on port 1 and 2 is negative (negative negative).

For each component, total energy consumption and efficiency are calculated based on test data and our assumptions. Figure 54 and Figure 55 show the final diagrams from Autonomie graphical interface after post-processing for the energy balance on the UDDS and HWFET cycles. Note that the efficiency of some components (transmission, alternator, reduction gear, torque converter) is taken into account in our assumptions.

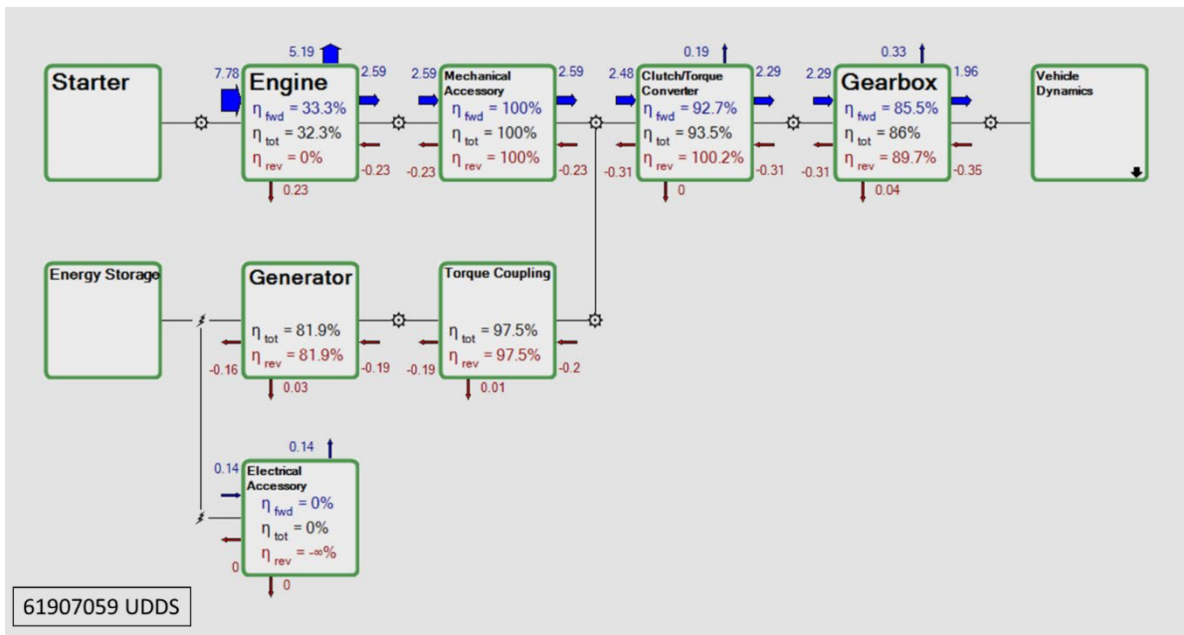


Figure 54. Energy balance diagram for the UDDS cycle in Autonomie

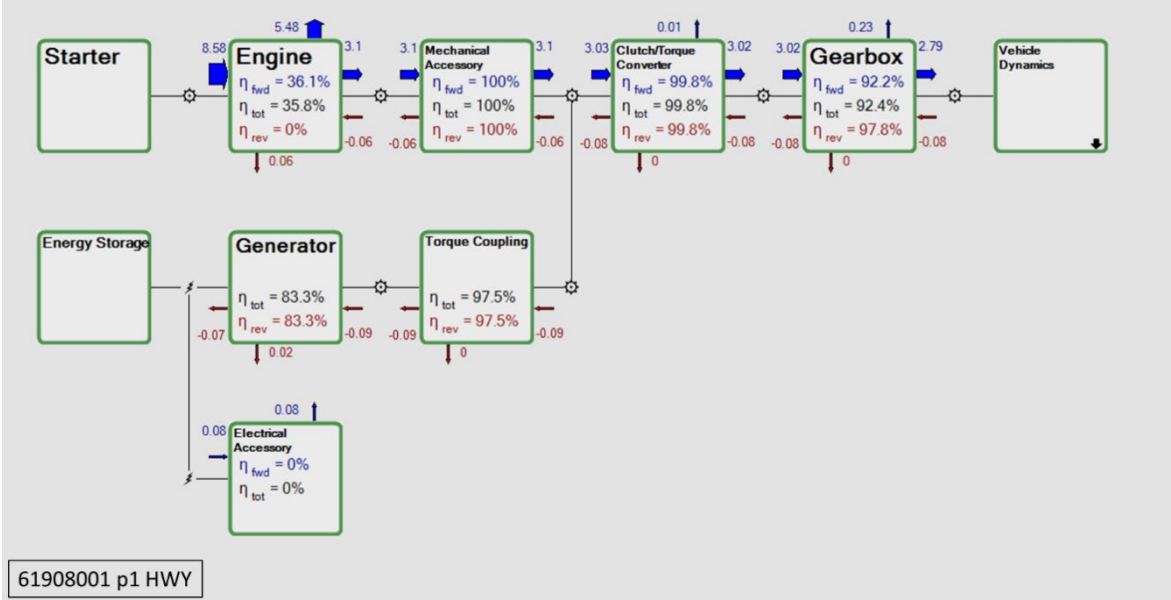


Figure 55. Energy balance diagram for the HWFET cycle in Autonomie

6. Autonomie Model Validation

Analysis of vehicle-level control from vehicle test data was performed to merge the separately developed vehicle component models into a vehicle simulation model. The component controls include transmission shifting, torque converter lockup, engine fuel cutoff, and so on. The component models analyzed, including the control model, were implemented and integrated in Autonomie for a vehicle simulation model for the 2019 Infiniti QX50. Note, however, that the vehicle model was simulated as a “warmed up” vehicle. Since all the simulations considered in this report assume a hot start, in which the engine coolant temperature is steady at about 95 °C, the cold start condition was not a factor for the simulations. The validation process for this study is shown in Figure 56.

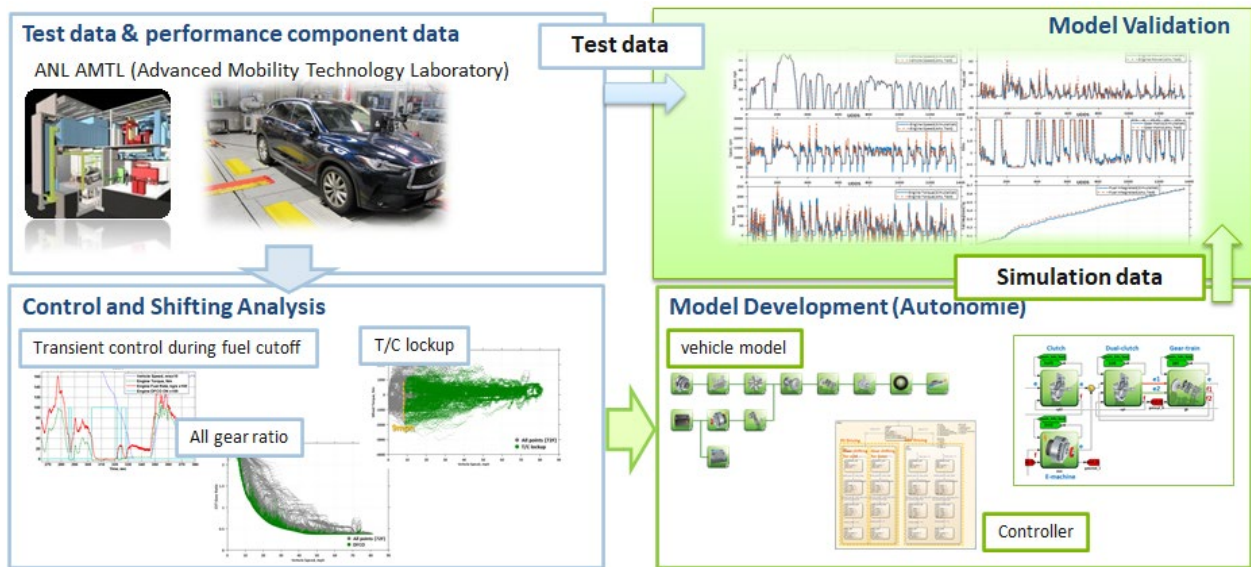


Figure 56. Validation process for 2019 Infiniti QX50 on Autonomie

The simulation was conducted in the UDDS and HWFET cycles. Figure 57 and Figure 58 show the simulation results and test data for vehicle speed, engine speed, engine torque, wheel power, gear number, and fuel integrated for the two drive cycles, respectively. The simulation results and test data for each cycle matched well.

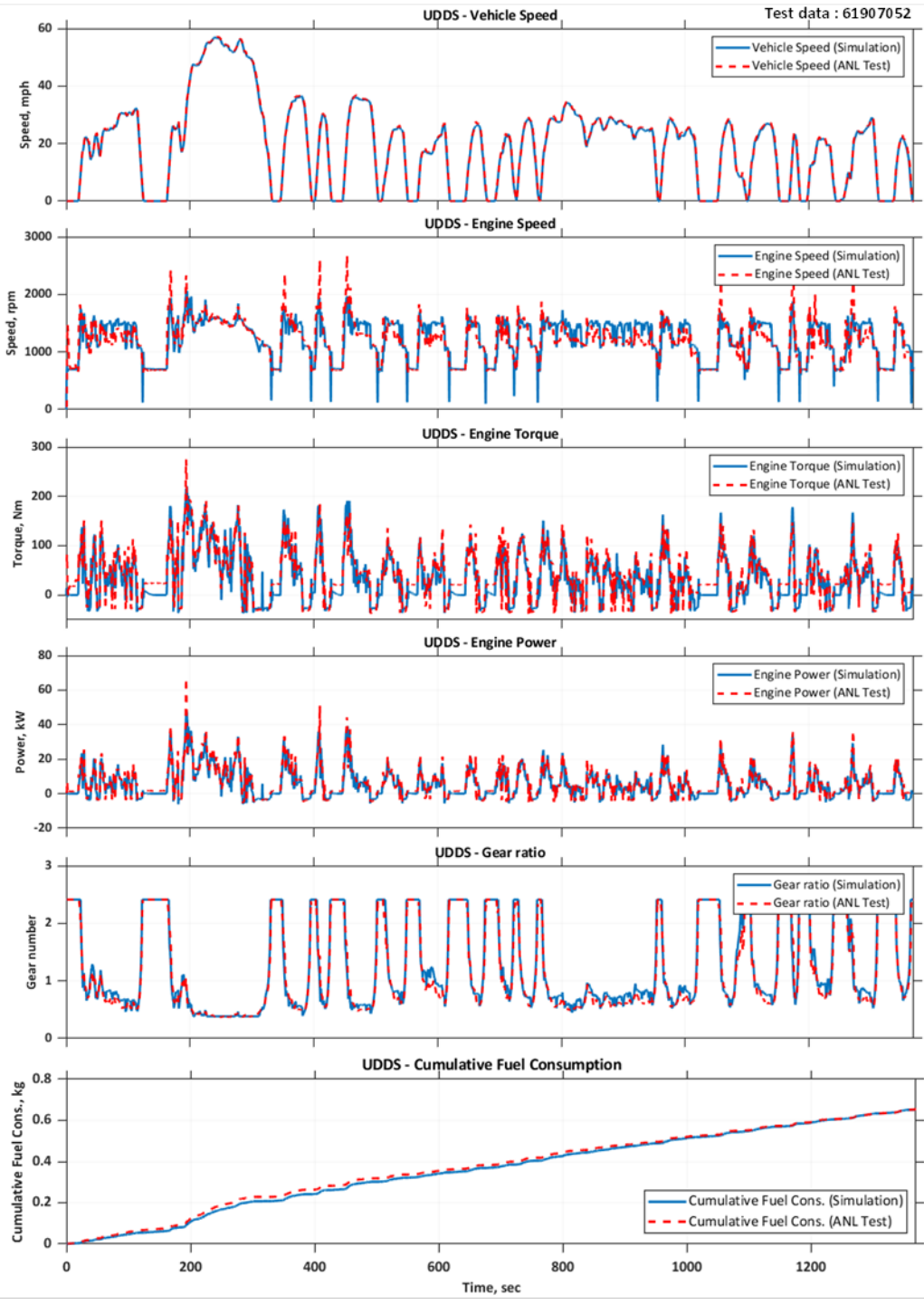


Figure 57. Simulation and test results for the UDDS cycle

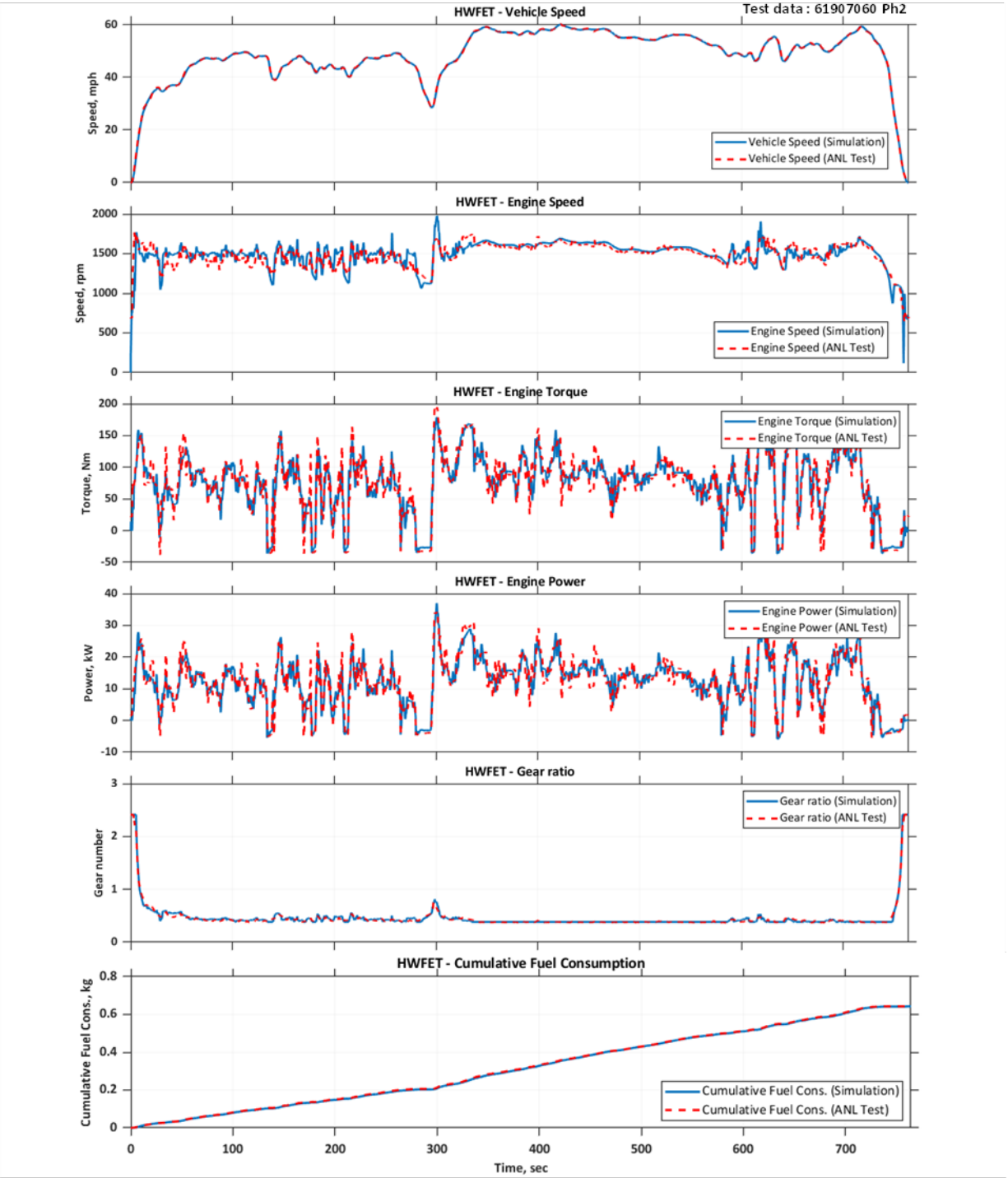


Figure 58. Simulation and test results for the HWFET cycle

Normalized cross-correlation power (NCCP) was used to compare second-by-second time-varying signal traces between test and simulation [6]. The NCCP was calculated using Equation 8 and Equation 9, where x and y represent individual signals. When applied to a test signal and a simulation signal of the same quantity, a value of NCCP equal to or greater than 0.9 indicates a high level of correlation. Conversely, a value less than 0.9 indicates a relatively poor correlation.

$$NCCP = \frac{\max\{R_{xy}(\tau)\}}{\max\{R_{xx}(\tau), R_{yy}(\tau)\}}$$

Equation 8

$$R_{xy}(\tau) = \lim_{T \rightarrow \infty} \frac{1}{T} \int_0^T x(t) \times y(t - \tau) dt$$

Equation 9

The NCCP values for the simulation results for the UDDS and HWFET cycles are given in Table 14. The values for vehicle speed, gear number, and engine speed, which exceeded 0.9, indicated a high level of correlation, whereas there was slightly low correlation for engine torque.

Table 14. NCCP value for the UDDS and HWFET cycles

	UDDS Cycle (test data 61907052)	HWFET Cycle (test data 61907060 Ph2)
Vehicle speed	0.989	0.999
Gear ratio	0.971	0.984
Engine speed	0.971	0.990
Engine torque	0.898	0.960

Figure 59 and Figure 60 show the vehicle speed at which the torque converter was locked up and engine fuel cutoff occurred, respectively. shows the simulation results for the torque converter lockup status according to vehicle speed compared with those for the test results for the UDDS (test data 61907052) and HWFET (test data 61907060 Ph2) cycles in Figure 59, which shows that the operation of the torque converter in the simulation was similar to that in the test. Figure 60 shows the simulation results for the engine fuel cutoff status compared with the test results for the UDDS (test data 61907052) and HWFET (test data 61907060 Ph2) cycles.

The percentage of time for torque converter lockup and engine fuel cutoff for the UDDS and HWFET cycles are given in Table 15.

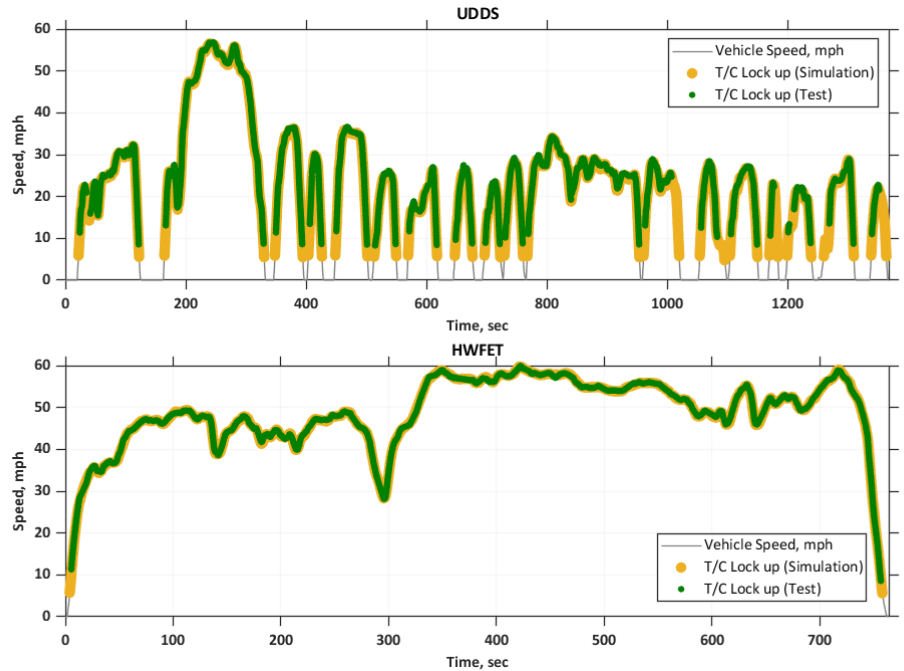


Figure 59. Vehicle speed at which torque converter locked up

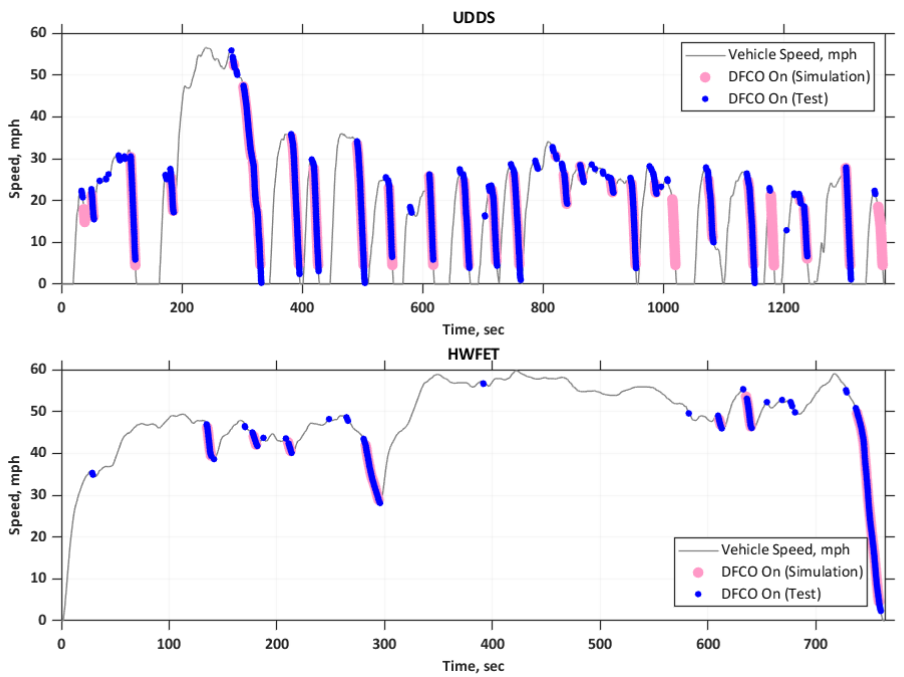


Figure 60. Vehicle speed at which engine fuel cutoff occurred

Table 15. Percentage of time for torque converter lockup and engine fuel cutoff

		UDDS Cycle (test data 61907052)	HWFET Cycle (test data 61907060 Ph2)
Torque converter lockup	Test	65.8%	98.3%
	Simulation	74.8%	98.7%
Engine fuel cutoff	Test	17.0%	8.3%
	Simulation	12.8%	6.0%

The simulation results for fuel consumption were compared to the test results for average fuel consumption to validate the simulation performance in Table 15. The results showed that the fuel consumption in the simulation was 7.406 and 5.266 L/100 km for the UDDS and HWFET cycles, which was different from that in the test by 1.36% and -0.02%, respectively.

Table 16. Fuel consumption in testing and simulation of UDDS and HWFET cycles

	Fuel Economy (L/100 km)	
	UDDS Cycle	HWFET Cycle
Test	7.31	5.27
Simulation (error)	7.41 (1.4%)	5.27 (0.0%)

7. Conclusions

NHTSA sets CAFE standards for passenger cars, light trucks, and medium-duty passenger vehicles. NHTSA has contracted with Argonne to conduct a full vehicle simulation using Autonomie (<https://www.autonomie.net/>) to provide input into the CAFE model to determine the optimum average fuel economy based on numerous technological and economic factors. Autonomie relies on vehicle technology assumptions for model development and validation. NHTSA funded the Argonne AMTL to perform a benchmark study of a 2019 Infiniti QX50 mid-sized passenger car and to provide data to Autonomie and assess the fuel-saving technologies of that powertrain.

The vehicle benchmarked in this report is a 2019 Infiniti QX50 equipped with the 2.0-liter, inline, 4-cylinder VCR turbo engine coupled to a continuously variable transmission. This particular powertrain configuration delivers favorable fuel economy results while providing significant vehicle performance. The focus of the benchmark study is to understand the usage of the critical powertrain components and their impact on vehicle efficiency. The vehicle was instrumented to provide data to support model development and validation in conjunction with providing the data for the analysis in the report. The vehicle was tested on a chassis dynamometer in the controlled laboratory environment in a range of certification tests. Further tests were performed to map the different powertrain components.

8. References

1. Infiniti, USA. (2016, September 29). *VC-Turbo Engine Technology*. Retrieved from <http://www1.infiniti.com/now/technology/vc-turbo-engine>
2. Infiniti press packs, *XTRONIC CVT Smooth-Shifting XTRONIC CVT: The Ideal Partner for VC-Turbo*. June, 2020. Retrieved from <https://infinitipresspacks.com/en/qx50/vc-turbo/xtronic-cvt.html>
3. U.S. Environmental Protection Agency. (2019). *EPA 2019 Test Car List*. Retrieved from www.epa.gov/compliance-and-fuel-economy-data/data-cars-used-testing-fuel-economy
4. Stutenberg K, Lohse-Busch H, Duoba M, Iliev S, Jehlik F, Di Russo M, *An Overview of Argonne's Advanced Mobility Technology Laboratory Vehicle Systems Instrumentation and Evaluation Methodology* (ANL/ESD 2021). <https://anl.box.com/v/AMTL-testing-reference>
5. SAE J2951_201111, Drive Quality Evaluation for Chassis Dynamometer Testing, Society of Engineers
6. Islam, E., Moawad, A., Kim, N., Rousseau, A. 2020. A Detailed Vehicle Simulation Process to Support CAFE and CO2 Standards for the MY 2021–2026 Final Rule Analysis (ANL/ESD-19/9)
7. Meng, Y., Jennings, M., Tsou, P., Brigham, D. et al., *Test Correlation Framework for Hybrid Electric Vehicle System Model*, SAE Int. J. Engines 4(1):1046-1057, 2011, <https://doi.org/10.4271/2011-01-0881>

9. Acknowledgements

This work has been funded by NHTSA. Special thanks go to Seiar Zia for his technical guidance. The authors appreciate the opportunity to perform the laboratory testing and the data analysis of this vehicle.

Finally, the authors acknowledge that this work would not have been possible without the entire team at the Center for Transportation Research. Special thanks go to Mike Kern, Geoffrey Amann, and George Tsigolis for their support during the vehicle evaluation process.

Appendix A: Vehicle Build Sheet



2019 INFINITI QX50 ESSENTIAL AWD

EMPOWER THE DRIVE™

Standard Equipment Included at No Extra Charge

PERFORMANCE:

2.0L Variable Compression-Turbo
4-cylinder engine
268 horsepower
280 lb-ft torque
All wheel drive (AWD)
INFINITI Drive Mode Selector
Continuously Variable Transmission (CVT)
19-inch aluminum alloy wheels
P235/55R19 all-season, run-flat tires
Dual exhaust finishers

COMFORT AND CONVENIENCE:

Leather-appointed seating
8-way power adjustable front seats
with 2-way driver power lumbar
Rear seat slide, recline, and fold flat
function (60/40 split)
Panoramic power sliding/tinted glass
moonroof with one-touch auto open/close
Power moonroof sunshade
Tri-zone automatic climate control
Leather wrapped steering wheel and
shift knob
Manual tilt and telescopic steering column
Paddle shifters
Rear privacy glass
Rear window defroster and wiper
Auto on/off LED headlights
LED signature daytime running lights
LED front fog lights
Auto-dimming inside mirror
Homelink™ Universal Garage Door Opener
Illuminated vanity mirrors
Roof rails
Electronic parking brake
Power adjustable, manual folding and heated
outside mirrors
Body colored door handles with chrome
accent and front LED welcome lights
Rain-sensing front windshield wipers

TECHNOLOGY:

Forward Emergency Braking (FEB) with
Pedestrian Detection
Predictive Forward Collision Warning (PFCW)
Blind Spot Warning (BSW)
Around View Monitor (AVM) with Moving
Object Detection (MOD)
Rear view monitor
Parking sensors (front and rear)
Remote engine start
INFINITI InTouch™ with Navigation and
INFINITI InTouch™ Services +
Voice recognition +
Bluetooth® hands-free phone and audio
streaming +
SiriusXM® Satellite Radio +
SiriusXM® Traffic and Travel Link +
AM/FM radio with CD player
4 USB ports
Power rear lift gate
Intelligent Key with Push Button Ignition
Power moonroof sunshade
Cruise Control
Hill Start Assist
Easy fill tire alert

SAFETY AND SECURITY:

INFINITI Advanced Air Bag System (AABS)
Supplemental front air bags (SRS)
Front seat mounted side impact supplemental
air bags
Roof mounted curtain side impact
supplemental air bags with
rollover sensor
Front driver and passenger knee supplemental
air bags
Lower Anchors and Tethers for Children
(LATCH)
Anti lock Braking System (ABS) with
brake assist
Traction Control System (TCS)
Vehicle Dynamic Control (VDC)
Electronic Brake force Distribution (EBD)
Independent Tire Pressure Monitoring System
(TPMS)
3 point front seatbelts with pretensioners
and load limiters

+For more information, see
dealer, owner's manual, or
www.infiniti.com/intouch/important
-information
++Replaces standard equipment

Manufacturer's Suggested
Retail Base Price: \$45,150.00

Options Included by Manufacturer
ProASSIST PACKAGE 550.00

Backup Collision Intervention (BCI)
Distance Control Assist (DCA)
Intelligent Cruise Control (ICC)
Rear Cross Traffic Alert (RCTA)
ProACTIVE PACKAGE 2,000.00

Steering Assist
Intelligent Cruise Control (ICC) with
Full Speed Range and Hold
Blind Spot Intervention (BSI)
Lane Departure Warning (LDW)
Lane Departure Prevention (LDP)

High Beam Assist (HBA)
Head-up Display (HUD)
Direct Adaptive Steering (DAS)
PREMIUM HEAT PACKAGE 1,200.00

Heated front seats
Memory driver seat, mirrors, and
steering wheel ++
Outside mirrors with reverse tilt-down ++
Power tilt and telescopic steering wheel ++
Heated steering wheel

ILLUMINATED KICK PLATES 465.00

CARGO PACKAGE 285.00

Reversible Cargo Mat, Cargo LOKs,
Console Net, Cargo Net
SPLASH GUARDS 185.00

DESTINATION CHARGES 995.00

Total* \$50,830.00

*Does not include dealer installed options and accessories, local taxes or license fees. This label has been applied pursuant to federal law. Do not remove prior to delivery to the ultimate purchaser.

EPA
DOT

Fuel Economy and Environment

Gasoline Vehicle

Fuel Economy

26 MPG
combined city/hwy

24 city
30 highway

3.8 gallons per 100 miles

SMALL SUVs range from 18 to 37 MPG.
The best vehicle rates 136 MPGe.

You spend
\$1,750
more in fuel costs
over 5 years
compared to the
average new vehicle.

Annual fuel cost
\$1,750

Fuel Economy & Greenhouse Gas Rating (tailpipe only)

5

1 5 10 Best

This vehicle emits 340 grams CO₂ per mile. The best emits 0 grams per mile (tailpipe only). Producing and distributing fuel also create emissions; learn more at fuelconomy.gov.

Smog Rating (tailpipe only)

5

1 5 10 Best

This vehicle emits 340 grams CO₂ per mile. The best emits 0 grams per mile (tailpipe only). Producing and distributing fuel also create emissions; learn more at fuelconomy.gov.

Actual results will vary for many reasons, including driving conditions and how you drive and maintain your vehicle. The average new vehicle gets 27 MPG and costs \$7,000 to fuel over 5 years. Cost estimates are based on 15,000 miles per year at \$3.00 per gallon. MPGe is miles per gasoline gallon equivalent. Vehicle emissions are a significant cause of climate change and smog.

fuelconomy.gov

Calculate personalized estimates and compare vehicles

GOVERNMENT 5-STAR SAFETY RATINGS

DELIVERY

Overall Vehicle Score Not Rated

Based on the combined ratings of frontal, side and rollover. Should ONLY be compared to other vehicles of similar size and weight.

Frontal Crash	Driver Not Rated	Passenger Not Rated
Based on the risk of injury in a frontal impact. Should ONLY be compared to other vehicles of similar size and weight.		
Side Crash	Front seat Not Rated	Rear seat Not Rated
Based on the risk of injury in a side impact.		
Rollover	Not Rated	
Based on the risk of rollover in a single-vehicle crash.		

VEHICLE COLORS:
EXT: HERMOSA BLUE
INT: GRAPHITE

FINAL ASSEMBLY POINT:
AGUAS(ABV.)MEX

TRANSPORT METHOD:
TRUCK

DEALER:
INFINITI OF ORLAND PARK
8751 W 159TH STREET
ORLAND PARK IL
60462

Star ratings range from 1 to 5 stars (*****), with 5 being the highest.
Source: National Highway Traffic Safety Administration (NHTSA)
www.safercar.gov or 1-888-327-4236

TOTAL OWNERSHIP EXPERIENCE

Every Infiniti Vehicle includes Infiniti's:

- 4-Year/60,000 Mile Basic Limited Warranty Coverage **
- 6-Year/70,000 Mile Powertrain Limited Warranty Coverage **
- 7-Year/Unlimited Mileage Corrosion Limited Warranty Coverage **
- 24-hour Roadside Assistance **
- Complimentary Service Loan Car ***

** Please see the Infiniti Warranty Information booklet for details.
*** Please ask your Infiniti retailer for details.

VIN: 3PCAJ5M39KF125022

EMS: 50 STATE EMISSIONS

MDL: 81419-125022 BW-5-G

OPT: D-V01V02X02N92M92B92
C03L11S55286

20180908004911AS71308

Appendix B: 2019 Infiniti QX50 Test Signals

Model Year	Represented Test Veh Make	Represented Test Veh Model	Test Veh ID	Test Veh Displacement (L)	Vehicle Type	Rated Horsepower	# of Cylinders	# of Gears	Drive System Description	Equivalent Test Weight (lbs.)	Test Number	Test Originator	Test Procedure Description	Test Fuel Type Cd	Test Fuel Type Description	RND_ADJ_FE_FU_UNIT	FE Bag 1	FE Bag 2	FE Bag 3	FE Bag 4	Target Coef A (lbF)	Target Coef B (lbF/mph)	Target Coef C (lbF/mph**2)
2019	BMW	X3 sDrive30i	LA13758	2.000	Both	248	4	8	2-Wheel Drive, Rear	4250	KBMX91003814	EPA	HWFE	61	Tier 2 Cert Gasoline	44.1	MPG				51.300	-0.3480	0.02599
2019	BMW	X3 sDrive30i	LA13758	2.000	Both	248	4	8	2-Wheel Drive, Rear	4250	KBMX91003817	EPA	Federal fuel 2-day exhaust (w/can load)	61	Tier 2 Cert Gasoline	29.6	MPG	27.792771	30.1888738	29.8563864	51.300	-0.3480	0.02599
2019	BMW	X3 sDrive30i	LA13758	2.000	Both	248	4	8	2-Wheel Drive, Rear	4250	KBMX91003842	EPA	Federal fuel 2-day exhaust (w/can load)	61	Tier 2 Cert Gasoline	29.3	MPG	27.3488706	29.9432216	29.610576	51.300	-0.3480	0.02599
2019	BMW	X3 sDrive30i	LA13758	2.000	Both	248	4	8	All Wheel Drive	4250	KBMX10052117	MFR	HWFE	61	Tier 2 Cert Gasoline	42.1	MPG				55.100	-0.3410	0.02760
2019	BMW	X3 sDrive30i	LA13758	2.000	Both	248	4	8	All Wheel Drive	4250	KBMX10052119	MFR	Federal fuel 3-day exhaust	61	Tier 2 Cert Gasoline	29.6	MPG	27.1000000	30.5000000	29.7000000	55.100	-0.3410	0.02760
2019	BMW	X3 sDrive30i	LA13758	2.000	Both	248	4	8	All Wheel Drive	4500	IBMX10048287	MFR	Federal fuel 3-day exhaust	61	Tier 2 Cert Gasoline	27.8	MPG	25.6000000	28.6000000	28.1000000	59.600	-0.3590	0.02789
2019	BMW	X3 sDrive30i	LA13758	2.000	Both	248	4	8	All Wheel Drive	4500	IBMX10048471	MFR	HWFE	61	Tier 2 Cert Gasoline	41.2	MPG				59.600	-0.3590	0.02789
2019	BMW	X3 sDrive30i	LA13758	2.000	Both	248	4	8	All Wheel Drive	4500	IBMX10049259	MFR	Federal fuel 3-day exhaust	61	Tier 2 Cert Gasoline	27.8	MPG	26.1000000	28.4000000	28.0000000	57.700	-0.3670	0.02655
2019	BMW	X3 sDrive30i	LA13758	2.000	Both	248	4	8	All Wheel Drive	4500	IBMX10049266	MFR	HWFE	61	Tier 2 Cert Gasoline	42.2	MPG				57.700	-0.3670	0.02655
2019	Alfa Romeo	Stelvio	L8GUF1855	2.000	Both	280	4	8	2-Wheel Drive, Rear	4250	KCRX10054350	MFR	Federal fuel 2-day exhaust (w/can load)	61	Tier 2 Cert Gasoline	29.7	MPG	26.4600000	29.9800000	32.2400000	38.950	-0.0211	0.02616
2019	Alfa Romeo	Stelvio	L8GUF1855	2.000	Both	280	4	8	2-Wheel Drive, Rear	4250	KCRX10054351	MFR	HWFE	61	Tier 2 Cert Gasoline	42.8	MPG				38.950	-0.0211	0.02616
2019	Alfa Romeo	Stelvio	L8GUF1855	2.000	Both	280	4	8	2-Wheel Drive, Rear	4250	KCRX10054352	MFR	Federal fuel 2-day exhaust (w/can load)	61	Tier 2 Cert Gasoline	28.8	MPG	25.8500000	28.7200000	31.4500000	38.950	-0.0211	0.02616
2019	Alfa Romeo	Stelvio	L8GUF1855	2.000	Both	280	4	8	2-Wheel Drive, Rear	4250	KCRX10054353	MFR	HWFE	61	Tier 2 Cert Gasoline	40.6	MPG				38.950	-0.0211	0.02616
2019	Alfa Romeo	Stelvio AWD	L7GAG0709	2.000	Both	280	4	8	2-Wheel Drive, Rear	4250	JCRX10047623	MFR	Federal fuel 2-day exhaust (w/can load)	61	Tier 2 Cert Gasoline	27.8	MPG	25.3100000	27.3300000	30.9400000	37.020	0.0207	0.02771
2019	Alfa Romeo	Stelvio AWD	L7GAG0709	2.000	Both	280	4	8	2-Wheel Drive, Rear	4250	JCRX10047624	MFR	HWFE	61	Tier 2 Cert Gasoline	40.5	MPG				37.020	0.0207	0.02771
2019	Alfa Romeo	Stelvio AWD	L7GAG0709	2.000	Both	280	4	8	2-Wheel Drive, Rear	4250	JCRX10047625	MFR	Federal fuel 2-day exhaust (w/can load)	61	Tier 2 Cert Gasoline	27.9	MPG	25.4000000	27.4100000	31.2600000	37.020	0.0207	0.02771
2019	Alfa Romeo	Stelvio AWD	L7GAG0709	2.000	Both	280	4	8	2-Wheel Drive, Rear	4250	JCRX10047626	MFR	HWFE	61	Tier 2 Cert Gasoline	40.6	MPG				37.020	0.0207	0.02771
2019	Lincoln	MKC	HUJ00015	2.000	Truck	245	4	6	2-Wheel Drive, Front	4250	HFMX10083472	MFR	Federal fuel 2-day exhaust (w/can load)	61	Tier 2 Cert Gasoline	24.1	MPG	23.0000000	23.3000000	26.7000000	44.290	0.2945	0.02493
2019	Lincoln	MKC	HUJ00015	2.000	Truck	245	4	6	2-Wheel Drive, Front	4250	HFMX10083473	MFR	HWFE	61	Tier 2 Cert Gasoline	35.5	MPG				44.290	0.2945	0.02493
2019	Lincoln	MKC	HUJ00031	2.300	Truck	275	4	6	2-Wheel Drive, Front	4250	HFMX10050992	MFR	Federal fuel 2-day exhaust (w/can load)	61	Tier 2 Cert Gasoline	22.1	MPG	21.1946929	21.169346	24.9721603	44.220	0.2681	0.02512
2019	Lincoln	MKC	HUJ00031	2.300	Truck	275	4	6	2-Wheel Drive, Front	4250	HFMX10050993	MFR	HWFE	61	Tier 2 Cert Gasoline	34.6	MPG				44.220	0.2681	0.02512
2019	Lincoln	MKC	HUJ00031	2.300	Truck	275	4	6	2-Wheel Drive, Front	4250	HFMX10053476	MFR	Federal fuel 2-day exhaust (w/can load)	61	Tier 2 Cert Gasoline	22.0	MPG	21.1000000	21.0000000	24.9000000	44.220	0.2681	0.02512
2019	Lincoln	MKC	HUJ00031	2.300	Truck	275	4	6	2-Wheel Drive, Front	4250	HFMX10053477	MFR	HWFE	61	Tier 2 Cert Gasoline	34.4	MPG				44.220	0.2681	0.02512
2019	Lincoln	MKC	HUJ00039	2.000	Truck	245	4	6	2-Wheel Drive, Front	4250	HFMX10040667	MFR	HWFE	61	Tier 2 Cert Gasoline	35.5	MPG				44.220	0.2681	0.02512
2019	Lincoln	MKC	HUJ00039	2.000	Truck	245	4	6	2-Wheel Drive, Front	4250	HFMX10040668	MFR	Federal fuel 2-day exhaust (w/can load)	61	Tier 2 Cert Gasoline	24.3	MPG	23.2793958	23.6707798	26.5177648	44.220	0.2681	0.02512
2019	Lincoln	MKC	HUJ00023	2.000	Truck	245	4	6	2-Wheel Drive, Front	4250	KFMX10052724	MFR	Federal fuel 2-day exhaust (w/can load)	61	Tier 2 Cert Gasoline	25.1	MPG	24.2789145	24.2957458	27.5354579	32.730	0.2433	0.02383
2019	Lincoln	MKC	HUJ00023	2.000	Truck	245	4	6	2-Wheel Drive, Front	4250	KFMX91003847	EPA	HWFE	61	Tier 2 Cert Gasoline	38.8	MPG				32.730	0.2433	0.02383
2019	CADILLAC	XT4 AWD	206KZV4337	2.000	Truck	237	4	9	2-Wheel Drive, Front	4250	KGMX10052280	MFR	Federal fuel 3-day exhaust	61	Tier 2 Cert Gasoline	27.5	MPG	26.2000000	26.7000000	30.3000000	29.400	0.4064	0.02238
2019	CADILLAC	XT4 AWD	206KZV4337	2.000	Truck	237	4	9	2-Wheel Drive, Front	4250	KGMX10052281	MFR	HWFE	61	Tier 2 Cert Gasoline	41.1	MPG				29.400	0.4064	0.02238
2019	CADILLAC	XT4 FWD	206KZV4337	2.000	Truck	237	4	9	2-Wheel Drive, Front	4000	KGMX10055320	MFR	Federal fuel 3-day exhaust	61	Tier 2 Cert Gasoline	30.9	MPG	28.5000000	30.7000000	33.3000000	23.630	0.3282	0.02452
2019	CADILLAC	XT4 FWD	206KZV4337	2.000	Truck	237	4	9	2-Wheel Drive, Front	4000	KGMX10055321	MFR	HWFE	61	Tier 2 Cert Gasoline	43.4	MPG				23.630	0.3282	0.02452
2019	ACURA	RDX AWD	EKYF2A	2.000	Truck	272	4	10	2-Wheel Drive, Front	4250	KHXX10052757	MFR	Federal fuel 2-day exhaust (w/can load)	61	Tier 2 Cert Gasoline	27.2	MPG	25.5000000	26.7000000	29.7000000	33.890	0.2274	0.02720
2019	ACURA	RDX AWD	EKYF2A	2.000	Truck	272	4	10	2-Wheel Drive, Front	4250	KHXX10052758	MFR	HWFE	61	Tier 2 Cert Gasoline	39.0	MPG				33.890	0.2274	0.02720
2019	ACURA	RDX AWD A-SPEC	EKYF2A	2.000	Truck	272	4	10	2-Wheel Drive, Front	4250	KHXX10052103	MFR	US06	61	Tier 2 Cert Gasoline	24.2	MPG	16.6000000	27.7000000		36.560	0.1346	0.02838
2019	ACURA	RDX AWD A-SPEC	EKYF2A	2.000	Truck	272	4	10	2-Wheel Drive, Front	4250	KHXX10052755	MFR	Federal fuel 2-day exhaust (w/can load)	61	Tier 2 Cert Gasoline	26.6	MPG	24.6000000	26.3000000	29.0000000	36.560	0.1346	0.02838
2019	ACURA	RDX AWD A-SPEC	EKYF2A	2.000	Truck	272	4	10	2-Wheel Drive, Front	4250	KHXX10052756	MFR	HWFE	61	Tier 2 Cert Gasoline	38.5	MPG				36.560	0.1346	0.02838
2019	ACURA	RDX FWD	EKYF3A	2.000	Truck	272	4	10	2-Wheel Drive, Front	4000	KHXX10052099	MFR	HWFE	61	Tier 2 Cert Gasoline	40.2	MPG				34.500	-0.0405	0.02915
2019	ACURA	RDX FWD	EKYF3A	2.000	Truck	272	4	10	2-Wheel Drive, Front	4000	KHXX10052760	MFR	Federal fuel 2-day exhaust (w/can load)	61	Tier 2 Cert Gasoline	28.4	MPG	26.5000000	27.8000000	31.0000000	34.500	-0.0405	0.02915
2019	ACURA	RDX FWD A-SPEC	EKYF3A	2.000	Truck	272	4	10	2-Wheel Drive, Front	4250	KHXX10052108	MFR	HWFE	61	Tier 2 Cert Gasoline	39.8	MPG				37.410	-0.0369	0.02915
2019	ACURA	RDX FWD A-SPEC	EKYF3A	2.000	Truck	272	4	10	2-Wheel Drive, Front	4250	KHXX10052109	MFR	US06	61	Tier 2 Cert Gasoline	24.8	MPG	16.7000000	28.7000000		37.410	-0.0369	0.02915
2019	ACURA	RDX FWD A-SPEC	EKYF3A	2.000	Truck	272	4	10	2-Wheel Drive, Front	4250	KHXX10052759	MFR	Federal fuel 2-day exhaust (w/can load)	61	Tier 2 Cert Gasoline	27.4	MPG	25.9000000	26.9000000	29.8000000	37.410	-0.0369	0.02915

Appendix C: 2019 Infiniti QX50 Test Signals

The following signals were collected at 10 Hz for each test. Note that the signal sampling rate for CAN and diagnostic messages is dependent on the vehicle, and the actual transmission rate may be faster or slower than the 10-hz sample rate.

Table 17. Facility and Vehicle Signal list

Facility, dyno and cell data	Analog data from vehicle	Modal tailpipe emissions
DAQ_Time[s]	DAQ_Time[s]_RawVehicleDAQ	AMA_Dilute_THC[mg/s]
Time[s]_RawFacilities	Time[s]_RawVehicleDAQ	AMA_Dilute_CH4[mg/s]
Dyno_Spd[mph]	Engine_Oil_Dipstick_Temp[C]	AMA_Dilute_NOx[mg/s]
Dyno_TractiveForce[N]	Radiator_Air_Outlet_Temp[C]	AMA_Dilute_COlow[mg/s]
Dyno_LoadCell[N]	Engine_Bay_Temp[C]	AMA_Dilute_COmid[mg/s]
Distance[mi]	Cabin_Temp[C]	AMA_Dilute_CO2[mg/s]
Dyno_Spd_Front[mph]	Cabin_Upper_Vent_Temp[C]	AMA_Dilute_HFID[mg/s]
Dyno_TractiveForce_Front[N]	Cabin_Lower_Vent_Temp[C]	AMA_Dilute_NMHC[mg/s]
Dyno_LoadCell_Front[N]	Solar_Array_Ind_Temp[C]	AMA_Dilute_Fuel[g/s]
Dyno_Spd_Rear[mph]	Eng_FuelFlow_Direct2[gps]	
Dyno_LoadCell_Rear[N]	12VBatt_Volt_Hioki_U1[V]	
Dyno_TractiveForce_Rear[N]	12VBatt_Curr_Hioki_I1[A]	
DilAir_RH[%]	12VBatt_Power_Hioki_P1[W]	
Tailpipe_Press[inH2O]	Alternator_Curr_Hioki_I2[A]	
Cell_Temp[C]	Alternator_Power_Hioki_P2[W]	
Cell_RH[%]	12VBatt_Curr_Hioki_I3[A]	
Cell_Press[inHg]	12VBatt_Power_Hioki_P3[W]	
Tire_Front_Temp[C]	Eng_FuelFlow_Direct[ccps]	
Tire_Rear_Temp[C]	Eng_Fuel_Temp_Direct[C]	
Drive_Schedule_Time[s]	Eng_Fuel_Temp_Direct3[C]	
Drive_Trace_Schedule[mph]		
Exhaust_Bag		

Table 18. CAN Signal list

Engine	Transmission
Eng_torque_TCM_Nm	Eng_torque_CVT_input_shaft_TCM_Nm
Eng_spd_CAN2_rpm	Input_CVT_Shaft_Rev_TCM_rpm
Eng_turbo_boost_pressure_PCM_psi	Trans_CVT_fluid_temp_CAN2_C
Eng_wategate_act_position_PCM_cm	Trans_CVT_fluid_temp_TCM_C
Eng_load_calc_PCM_per	Trans_gear_demand_CAN2
Eng_map_sensor_PCM_psi	Trans_gear_engaged_CAN2
Eng_cam_exhaust_adv_ang_PCM_deg	Trans_primary_pulley_speed_CAN2_rpm
Eng_cam_intake_adv_ang_PCM_deg	Trans_PRNDL_demand_CAN2
Eng_fuel_DI_inj_pulse_B1_PCM_ms	Trans_PRNDL_engaged_CAN2
Eng_fuel_inj_base_schdl_PCM_ms	Trans_pulley_gear_ratio_TCM
Eng_fuel_PFI_inj_pulse_B1_PCM_ms	Trans_secondary_pulley_speed_CAN2_rpm
Eng_ignition_timing_PCM_deg	Trans_slip_speed_TCM_rpm
Eng_intake_manifold_pos_tumble_PCM_V	Trans_target_gear_ratio_CAN2
Eng_intake_mani_runner_swirl_ctrl_valve_PCM	Trans_torque_converter_clutch_pressure_TCM_Mpa
Eng_mass_airflow_PCM_gs	Trans_line_pressure_TCM_Mpa
Eng_oil_pressure_PCM_MPa	Trans_sec_pressure_TCM_Mpa
Eng_oil_temp_CAN2_C	Trans_primary_pressure_TCM_Mpa
Eng_oil_temp_PCM_C	
Int_air_temp_PCM_C	
VCR_angle_actual_CAN5_deg	
VCR_angle_CAN5_deg	
Eng_fuel_press_PCM_mpa	
Eng_fuel_hp_pump_PCM_deg	
Eng_airfuel_sen_B1_PCM_V	

Driver Input and Vehicle Signals	Cooling system
Drive_trace_grade__per	Engine_coolant_bypass_valve_pos_PCM__deg
Drive_trace_speed__mph	Eng_coolant_temp_CAN2__C
Pedal_accel_CAN2__per	Eng_fan_duty_PCM__per
Pedal_accel_CAN2__per	Eng_radiator_coolant_temp_PCM__C
Wheel_speed_FL_CAN4	Eng_coolant_temp_PCM__C
Wheel_speed_FR_CAN4	
Wheel_speed_RL_CAN4	
Wheel_speed_RR_CAN4	
Veh_brake_press_sensor_ABS_bar	

Appendix D: Test Summary

Test ID [#]	Cycle	Test Time	Start Comments	End Comments	Test Cell Temp [C]	Test weight [lb]	Dyno Target A	Dyno Target B	Dyno Target C	Cycle Distance [mi]	Cycle Fuel Consumed [gal] (Emiss Raw)	Cycle Fuel economy [mpg] (Emiss Bag)	Fuel used modal [gal]	Fuel Economy Modal [mpg]	Fuel used Scale [gal]	Fuel Economy Scale [mpg]	Test Driver	APTime	ASCR	ASC_d	ASC_1	CE_d	CE_1	EER	ER	IWR	
Day 9 - repeat of HWY																											
61908001	Highway	08/01/19, 10:16:25 A	Hwyx2, 2 bag, repeat from CERT cycles due to fuel scale dropout	ok	25	4250	45.47	-0.1558	0.02832	10.27	0.290	35.3	0.290	35.4	0.26	40.05	GA	1,992.78	3.12	1,348	1,307	8.97	8.97	-0.02	0.06	0.25	
61908001	Highway	08/01/19, 10:16:25 A	Hwyx2, 2 bag, repeat from CERT cycles due to fuel scale dropout	ok	25	4250	45.47	-0.1558	0.02832	10.27	0.269	38.2	0.269	38.4	0.24	43.33	GA	1,993.09	4.66	1,368	1,307	8.95	8.97	-0.29	-0.17	0.25	
61908002	Power cycle	08/01/19, 10:56:27 A	Quoba mapping cycle, 1 bag warm start, bags OFF	ok	22	4250	45.47	-0.1558	0.02832	7.76			0.334	23.2	0.32	24.56	GA	1,772.79	0.78	5,260	5,220	10.52	10.37	1.08	1.42	0.64	
Day 10 - HWY coast down check																											
61908003	Coast down check	08/05/19, 10:40:27 A	Hwyx2, 2 bag with vehicle on coastdown to verify vehicle losses	ok	25	4250	45.47	-0.1558	0.02832	10.23	0.290	35.3	0.289	35.5	0.26	39.00	MK	1,992.93	5.98	1,385	1,307	9.94	8.97	-0.01	-0.26	0.25	
61908003	Coast down check	08/05/19, 10:40:27 A	Hwyx2, 2 bag with vehicle on coastdown to verify vehicle losses	ok	25	4250	45.47	-0.1558	0.02832	10.23	0.267	38.3	0.266	38.5	0.24	43.28	MK	1,993.25	7.63	1,407	1,307	8.93	8.97	-0.22	-0.43	0.25	
61908004	UDDS	08/05/19, 02:45:49 PM	UDDS, 1 bag prep for COLD FTP in 20°F test cell with HVAC AUTO-72°F	ok	-7	4250	45.47	-0.1558	0.02832	7.41	0.309	24.0	0.308	24.1	0.28	26.85	MK	1,877.58	2.26	5,589	5,466	6.75	6.69	1.51	0.94	0.61	
Day 11 - 20F APRF testing																											
61908005	UDDS	08/06/19, 08:20:33 A	UDDSx2, 4 bag (FTP), COLD FTP in 20°F test cell with HVAC AUTO-72°F	ok	-6	4250	45.47	-0.1558	0.02832	3.59	0.211	17.0	0.210	17.1	0.21	17.24	MK/GA	2,465.40	4.89	2,149	2,049	3.57	3.49	2.35	2.27	0.55	
61908005	UDDS	08/06/19, 08:20:33 A	UDDSx2, 4 bag (FTP), COLD FTP in 20°F test cell with HVAC AUTO-72°F	ok	-7	4250	45.47	-0.1558	0.02832	2.85	0.190	21.4	0.179	21.5	0.16	24.75	MK/GA	1,514.54	3.36	3,531	3,416	3.26	3.20	2.26	1.98	0.67	
61908005	UDDS	08/06/19, 08:20:33 A	UDDSx2, 4 bag (FTP), COLD FTP in 20°F test cell with HVAC AUTO-72°F	ok	-6	4250	45.47	-0.1558	0.02832	7.43	0.391	19.04	0.389	19.12	0.36	20.45											
61908005	UDDS	08/06/19, 08:20:33 A	UDDSx2, 4 bag (FTP), COLD FTP in 20°F test cell with HVAC AUTO-72°F	ok	-6	4250	45.47	-0.1558	0.02832	3.60	0.144	25.1	0.142	25.4	0.13	27.52	MK/GA	2,464.17	1.80	2,086	2,049	3.56	3.49	1.47	1.84	0.55	
61908005	UDDS	08/06/19, 08:20:33 A	UDDSx2, 4 bag (FTP), COLD FTP in 20°F test cell with HVAC AUTO-72°F	ok	-7	4250	45.47	-0.1558	0.02832	3.88	0.159	24.3	0.159	24.3	0.14	28.24	MK/GA	1,514.22	2.31	3,495	3,416	3.31	3.20	3.00	3.51	0.67	
61908005	UDDS	08/06/19, 08:20:33 A	UDDSx2, 4 bag (FTP), COLD FTP in 20°F test cell with HVAC AUTO-72°F	ok	-6	4250	45.47	-0.1558	0.02832	7.48	0.303	24.67	0.302	24.80	0.27	27.89											
61908006	UDDS	08/06/19, 09:38:23 A	UDDS #3, 2 bag, warm start in 20°F test cell with HVAC AUTO-72°F	ok	-6	4250	45.47	-0.1558	0.02832	3.61	0.143	25.1	0.141	25.5	0.13	27.67	GA	2,477.70	0.80	2,065	2,049	3.53	3.49	0.79	1.21	0.55	
61908006	UDDS	08/06/19, 09:38:23 A	UDDS #3, 2 bag, warm start in 20°F test cell with HVAC AUTO-72°F	ok	-7	4250	45.47	-0.1558	0.02832	3.88	0.157	24.7	0.159	24.4	0.14	28.21	GA	1,527.08	1.16	3,456	3,416	3.29	3.20	2.15	2.82	0.67	
61908006	UDDS	08/06/19, 09:38:23 A	UDDS #3, 2 bag, warm start in 20°F test cell with HVAC AUTO-72°F	ok	-6	4250	45.47	-0.1558	0.02832	7.49	0.300	24.93	0.300	24.93	0.27	27.95											
61908007	Highway	08/06/19, 10:17:12 A	Hwyx2, 2 bag, warm start in 20°F test cell with HVAC AUTO-72°F	ok	-4	4250	45.47	-0.1558	0.02832	10.24	0.305	33.5	0.304	33.7	0.28	37.03	MK	1,992.89	4.89	1,371	1,307	8.94	8.97	-0.11	-0.25	0.25	
61908007	Highway	08/06/19, 10:17:12 A	Hwyx2, 2 bag, warm start in 20°F test cell with HVAC AUTO-72°F	ok	-5	4250	45.47	-0.1558	0.02832	10.25	0.293	34.9	0.292	35.1	0.26	39.40	MK	1,993.23	6.33	1,390	1,307	8.93	8.97	-0.30	-0.39	0.25	
61908008	SSS	08/06/19, 11:03:08 A	SSS, 0-80-0, 3 bag at 0%, 3% and 6% grade, warm start in 20°F test cell	ok	-3	4250	45.47	-0.1558	0.02832	6.24			0.254	27.6	0.21	29.83	GA	1,388.30	24.25	889	715	6.55	6.55	-0.36	-0.08	0.19	
61908008	SSS	08/06/19, 11:03:08 A	SSS, 0-80-0, 3 bag at 0%, 3% and 6% grade, warm start in 20°F test cell	ok	-5	4250	45.47	-0.1558	0.02832	6.23			0.256	17.6	0.21	18.92	GA	1,388.22	25.81	900	715	6.53	6.55	-0.62	-0.41	0.19	
61908008	SSS	08/06/19, 11:03:08 A	SSS, 0-80-0, 3 bag at 0%, 3% and 6% grade, warm start in 20°F test cell	ok	-4	4250	45.47	-0.1558	0.02832	6.22			0.512	12.2	0.48	12.85	GA	1,388.72	37.97	987	715	6.59	6.55	0.51	0.55	0.19	
61908009	US06	08/06/19, 11:54:30 A	US06x2, 4 (split), warm start in 20°F test cell with HVAC AUTO-72°F	ok	-5	4250	45.47	-0.1558	0.02832	1.79	0.122	14.7	0.120	15.0	0.11	15.73	GA	5,688.95	-0.20	2,455	2,460	3.30	3.31	-1.29	-0.29	0.79	
61908009	US06	08/06/19, 11:54:30 A	US06x2, 4 (split), warm start in 20°F test cell with HVAC AUTO-72°F	ok	1	4250	45.47	-0.1558	0.02832	6.25	0.249	25.1	0.248	25.2	0.23	27.08	GA	#####	-3.67	1,098	1,139	7.99	7.97	0.13	0.30	0.31	
61908009	US06	08/06/19, 11:54:30 A	US06x2, 4 (split), warm start in 20°F test cell with HVAC AUTO-72°F	ok	-2	4250	45.47	-0.1558	0.02832	8.04	0.371	21.66	0.367	21.87	0.34	23.33											
61908009	US06	08/06/19, 11:54:30 A	US06x2, 4 (split), warm start in 20°F test cell with HVAC AUTO-72°F	ok	-6	4250	45.47	-0.1558	0.02832	1.78	0.120	14.9	0.117	15.2	0.11	16.16	GA	5,663.57	0.11	2,462	2,460	3.31	3.31	-0.75	-0.09	0.79	
61908009	US06	08/06/19, 11:54:30 A	US06x2, 4 (split), warm start in 20°F test cell with HVAC AUTO-72°F	ok	-2	4250	45.47	-0.1558	0.02832	6.25	0.246	25.4	0.243	25.7	0.23	27.66	MK/GA	#####	-3.19	1,103	1,139	7.92	7.97	-0.75	-0.57	0.31	
61908009	US06	08/06/19, 11:54:30 A	US06x2, 4 (split), warm start in 20°F test cell with HVAC AUTO-72°F	ok	-4	4250	45.47	-0.1558	0.02832	8.03	0.365	21.97	0.361	22.27	0.34	23.88											

Appendix E: Certification Fuel Specifications

Table 19. Certificate of Analysis for Tier 2 test fuel used for all the testing

APRF REC'D 3 DRUMS (TOTAL)
7/30/18



haltermannsolutions
Telephone: (800) 969-2542

Certificate of Analysis
FAX: (281) 457-1469

PRODUCT: **EPA TIER II EEE
FEDERAL REGISTER** Batch No.: GE3121GP10
PRODUCT CODE: **HF0437** Tank No.: Drums
Date: 6/26/2018

TEST	METHOD	UNITS	HALTERMANN Specs			RESULTS
			MIN	TARGET	MAX	
Distillation - IBP	ASTM D86 ²	"F	75		95	87
5%		"F				110
10%		"F	120		135	123
20%		"F				140
30%		"F				160
40%		"F				187
50%		"F	200		230	216
60%		"F				231
70%		"F				242
80%		"F				259
90%		"F	305		325	316
95%		"F				340
Distillation - EP		"F			415	400
Recovery		vol %		Report		97.5
Residue		vol %		Report		0.7
Loss		vol %		Report		1.8
Gravity	ASTM D4052 ²	"API	58.7		61.2	58.9
Density	ASTM D4052 ²	kg/l	0.734		0.744	0.743
Reid Vapor Pressure	ASTM D5191 ²	psi	8.7		9.2	8.9
Carbon	ASTM D3343 ¹	wt fraction		Report		0.8665
Carbon	ASTM D5291 ²	wt fraction		Report		0.8663
Hydrogen	ASTM D5291 ²	wt fraction		Report		0.1337
Hydrogen/Carbon ratio	ASTM D5291 ²	mole/mole		Report		1.839
Stoichiometric Air/Fuel Ratio				Report		14.567
Oxygen	ASTM D4815 ²	wt %		0.05		None Detected
Sulfur	ASTM D5453 ²	wt %	0.0025		0.0035	0.0032
Lead	ASTM D3237 ²	g/gal		0.01		None Detected
Phosphorus	ASTM D3231 ²	g/gal		0.005		None Detected
Silicon	ASTM 5184 ²	mg/kg		4		None Detected
Composition, aromatics	ASTM D1319 ²	vol %		35		31
Composition, olefins	ASTM D1319 ²	vol %		10		1
Composition, saturates	ASTM D1319 ²	vol %		Report		69
Particulate matter	ASTM D5452 ²	mg/l		1		0
Oxidation Stability	ASTM D525 ²	minutes	240			1000+
Copper Corrosion	ASTM D130 ²			1		1a
Gum content, washed	ASTM D381 ²	mg/100mls		5		<0.5
Fuel Economy Numerator/C Density	ASTM D5291 ¹		2401		2441	2432
C Factor	ASTM D5291 ¹			Report		0.9987
Research Octane Number	ASTM D2699 ²		96.0			97.3
Motor Octane Number	ASTM D2700 ²			Report		88.6
Sensitlivity	D2699/2700 ²		7.5			8.7
Net Heating Value, btu/lb	ASTM D3338 ¹	btu/lb		Report		18441
Net Heating Value, btu/lb	ASTM D240 ²	btu/lb		Report		18623
Color	VISUAL			Report		Undyed

Quality Assurance Technician

[Signature]

¹ Haltermann Solutions is accredited to ISO/IEC 17025 by ANAB for the tests referred to with this footnote.
² Tested by ISO/IEC 17025 accredited subcontractor.

Gasoline and diesel specialty fuels from Haltermann Solutions shall remain within specifications for a minimum of 3 years from the date on the COA so long as the drums are sealed and unopened in their original container and stored in a warehouse at ambient conditions. Specialty fuels that have been intentionally modified for aggressive or corrosive properties are excluded.

This report shall not be reproduced, except in full, without the written consent of Haltermann Solutions.

Main Lab, 15600 West Hardy Rd., Houston, TX 77060 USA

Page 1 of 1

Appendix F: Test ID to Figure Matrix

This appendix specifies the test IDs used to generate the figures on the report.

Figure #	Test IDs
Figure 1: Distribution of horsepower and equivalent test weight among comparable vehicles in the sample group	Not applicable
Figure 2: Distribution of FTP fuel economy for comparison vehicles	Not applicable
Figure 3: Distribution of adjusted HWFET fuel economy for comparison vehicles	Not applicable
Figure 4: Vehicle mounted for full testing inside the AMTL 4WD chassis dynamometer.	Not applicable
Figure 5: Instrumentation of port and direct fuel Injection systems	Not applicable
Figure 6: Direct fuel flow measurements via fuel scale and Coriolis flow meters, system overview, and actual measurement system	Not applicable
Figure 7: Wiring of Hioki Power Analyzer on the 2019 Infiniti QX50 test vehicle	Not applicable
Figure 8: CAN breakout on the 2019 Infiniti QX50	Not applicable
Figure 9: Overview of steady-state ramp drive cycle	61907056
Figure 10: Vehicle acceleration with varying constant pedal inputs	61907068
Figure 11: 2019 Infiniti QX50 test vehicle mounted to the chassis dynamometer inside the test cell	Not applicable
Figure 12: Infiniti QX50 powertrain operation on cold start UDDS	61907039
Figure 13: Daily drive cycle test sequence executed in the morning	61907039, 61907040, 61907041, 61907042
Figure 14: Raw fuel scale fuel economy results: UDDS and HWFET certification cycles from Argonne	Test Sequence #1: 61907039, 61907041 Test Sequence #2: 61907045, 61907047 Test Sequence #3: 61907051, 61907053
Figure 15: Raw fuel scale fuel economy results for certification cycles at different temperature conditions	20F: 61908005, 61908006, 61908007, 61908009 22C: 61907039, 61907040, 61907041, 61907042 95F: 61907071, 61907022C, 61907073, 61907075
Figure 16: Engine operation in the UDDS cycle at different temperatures	20F: 61908005 22C: 61907039 95F: 61907071
Figure 17: Powertrain and cabin temperature profiles at different temperature	20F: 61908005, 61908006, 61908007, 61908009 22C: 61907039, 61907040, 61907041, 61907042 95F: 61907071, 61907022C, 61907073, 61907075
Figure 22: Powertrain operation during the 55- to 80-mph passing maneuver	61907062
Figure 23: Powertrain operation during maximum acceleration	61907049

Figure #	Test IDs
Figure 24: PFI to DI transition and initial 240 sec of the idle fuel flow test	
Figure 25: Infiniti VCR of change for 25°C hot start, US06, and 0–80 mph maximum effort cycles	
Figure 26: Infiniti VCR operational overview for 25°C hot start UDDS, HWFET, and US06 cycles	
Figure 27: Infiniti VCR operational overview of positive tractive force for 25°C hot start UDDS, HWFET, and US06 cycles	
Figure 28: Infiniti VCR and boost operational map for 25°C hot start UDDS, HWFET, and US06 cycles	•
Figure 29: Infiniti VCR histogram overview of positive tractive force for 25°C hot start UDDS, HWFET, and US06 cycles	
Figure 30: Engine boost histogram overview of positive tractive force for 25°C hot start UDDS, HWFET, and US06 cycles	•
Figure 31: Comparison of ignition timing spark advance for UDDS, HWFET, and US06 cycles	
Figure 32: Comparison of percentage DI operation for UDDS, HWFET, and US06 cycles. Additional figure generalizes regions of DI operation.	

Appendix G: Comments From External Reviewers

This document contains the comments from external reviewers on the vehicle testing and validation reports for the following 4 vehicles

- Infiniti QX50, 2L Turbo VCR, CVT
- 2019 Acura MDX Sport Hybrid, 3L V6 VTEC, 7 spd DCT
- Toyota Camry, 2.5L I4, 8 spd AT
- Honda Accord, 1.5L turbo VTEC, CVT

Reviewer 1

Prof. Giorgio Rizzoni

Ford Motor Company Chair in ElectroMechanical Systems, is a Professor of Mechanical and Aerospace Engineering and of Electrical and Computer Engineering at Ohio State University (OSU).

Argonne National Lab (ANL) has operated the Advanced Mobility Technology Laboratory (AMTL, formerly Advanced Powertrain Research Facility, APRF) for over 20 years. This reviewer is quite familiar with the operation and characteristics of the AMTL, having served as an Associate Technical Team Member of the Vehicle Systems Analysis Technical Team of the U.S. DRIVE Partnership between 2013 and 2016. During this time, I had the opportunity to participate in numerous program reviews of the work done by ANL-APRF in characterizing and evaluating the fuel economy, energy efficiency and emissions of a number of vehicles, mostly with focus on alternative fuels and powertrains. During the course of these reviews, it became apparent that the test capabilities and instrumentation of the AMTL are of the highest quality, and far exceed the minimum requirements for certification testing. The four-wheel-drive chassis dynamometer is operated in an environmental chamber capable of low- and high-temperature testing, and the available instrumentation permits both non-intrusive and intrusive testing to evaluate not only the fuel economy and emissions of the vehicle, but also to perform distinct and specific tests to evaluate the energy efficiency and power consumption of specific subsystems and components in the vehicle. In addition, the APRF team has developed considerable software analysis capabilities that allow the team to present results in comprehensive and carefully thought-out graphical and tabular forms. In my 35-year career as an automotive researcher, I have not come across a public-domain test facility of this kind that matches the capabilities of the AMTL. The work presented in this report is of the highest quality.

The test plan is quite comprehensive, designed to address specific questions related to the fuel economy impact of the operation of various automotive subsystems, and far exceeds the minimum requirements of certification testing. I have no suggestions for further improvement.

The tests conducted in the study were comprehensive and evaluated vehicle fuel economy under different environmental conditions (72, 20, and 95 °F, the last with solar radiation emulation), and with fuels with different octane ratings (regular and premium). In addition to performing fuel economy tests following regulatory driving cycles (UDDS, HWFET, US06, and SC03, LA92 and JCo8), the testing included steady speed tests at different grades, tests during passing maneuvers, and wide-open throttle and idle fuel consumption tests. The test program is as comprehensive as one could expect to implement in a chassis dynamometer test cell. The comparison with EPA CAFE test results is very valuable.

The graphical and tabular summary of the test results give a clear and concise representation of the results. I made some recommendations on minor improvements that I believe will be incorporated in the final report. The only item that is important to note is

the lack of consistency in the units used throughout the report. This is an industry-wide problem, wherein SI and English units are both used and not always both shown next to one another.

The energy analysis, including both fuel economy and overall efficiency, is comprehensive and includes consideration of thermal environment (both ambient temperature as well as cold and hot start conditions), and of different vehicle modes of operation (accel/decel, cruise, stop). The visual presentation of these results is excellent and gives the reader the opportunity to understand the results of complex tests.

As part of the peer review process, I took the time to carefully review the report, and made a number of editorial suggestions that, in my opinion, further enhanced the already excellent quality of the report. I believe that the final product is a well-organized, readable, clear and accurate report.

Vehicle specific comments:

Infinity QX50:

This report provides testing results for a 2019 Infiniti QX50 equipped with a turbocharged 2.0 liter in-line four-cylinder Variable Compression Ratio (VCR) Atkinson cycle-capable engine with dual fuel injection, coupled to the driveline by a CVT. The combination of features in this powertrain is novel, to best of this reviewer's knowledge, and is a very appropriate choice for testing and analysis at Argonne.

The additional analysis presented in the report on: details of VCR engine operation; dual fuel injection strategies; transmission operating strategy; torque converter lock-up strategies; vehicle performance (acceleration and passing maneuvers); fuel cut-off strategies; cycle thermal test conditions; comparison of fuels with different AKI ratings; and accessory load operation further enhances the quality and completeness of the report. The Autonomie Model Validation section is a valuable addition to the testing results and is very well executed.

Acura MDXSH

This report provides testing results for a 2019 Acura MDX Sport Hybrid equipped with a 3.0 V6 Variable Valve Timing and Lift Electronic Control (VTEC) engine coupled through a 7-speed dual clutch transmission (DTC) and a three-motor hybrid system. The 2019 Acura MDX sport hybrid "super-handling" all-wheel drive (SH-AWD) system includes a 143-kW engine coupled to a 7-speed dual clutch transmission (DCT) and a 35-kW electric motor in the front and two 27-kW electric motors on the rear axle, capable of driving each wheel independently, thus replacing the rear differential. The 3.0L V6 engine is port fuel injected and can perform cylinder deactivation for each bank to achieve higher low-load efficiencies. The configuration of the rear electric machines permits the implementation of torque-vectoring strategies and enable superior vehicle handling. This choice of this vehicle is appropriate as it represents a trend towards achieving improved fuel economy while also providing improved performance.

Camry:

The vehicle tested in this report is equipped with a 2.5 L in-line four-cylinder engine coupled to an 8-speed automatic transmission. The engine is a high expansion ratio Atkinson cycle engine with very high peak thermal efficiency (40%), dual variable valve timing, cooled EGR. The 8-speed transmission is a new development that replaces the previously employed 6-speed

transmission. The vehicle is claimed to offer outstanding fuel economy while delivering impressive performance. The results presented in the report clearly support these statements and suggest that the technologies embodied in this vehicle are representative of future trends for conventional (i.e.: non-hybrid) powertrains in mid-size sedans.

Accord

The vehicle tested in this report is equipped with a best-in-class powertrain, featuring a turbocharged 1.5 L in-line four-cylinder engine with variable valve timing and lift electronic control (VTEC) paired with a direct injection system and a continuously variable transmission. The Honda's VTEC turbo technology is marketed as part of the powertrain technologies marketed by Honda as "Earth Dreams Technology." The vehicle is claimed to offer outstanding fuel economy while delivering impressive performance. The results presented in the report clearly support these statements and suggest that the technologies embodied in this vehicle are representative of future trends for conventional (i.e.: non-hybrid) powertrains in mid-size sedans.

The additional analysis presented in the report on: transmission and torque converter operating strategy (including different transmission operating modes); vehicle performance (acceleration and passing maneuvers); start-stop operation; vehicle fuel injection strategies; fuel cut-off strategies; cycle thermal test conditions; comparison of fuels with different AKI ratings; and accessory load operation further enhances the quality and completeness of the report. The Autonomie Model Validation section is a valuable addition to the testing results, and is very well executed.

Reviewer 2

Prof. David Foster

*Phil and Jean Myers Professor Emeritus,
Department of Mechanical Engineering, University of Wisconsin-Madison*

The experimental protocols and quality of the data taken is very good. It was also nice to see the extra dyno test runs that were developed to probe the vehicle control systems and performance for a more extensive range of operating conditions than the standardized certification tests. The use of this data to fit the Autonomie simulation was impressive as were the correlations between the simulation predictions and the certification cycle test data. Very nice work.

I have made many comments throughout the four reports. Some were generic to the descriptions of the experimental procedure and simulation tuning. Relative to these comments, I sometimes repeated them in the individual reports and other times merely said I had made a comment on the item being described in one of the reports previously reviewed. I hope that the individual teams will share the generic comments about operating procedure, etc. with each other.

Finally, I also had suggestions which I thought would increase the impact of this work. I think that the detail of the operating characteristics of the specific components of each vehicles powertrain contained in Autonomie puts you are in a position to quantify the incremental improvement each of the advanced powertrain technologies makes in the vehicles' fuel economy and performance relative to previous model vehicles as well as competitor vehicles. This is what I expected as part of the discussion on the insights gained from vehicle testing. I inferred this from reading the contract statement: "The focus of the evaluation was to understand the use of critical powertrain components and their impact on the vehicle efficiency," given in the introduction and/or conclusion of each report. In conclusion of each report I made an extended comment further detailing this thought – usually with specific reference to the technologies used in the vehicle reported on in the report.

Below is a copy of my conclusive comment from the Acura Performance Report:

"This is a similar comment to that made in the reports I have previously reviewed.

This is very good work. The experimental protocol, procedures and data taking techniques are of high quality. The component data extracted from the tests were used to tune Autonomie which was then used to simulate the vehicle with excellent results.

The reporting of the data in this report was pretty much just that; here is the data we got; we can see the different aspect of the powertrain engaging and disengaging; here are the results for the two different octane fuels that were tested, etc. However, there was very little discussion of, or attempts to quantify, the impact on fuel economy and performance improvement of the individual advanced technologies used in the vehicle. Also, to me it was disconcerting that when the testing showed no difference between the manufacturer's recommended high-octane fuel and the less expensive low octane fuel almost no discussion ensued. To me this was a significant finding.

I think you are well situated to make these assessments. The Autonomie simulation has energy flows and performance evaluation criteria for most, if not all, of the components and subsystems of the vehicle. I thought it would be possible to use the simulation, which reproduces the data well, to partition the energy flow from the fuel to the wheels for the various driving conditions tested and quantify the impact of the different technologies on fuel economy and performance.

By doing this for the different vehicles tested you would be able to offer a look-up type categorization of the potential benefits of different technologies, used either separately or synergistically, on overall vehicle performance.

Such an analysis would be a tremendous contribution to the technical and regulatory community, and it is what I inferred what the NHTSA was interested in. It is why I offer this comment on the highlighted phrase.”

The testing of the impact of the fuels octane number was particularly surprising. In general the octane number did not make a significance difference in the vehicles performance. In fact in the Acura, where the manufacturer recommends high octane gasoline, the low octane gasoline showed better performance. This is a significant finding which I do not understand. It was not discussed in any detail in the report.

There is no reason to discount the data in your tests. However, if this is true, why would the manufacturers recommend high octane gasoline when better performance could be obtained with a less expensive fuel? I made comments of this nature in the different vehicle reports because I think this is a significant finding. It is also one that your laboratory should make absolutely sure that nothing is strange with the data. I even suggested asking Honda about this. To that end, I think one needs to be sure that there are no caveats to this data before it is disseminated more widely in the public arena. This result is significant!

For more detail on this I am also including the extended comment I made in the fuels testing section of the Acura Performance report:

“Considering these tests relative to the fuel test results given in the Infinity makes me more confused. It seems to me that the most important test to perform for this evaluation is the one using the manufacturer’s recommended octane rating fuel – which should to be the focus of your results.

If the manufacturer recommends the lower octane fuel isn’t it safe to assume that they have optimized the engine for the lower-octane fuel, and have not included technologies that would optimize for higher octane? For example, the range of spark advance might be limited, the chosen compression ratio might not be optimal if a higher-octane fuel were used, In other words, using a high-octane fuel could very well result in significant knock margin being ‘left on the table’ because of this non optimal operation. In which case it would be easy to interpret results of such tests out of context and come to a more general conclusion that higher octane is not worth very much.

I commented in the Infinity testing that an opportunity may have been missed by not running a lower octane fuel in the vehicle which specifies high-octane. It might more clearly inform us on the magnitude of performance improvements that are available through the use of a high-octane fuel in a vehicle which has been optimized of that fuel. Or conversely, it could inform us of the performance degradation that will be experienced from using a low octane fuel in a vehicle designed for high octane fuel.

For this vehicle it appears that you are doing what I suggested in the Infinity report. (Although because of confusion in how the fuel specifications are given in Appendix D, I got confused trying to interpret the results.) I was hoping your data, when combined with the fuel testing data from the other vehicle performance evaluations, would show the performance detriments that may occur when an engine optimized for higher octane fuel is run on low octane fuel. It could

also give information about using a lower octane fuel in an engine optimized for high octane relative to the performance of an engine/vehicle optimized for a lower octane number fuel using the low octane fuel. And finally, it could assess if there is any benefit to using a high-octane fuel in an engine optimized for low octane.

Partitioning these efficiency contributions of both engine technology and fuel specifications would be a significant contribution to the larger technical community, regulatory agencies, and the public in general.”

Perhaps the level of energy flow partitioning I was hoping for is outside of the scope of the contract with NHTSA. If it is, fine, but I still think these data and the subsequent Autonomie simulation capabilities give ANL a unique opportunity to offer some quantification of the efficiency improvement potential for a wide array of advanced technology components that are being incorporated into new vehicles.

Reviewer 3

Prof. Douglas Nelson

Department of Mechanical Engineering, Virginia Tech

Comments on Toyota Camry report:

The ANL report documents vehicle testing and model development for the 2018 Toyota Camry XLE 2.5L

PFI/DI engine coupled to an eight-speed automatic transmission. This vehicle was selected to evaluate these technologies and to develop models in support of NHTSA's CAFE work. Overall, the report is of high quality and achieves the objectives set out in the report. The following comments are intended to help improve the report.

The report should add an Executive Summary that clearly states the results of the report. The Conclusions should also be revised and extended to include what is significant about the results; does the work provide new and better data, models, and control? Does this engine have improved efficiency beyond previous versions of direct and port fuel injection engines? Does the Atkinson cycle used in a conventional vehicle rather than a hybrid have any issues with operation of the engine?

The given reference [8] does not seem to be available (yet?) to the public. The data provided in the report is of very high quality and high value, but the errors and uncertainty are not adequately addressed. The excellent repeatability of some data has been shown. Even if the details are provided in [8] a brief summary of the overall testing data quality/uncertainty should be included in the report.

Comments on Infiniti QX50 report

The ANL report documents vehicle testing and model development for the 2019 Infiniti QX50 2.0L variable compression ratio (VCR) turbocharged engine coupled to a continuously variable transmission (CVT). This vehicle was selected to evaluate these technologies and to develop models in support of NHTSA's CAFÉ work. Overall, the report is of high quality and achieves the objectives set out in the report. The following comments are intended to help improve the report.

The Executive Summary should clearly state the results of the modeling and validation sections of the report. The Conclusions should also be revised and extended to include what is significant about the results; does the work provide new and better data, models, and control? Does this engine have improved efficiency beyond previous versions of direct and port fuel injection engines? Does the Atkinson cycle used in this conventional vehicle rather than a hybrid have any issues with operation of the engine? What are the advantages of VCR for efficiency vs performance? The given reference [4] does not seem to be available (yet?) to the public. The data provided in the report is of very high quality and high value, but the errors and uncertainty are not adequately addressed. The excellent repeatability of some data has been shown. Even if the details are provided in [4] a brief summary of the overall testing data quality/uncertainty should be included in the report.

Overall, the testing sections have good documentation and presentation of the complex interactions of VCR, boost, DI and ignition timing. The following comments are provided in the order of the report, and are not in any order of significance. In several places in the vehicle

comparison, the term “adjusted” fuel economy is used. The fuel economy results available from the EPA test car list (tcl) data (as referenced) are broadly understood to be unadjusted values that correspond to specific drive cycles and phases, while the label fuel economy available from fueconomy.gov are adjusted. CAFE is based on unadjusted fuel economy directly available from the EPA test car list data. That tcl data does have a header that says RND_ADJ_FE, but that ADJ is not in the same context. If you use the term adjusted with respect to the tcl data, please very specifically define what the adjustment means in this context. Is it the weighting of the cold start and hot start phases 1 and 3 of the UDDS test results to get the FTP? Then why are HwFET results also (sometimes) referenced as adjusted? Please just be very clear about this term as there is a lot of confusion about CAFÉ vs Label fuel economy.

The mix of using superscripted numbers for both footnotes and references is a bit confusing – suggest using references in [#] format as in the other reports.

Comments on the Accord report

The ANL report documents vehicle testing and model development for the 2018 Honda Accord LX 1.5L turbocharged engine coupled to a continuously variable transmission (CVT). This vehicle was selected to evaluate these technologies and to develop models in support of NHTSA’s CAFE work. Overall, the report is of high quality and achieves the objectives set out in the report. The following comments are intended to help improve the report.

The report should add an Executive Summary that clearly states the results of the report. The conclusions should also be revised and extended to include what is significant about the results; does the work provide new and better data, models, and control? Does this engine have improved efficiency beyond previous versions of turbocharged four-cylinder engines? Does the CVT have reduced losses in addition to improving the operation of the engine?

The given reference [8] does not seem to be available (yet?) to the public. The data provided in the report is of very high quality and high value, but the errors and uncertainty are not adequately addressed. The excellent repeatability of some data has been shown. Even if the details are provided in [8] a brief summary of the overall testing data quality/uncertainty should be included in the report.

Comments on Acura MDXSH

The ANL report documents vehicle testing and model development for the 2019 Acura MDX SH 3.0L VTEC engine coupled to a 7-speed dual clutch transmission and a 3-motor hybrid electric system. This AWD hybrid vehicle was selected to evaluate these technologies and to develop models in support of NHTSA’s CAFE work. Overall, the report is of high quality and achieves the objectives set out in the report. The following comments are intended to help improve the report.

The Executive Summary should clearly state the results of the modeling and validation sections of the report. The Conclusions should also be revised and extended to include what is significant about the results; does the work provide new and better data, models, and control? Does this hybrid vehicle have improved engine efficiency beyond previous hybrids? Does the DCT with integrated motor have significant fuel consumption benefits? What are the advantages of rear motors for efficiency vs performance?

The given reference [4] does not seem to be available (yet?) to the public. The data provided in the report is of very high quality and high value, but the accuracy and uncertainty are not

adequately addressed. The excellent repeatability of some data has been shown. Even if the details are provided in [4] a brief summary of the overall testing data quality/uncertainty should be included in the report.

Overall, the testing sections have good documentation and presentation of the complex interactions of hybrid strategy and components.

DOT HS 813 162
July 2021



U.S. Department
of Transportation
**National Highway
Traffic Safety
Administration**

